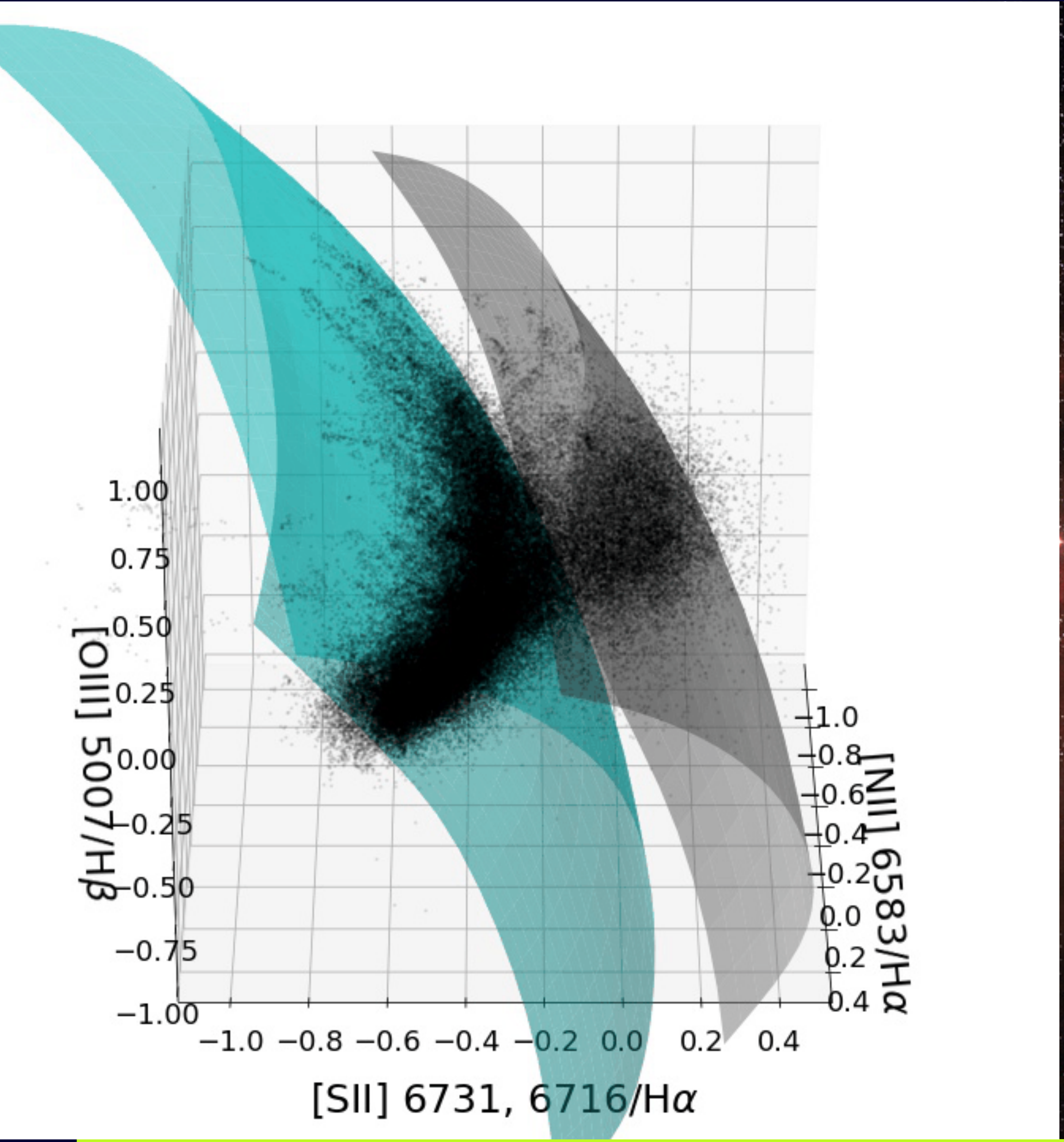

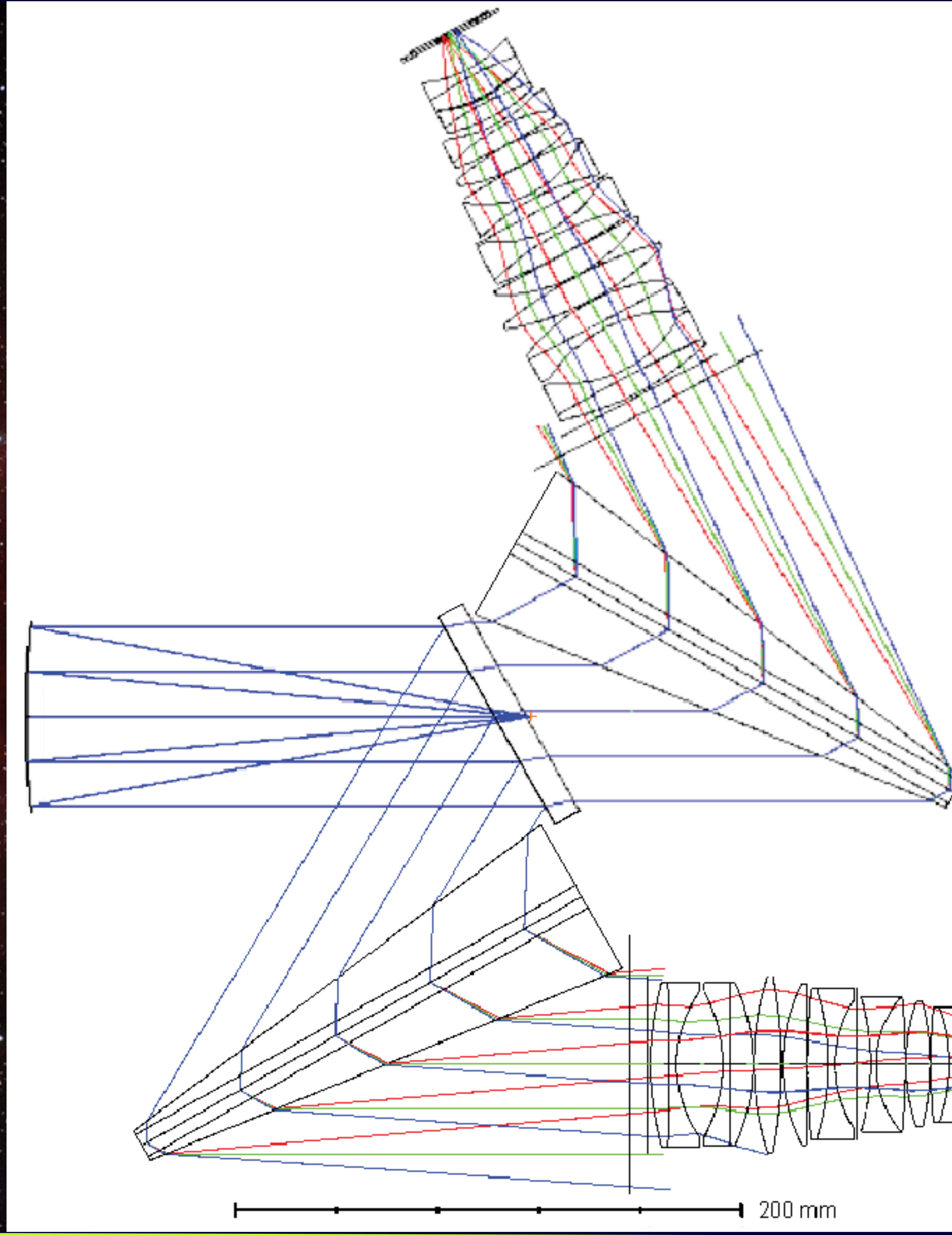

Towards Precision Astrophysics of Warm Ionized Gas

Renbin Yan (University of Kentucky)

@Tsinghua University, Dec 17, 2020

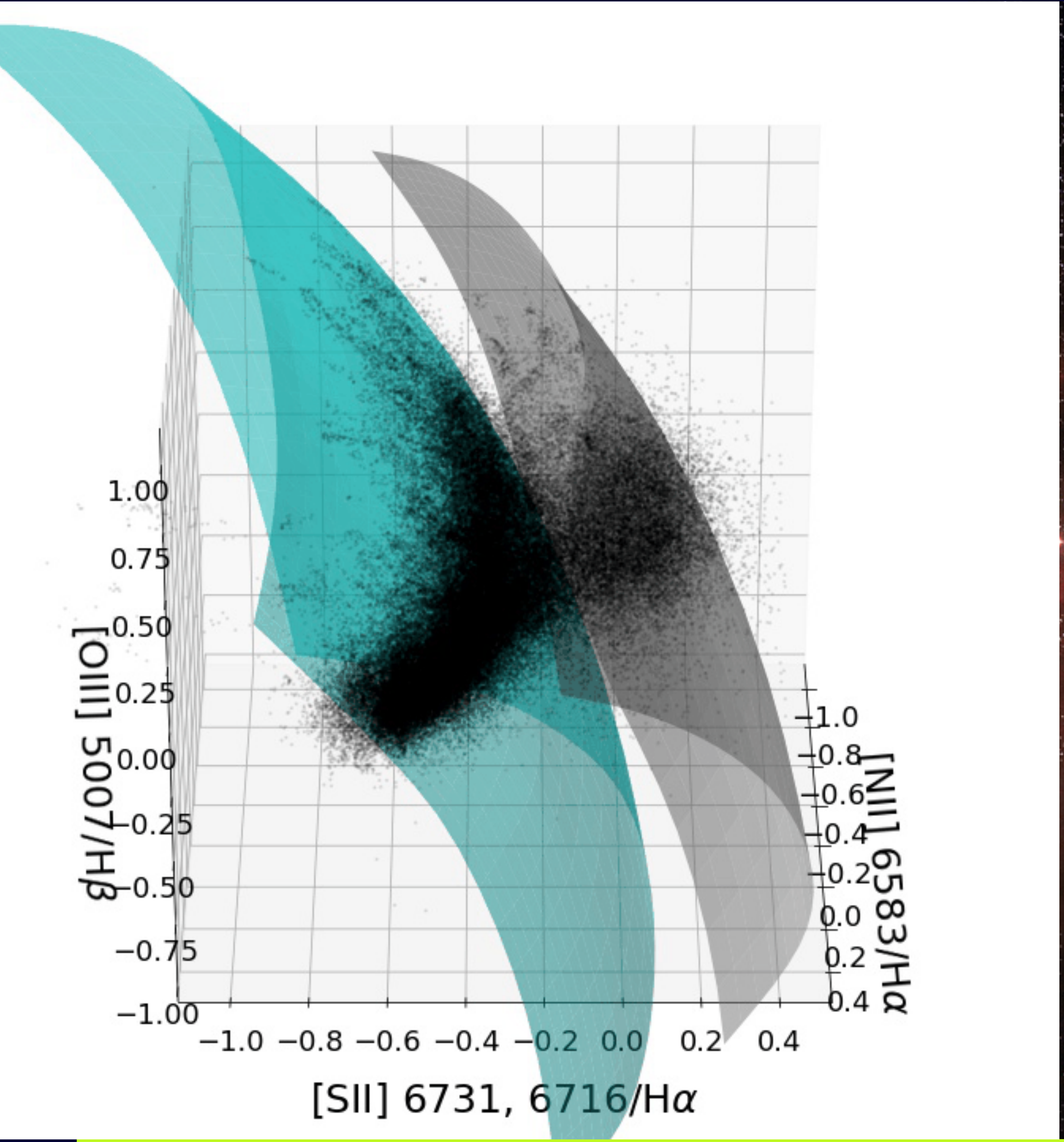

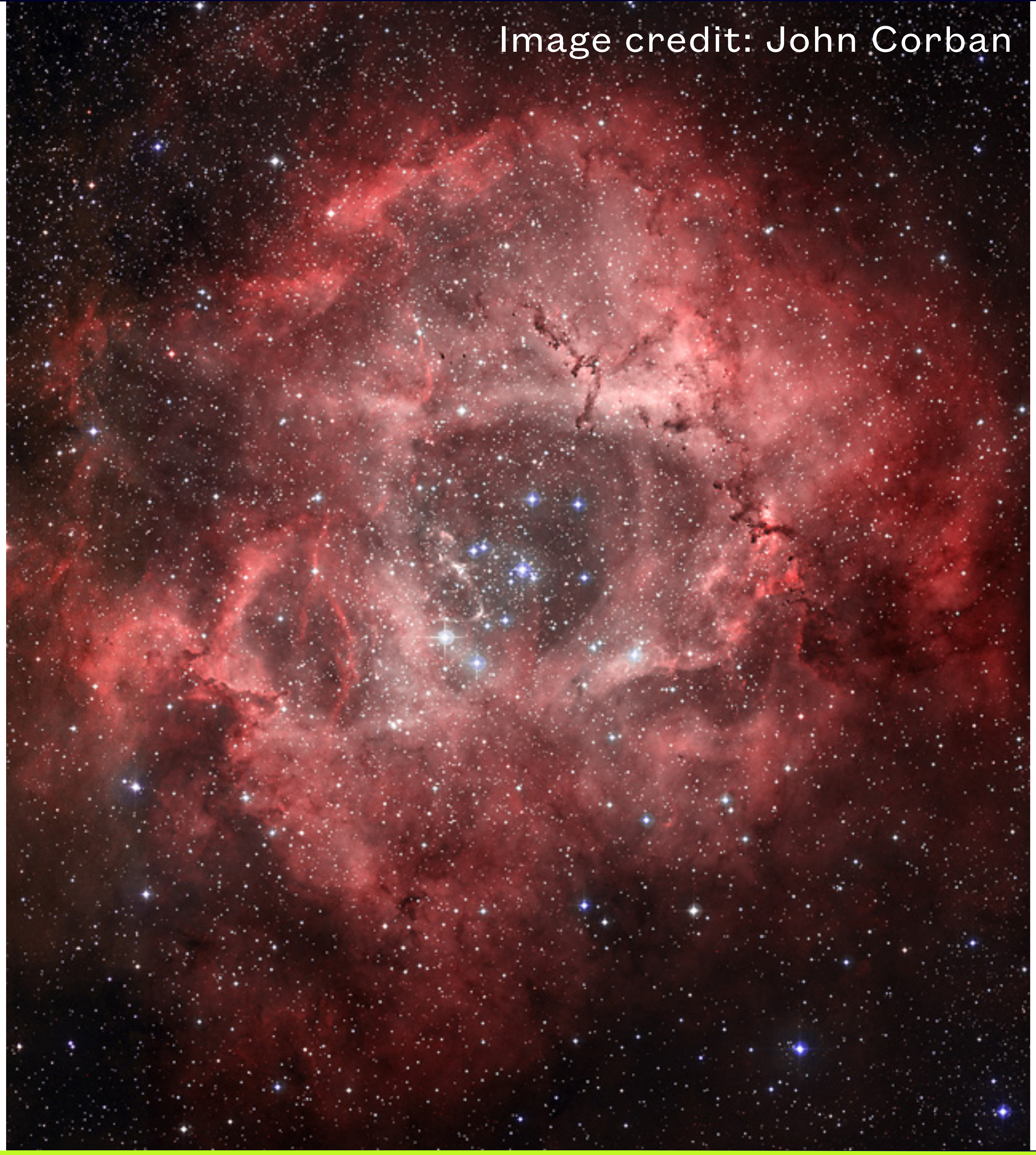

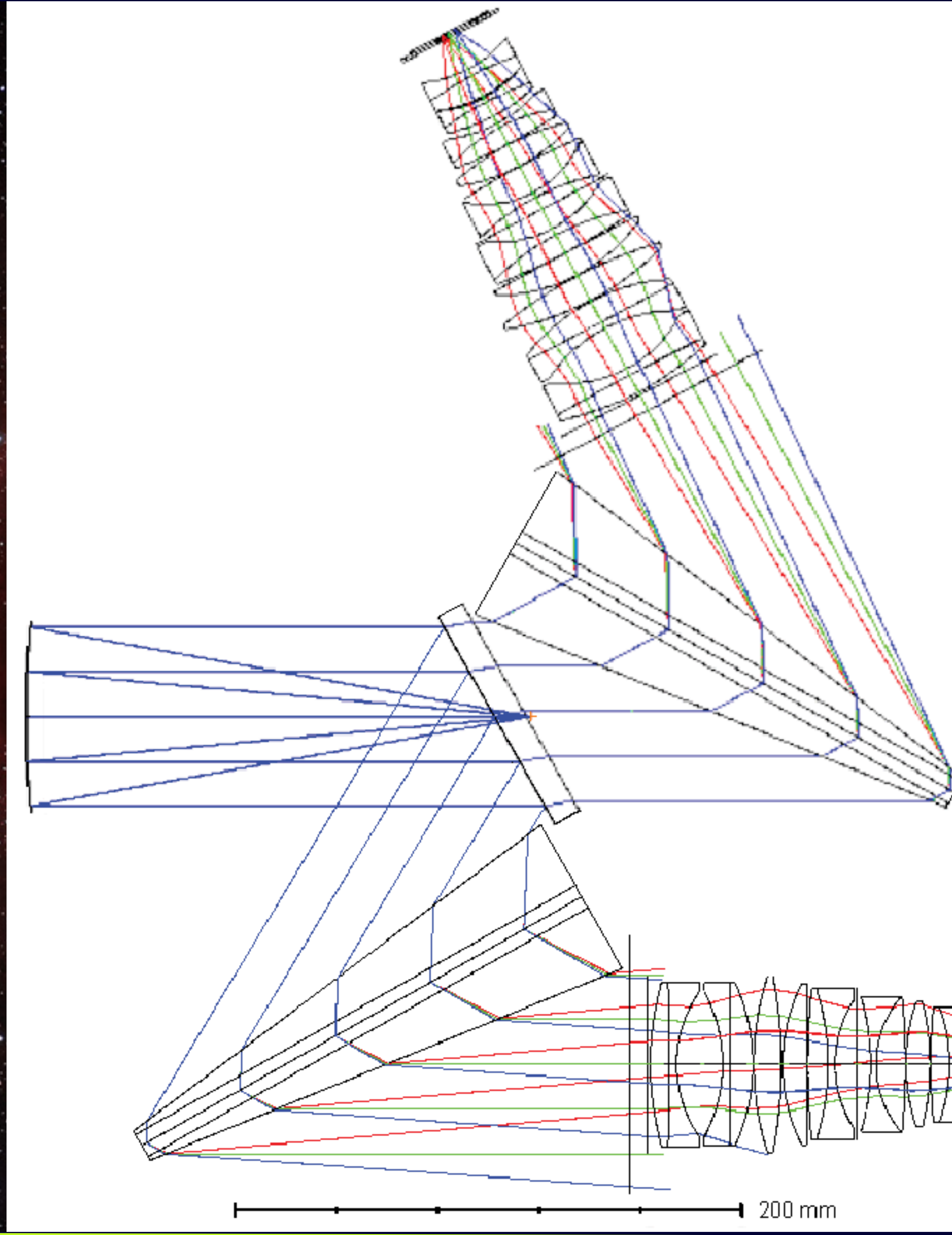

Towards Precision Astrophysics of Warm Ionized Gas

Renbin Yan (University of Kentucky)

@Tsinghua University, Dec 17, 2020

SDSS-IV/MaNGA
Mapping Nearby Galaxies at APO

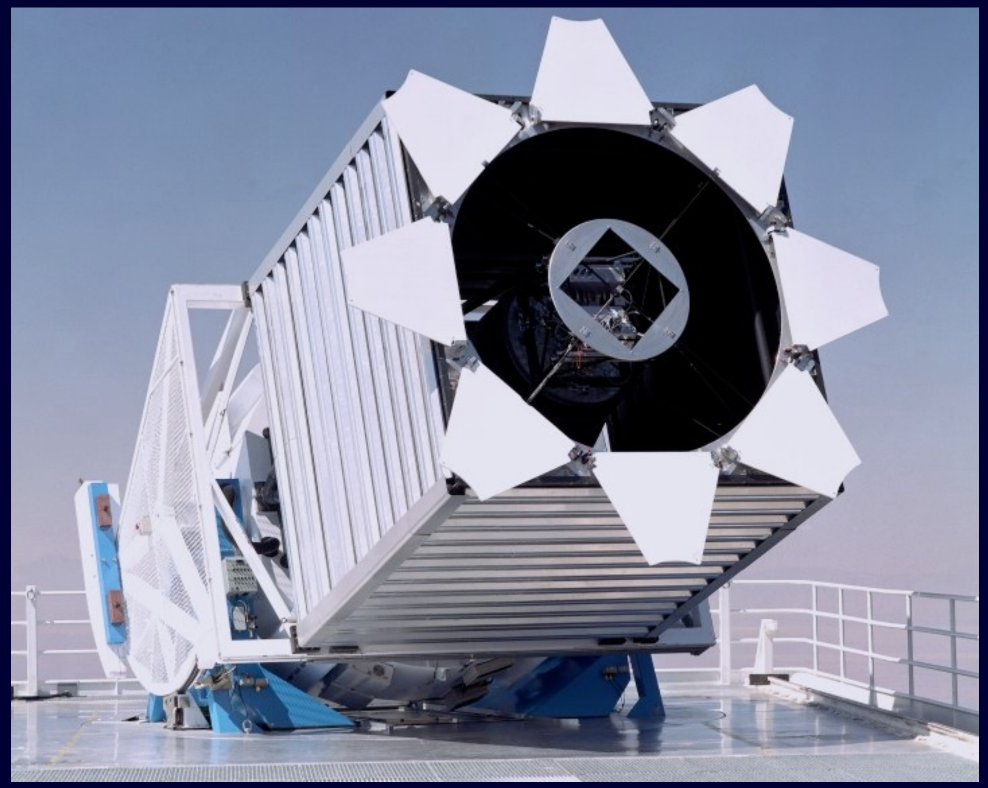

- Multi-object integral field spectroscopy survey of nearby galaxies.
- Spatial resolution: 2.5" (1-2kpc);
  Spectral resolution: 50-70 km/s (sigma), R~2000;
  Spectral coverage: 3,622-10,354A.

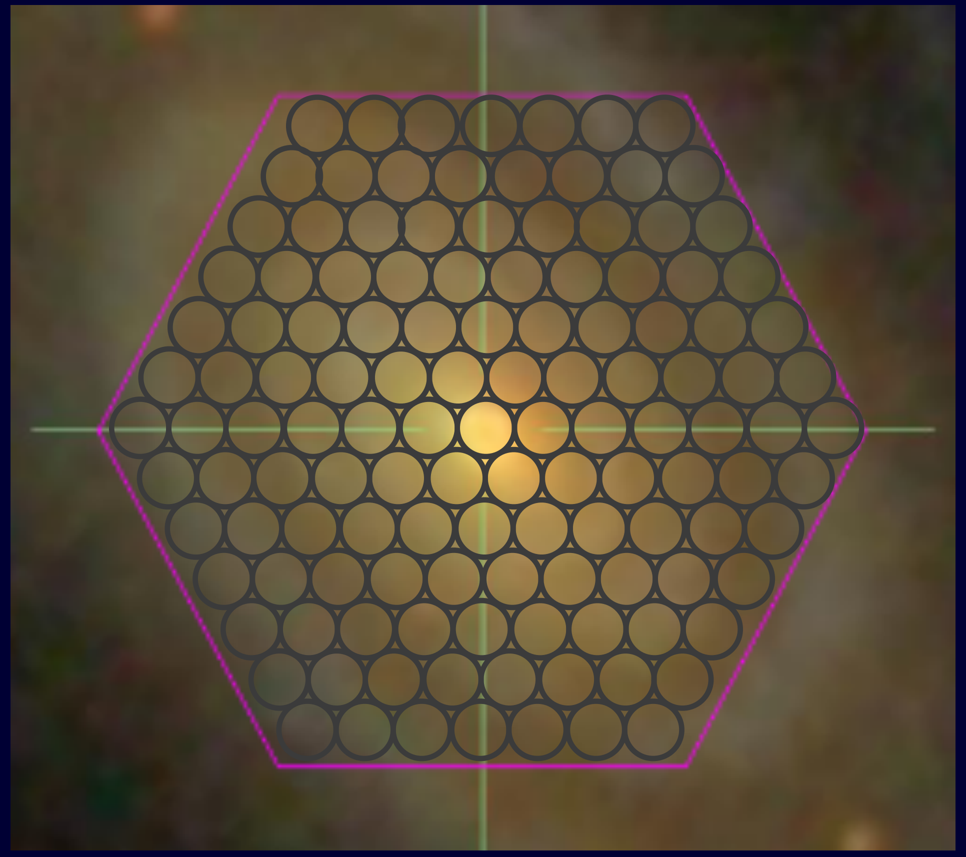

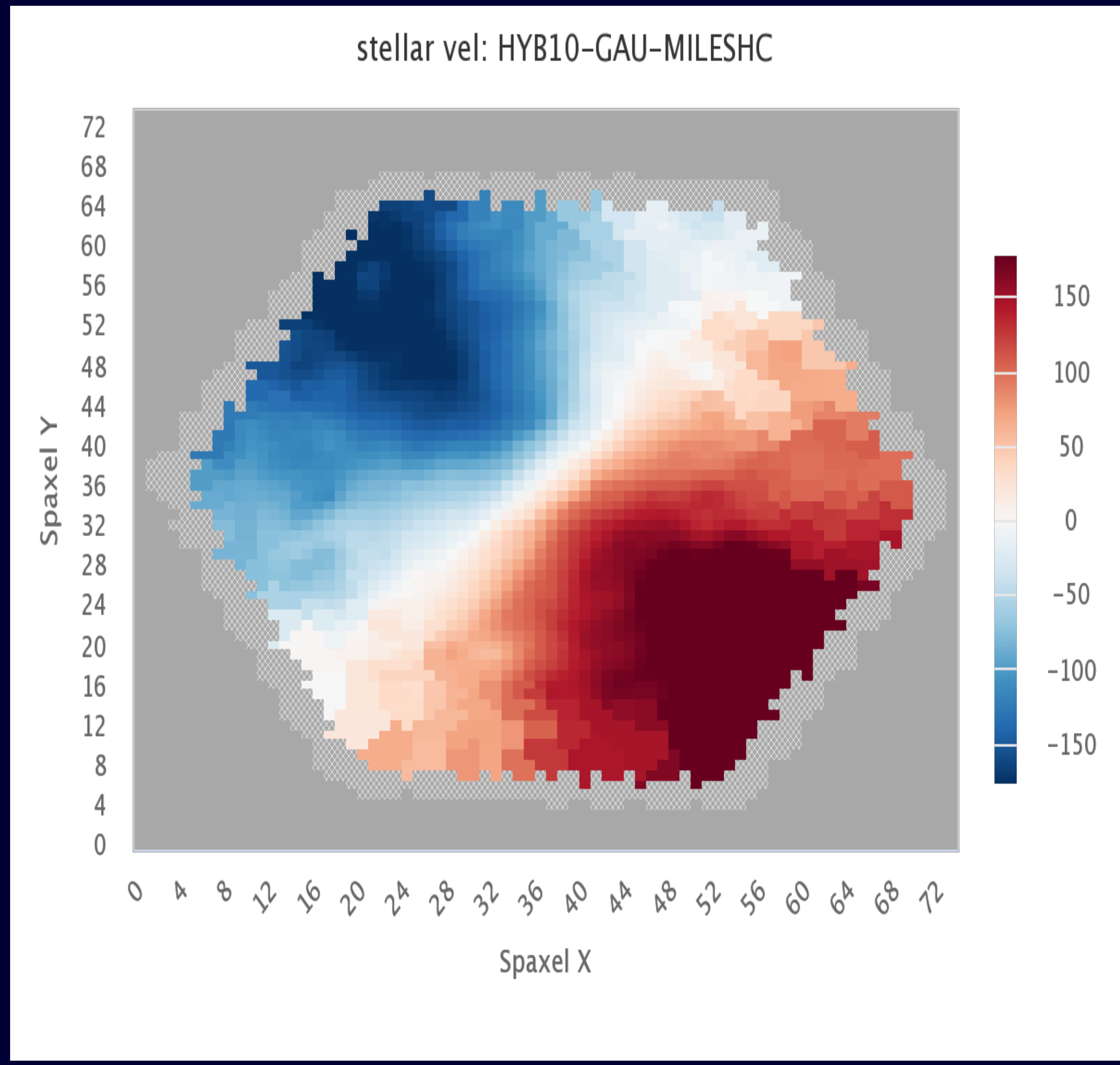

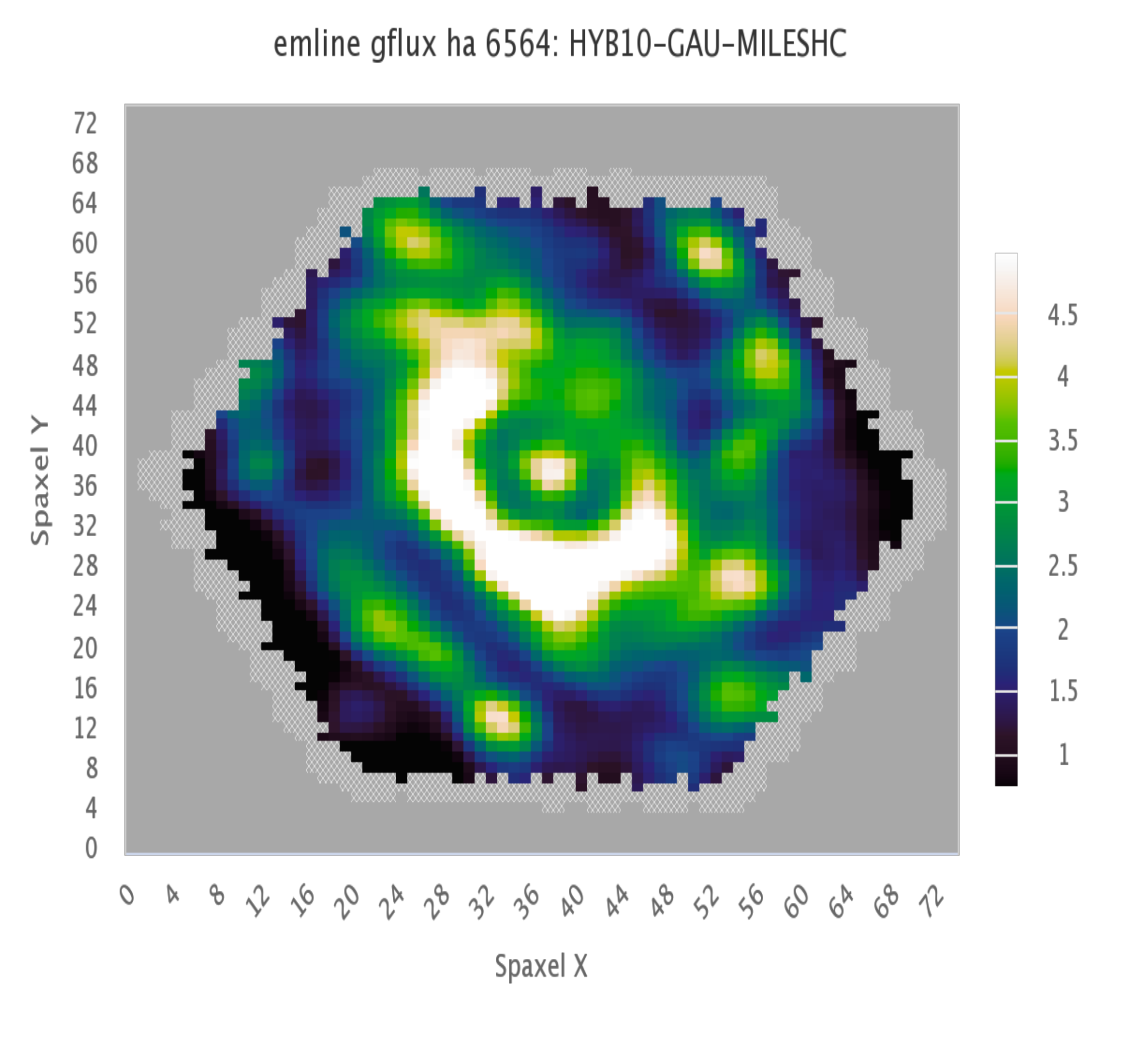

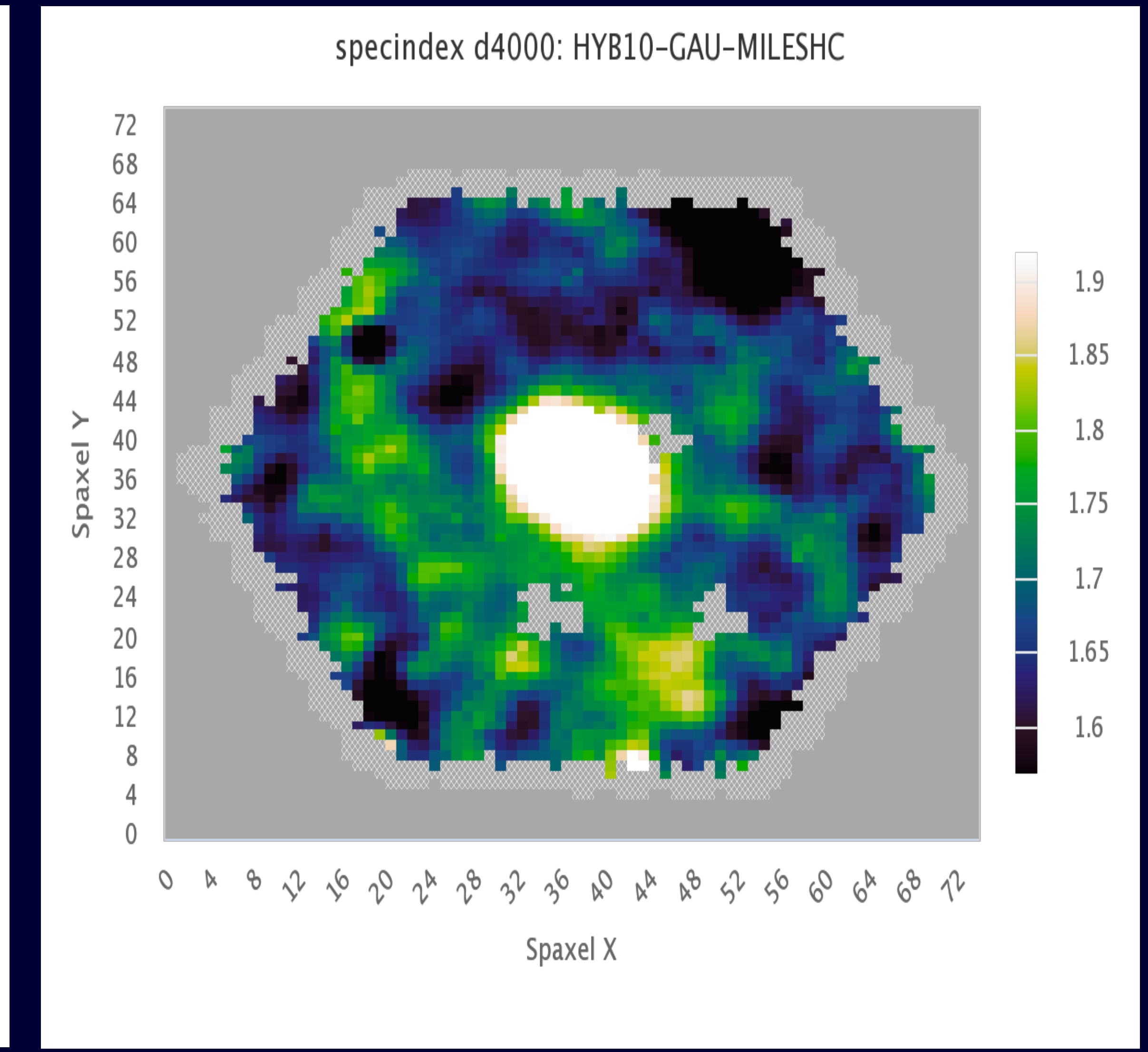

SDSS-IV/MaNGA
Mapping Nearby Galaxies at APO

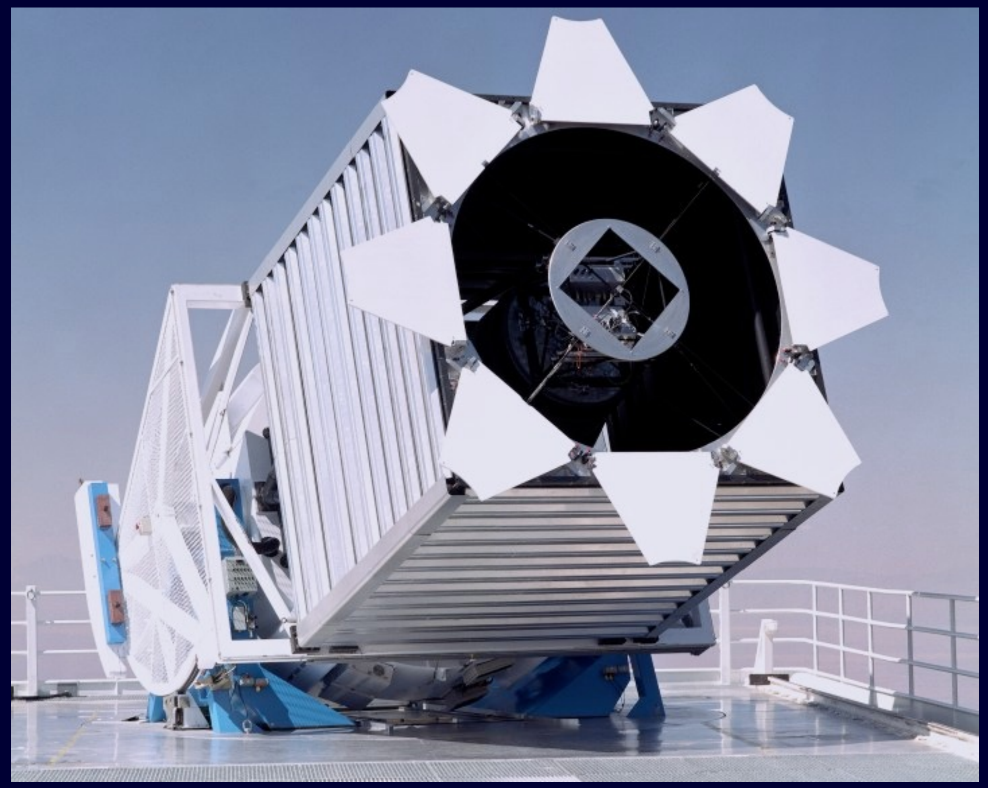

- Multi-object integral field spectroscopy survey of nearby galaxies.

- Spatial resolution: 2.5” (1-2kpc);
  Spectral resolution: 50-70 km/s (sigma), R~2000;
  Spectral coverage: 3,622-10,354A.

- Observations finished on Aug 24, 2020 !
  Final sample: 10,010 unique galaxies with high quality data.

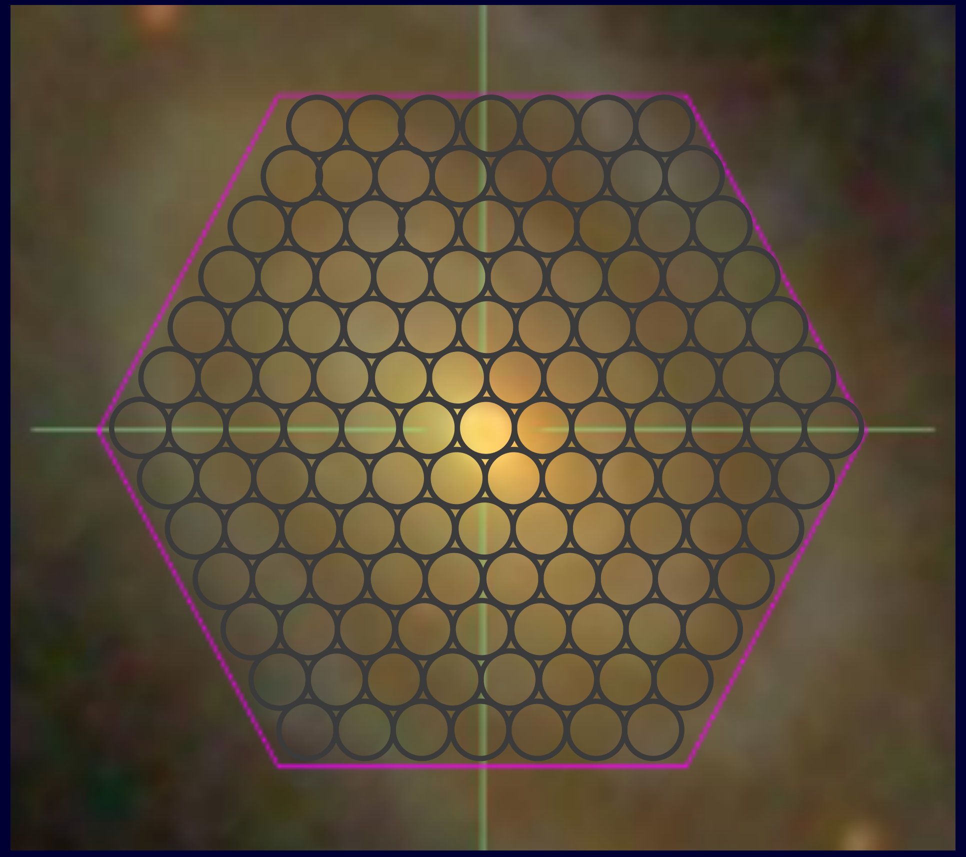

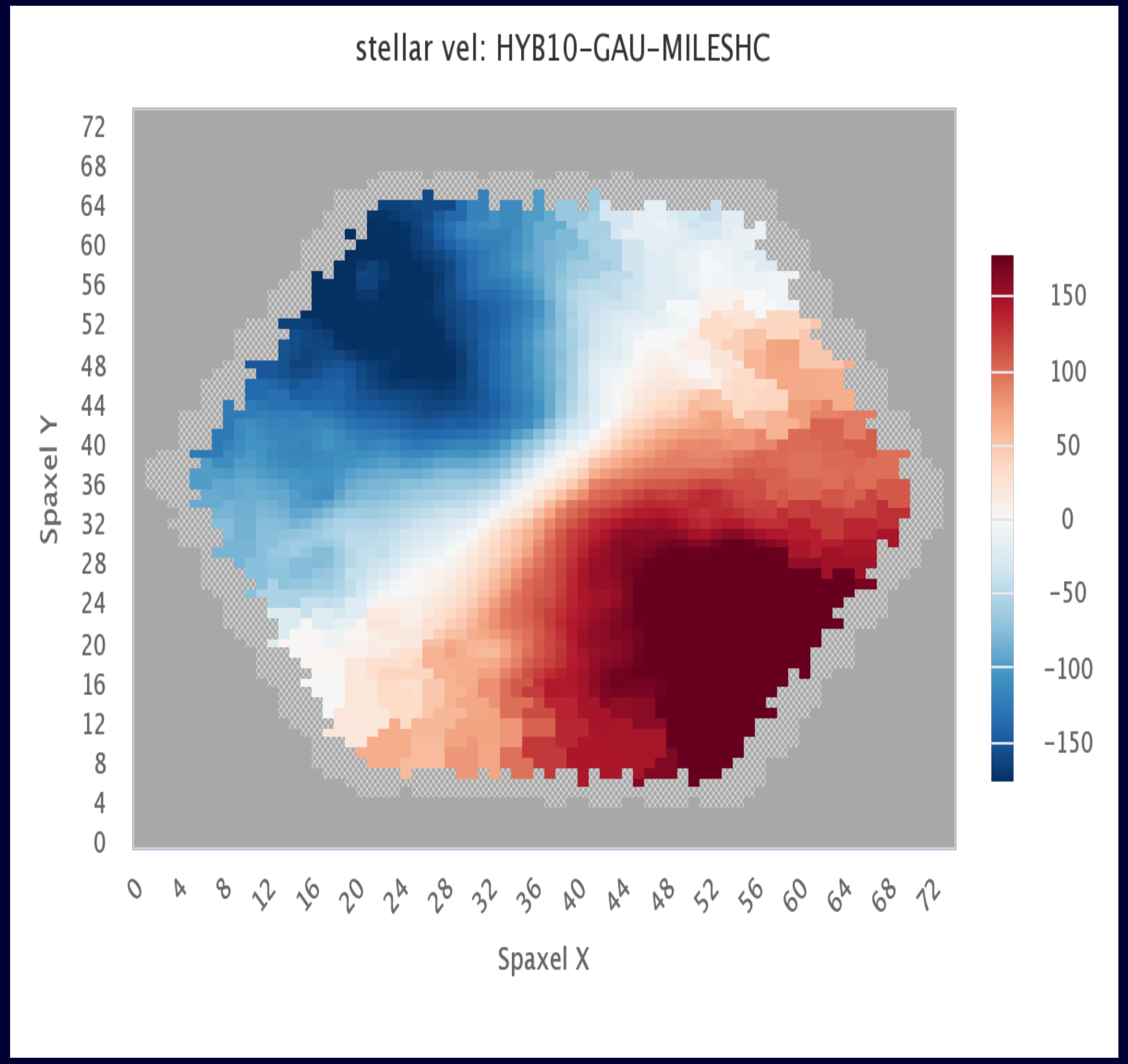

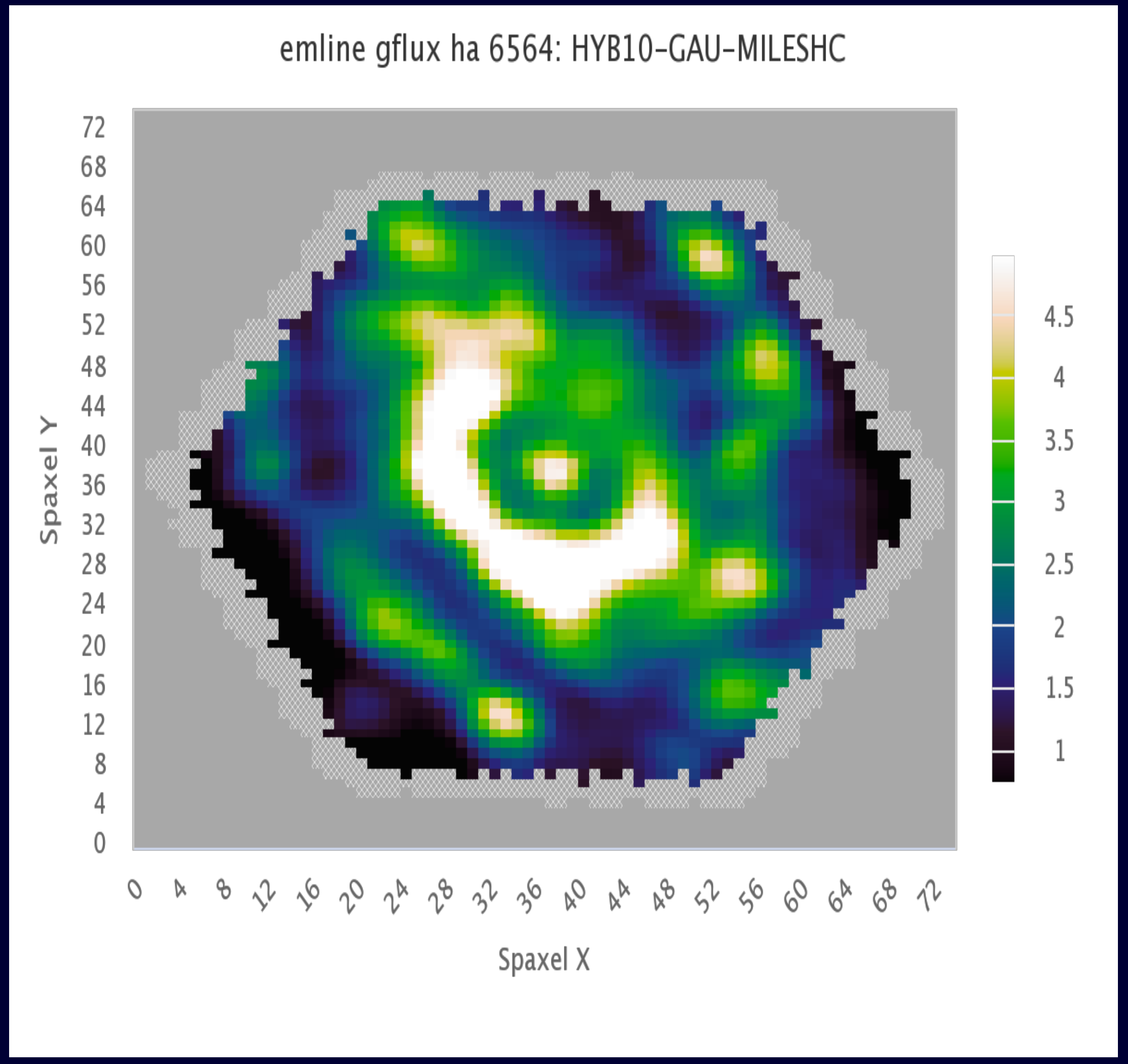

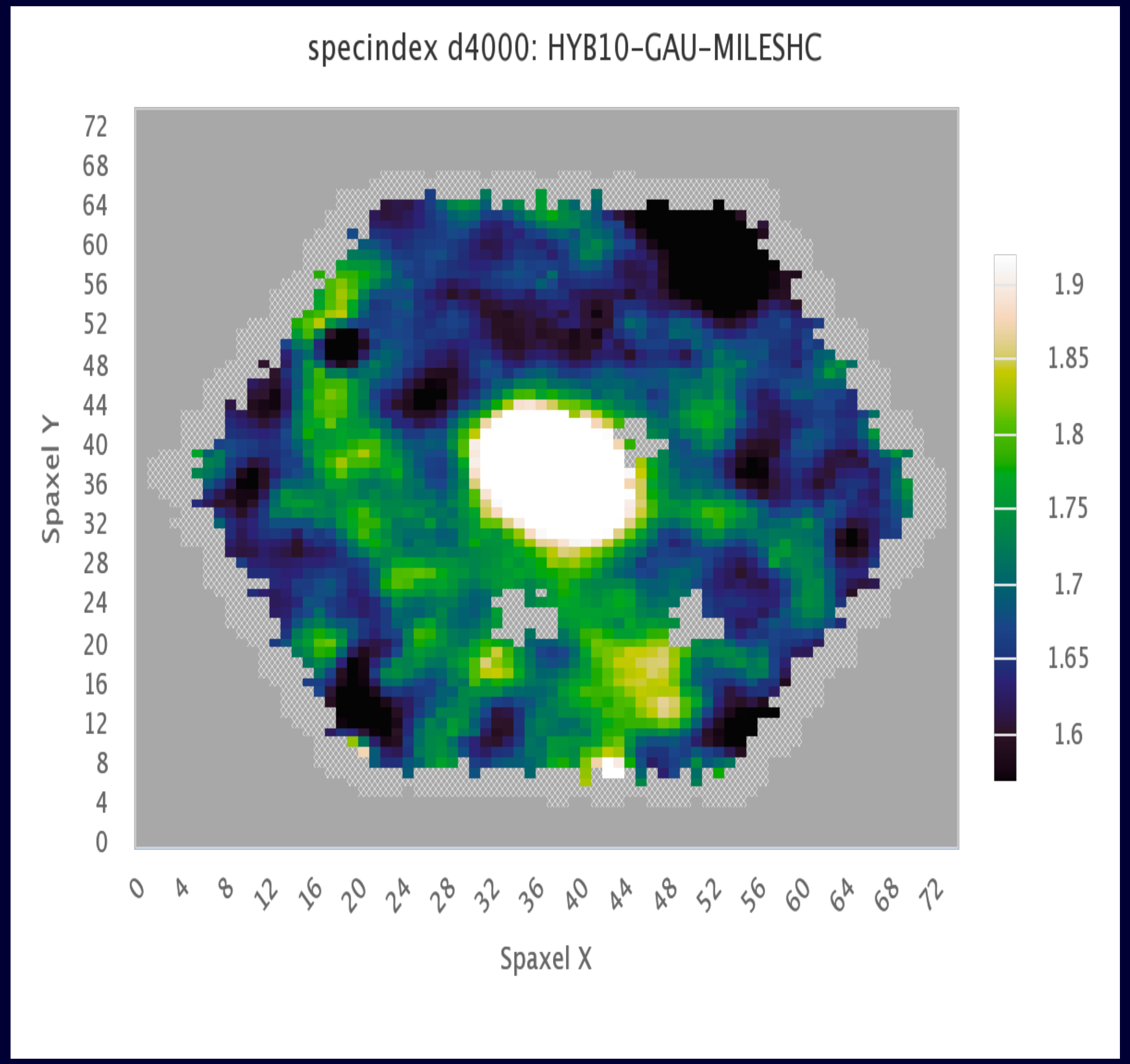

SDSS-IV/MaNGA
Mapping Nearby Galaxies at APO

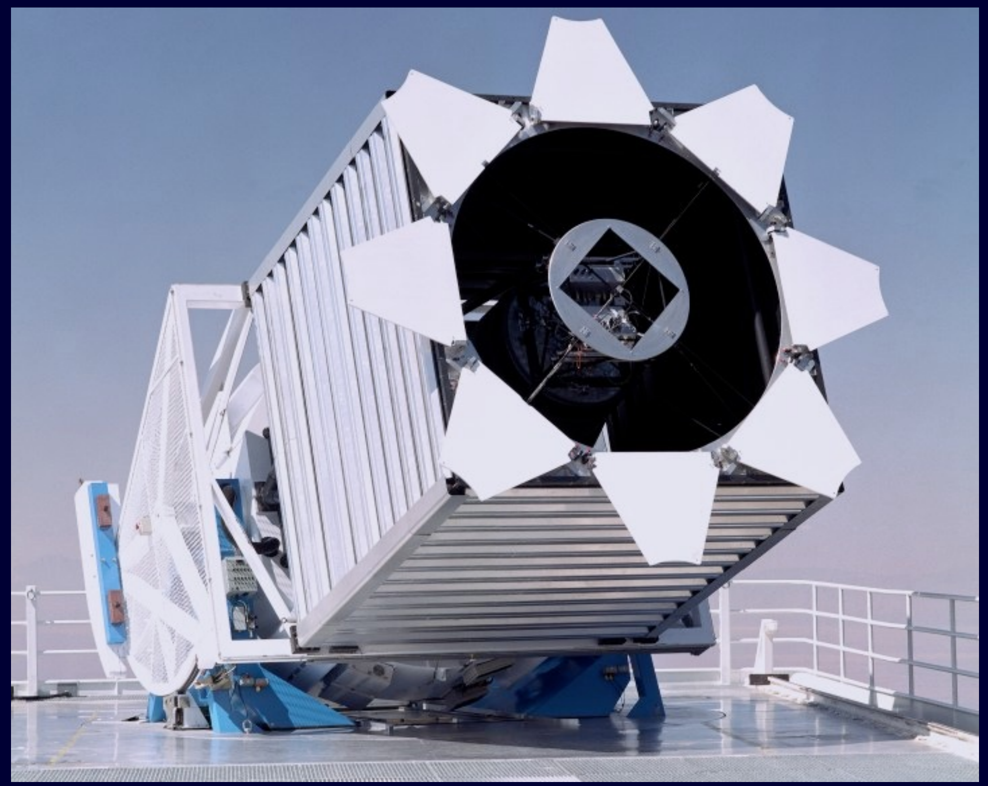

- Multi-object integral field spectroscopy survey of nearby galaxies.
- Spatial resolution: 2.5" (1-2kpc);
  Spectral resolution: 50-70 km/s (sigma), R~2000;
  Spectral coverage: 3,622-10,354A.
- Observations finished on Aug 24, 2020 !
  Final sample: 10,010 unique galaxies with high quality data.

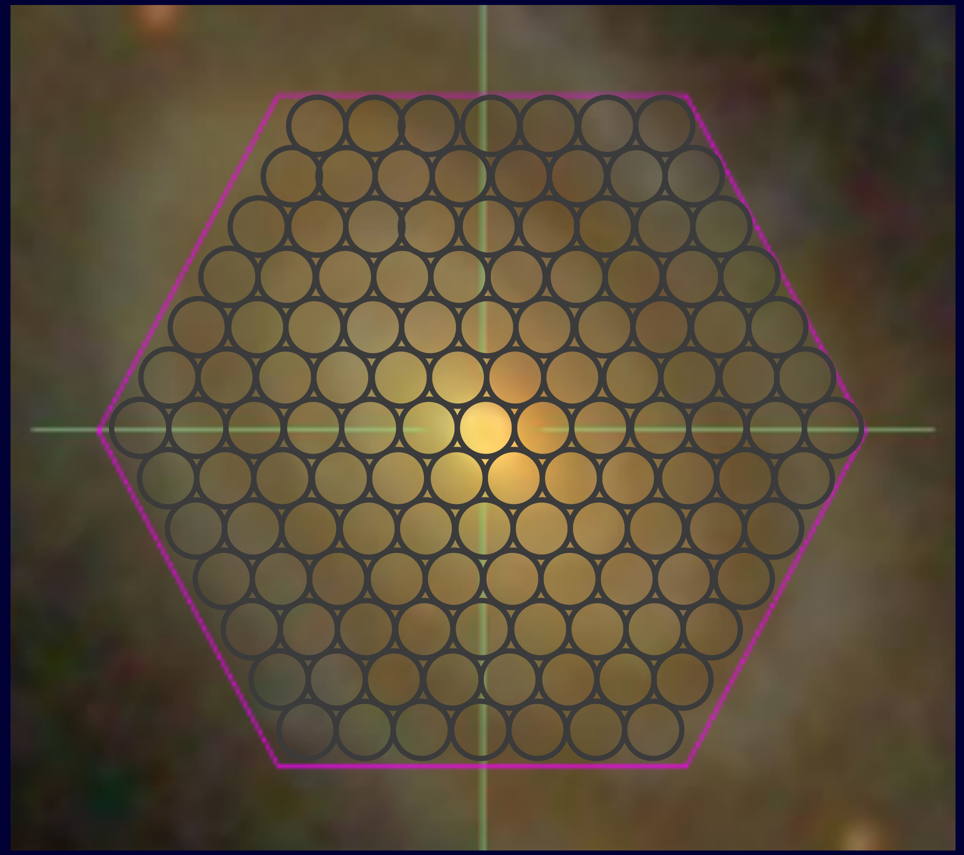

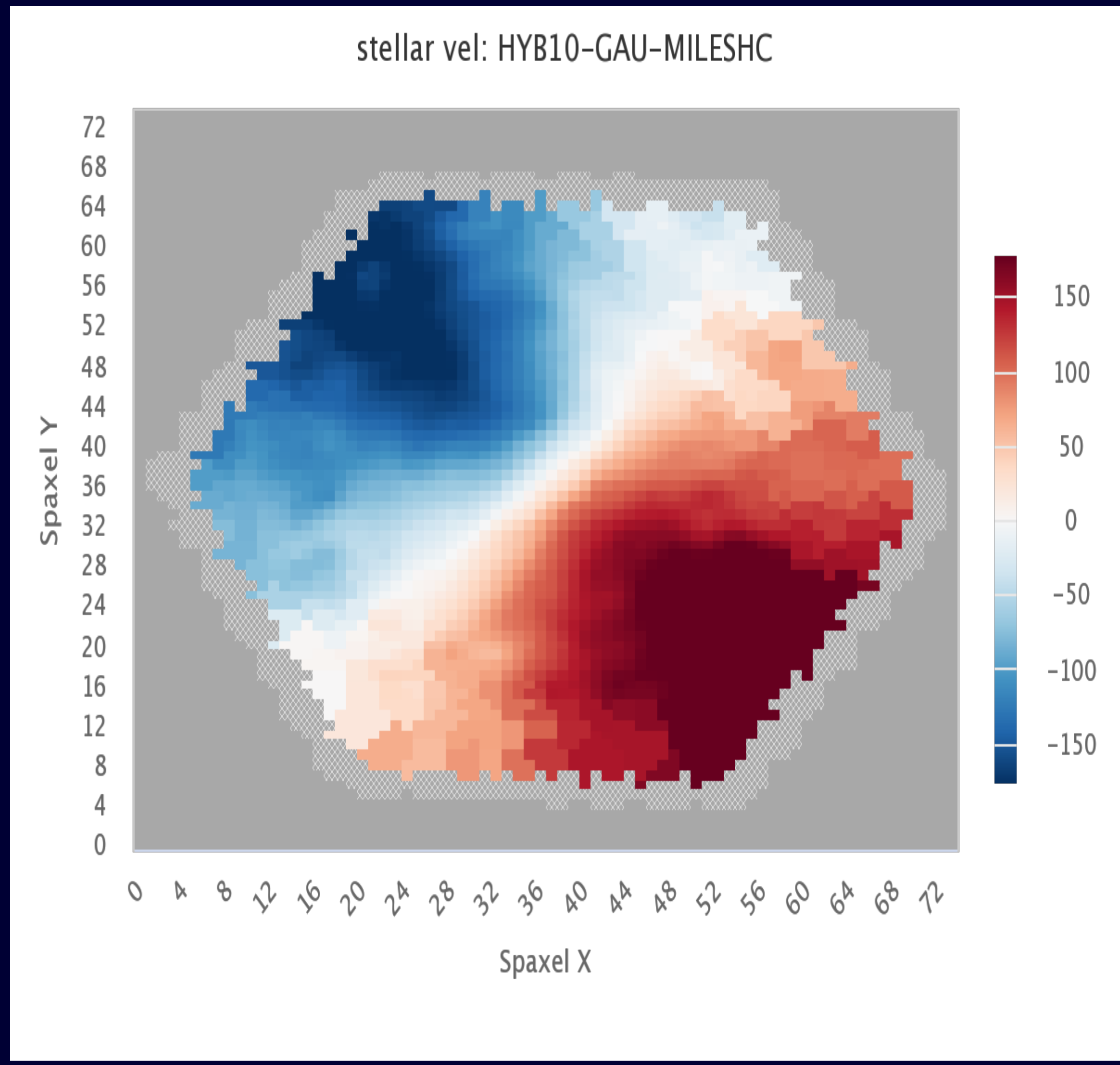

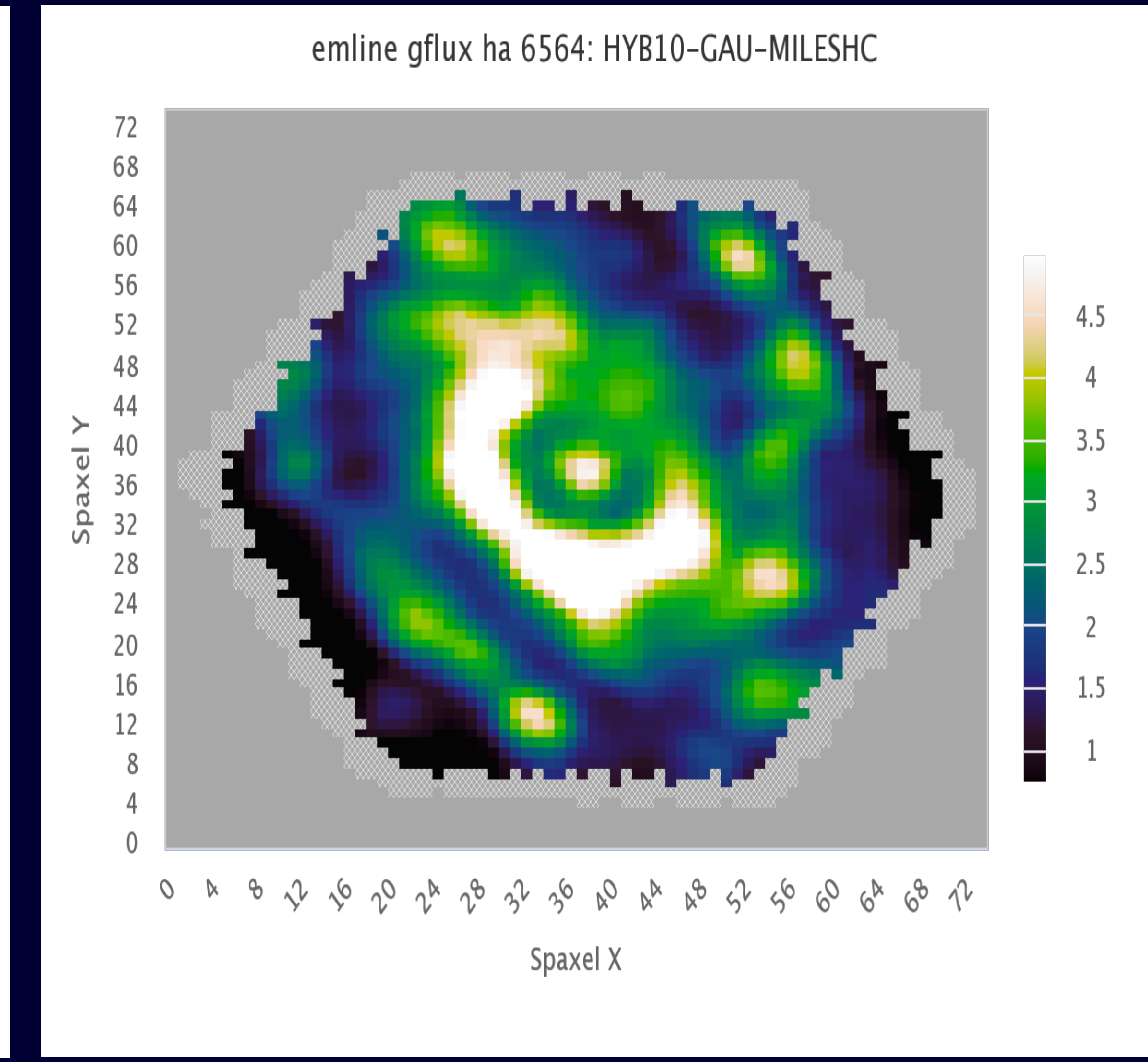

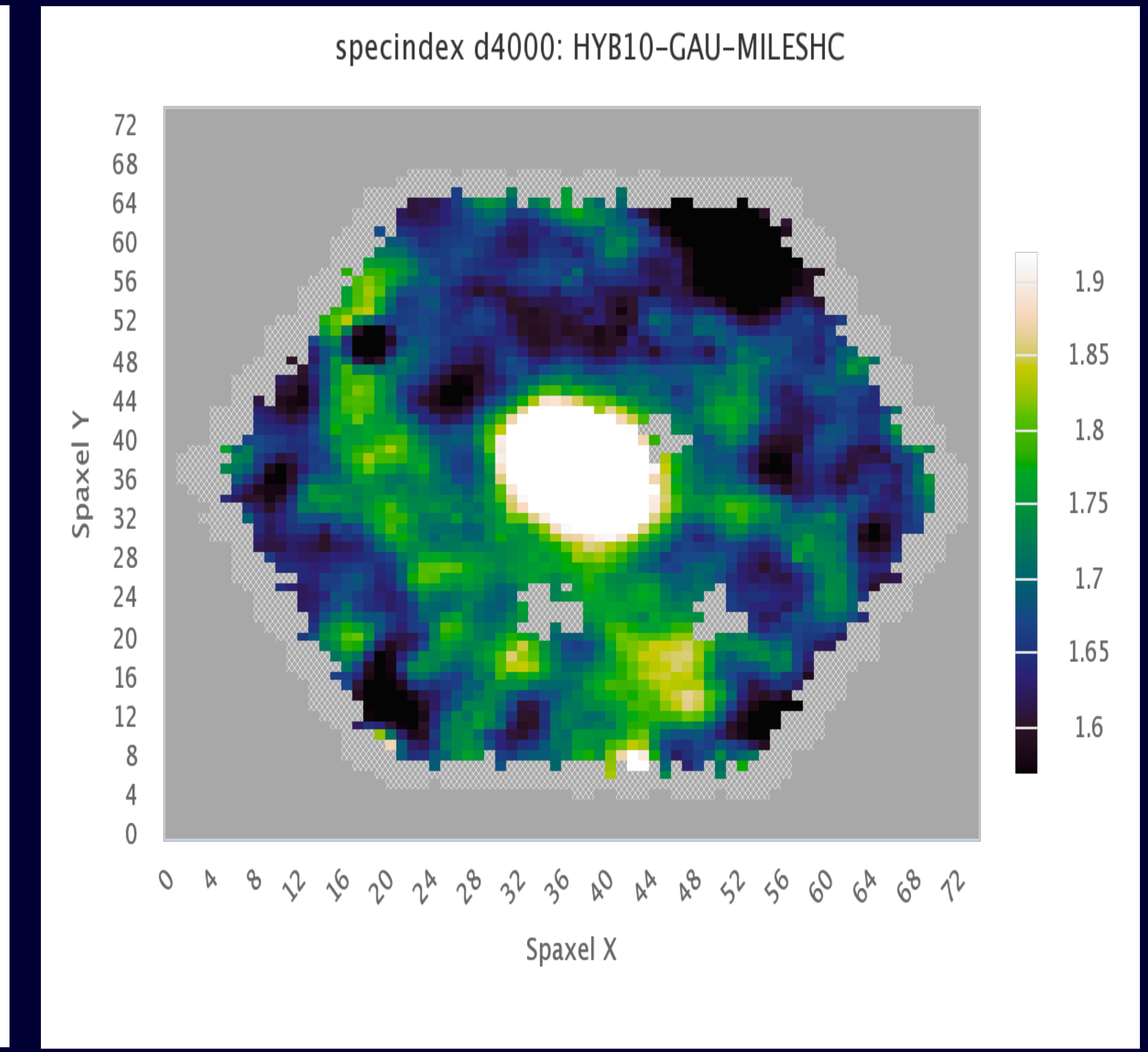

- MPL-11 in Jan/Feb 2021
- DR17 in Dec 2021.

MaNGA Stellar Library (MaStar)

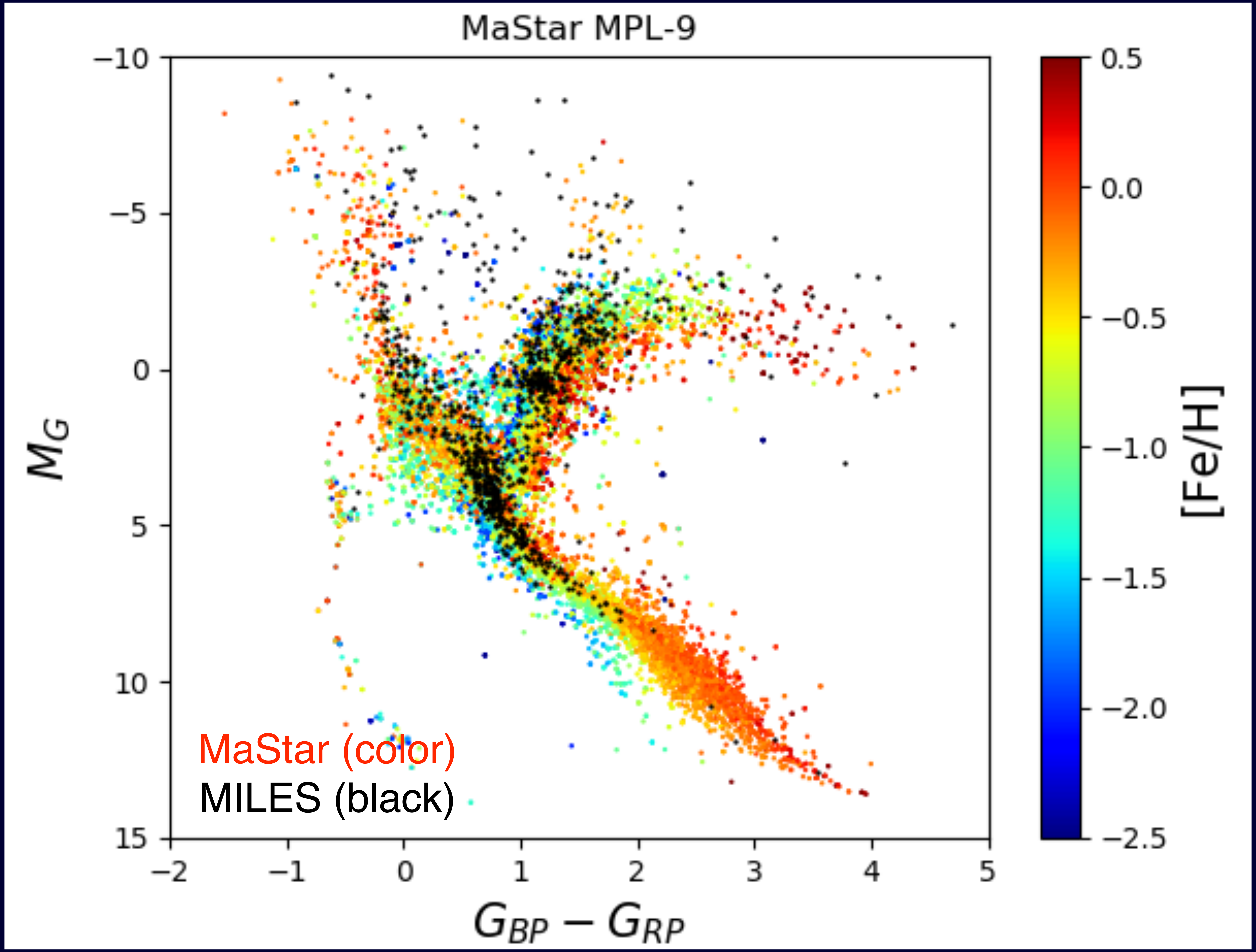

- >13,000 stars with >31,000 good quality visits
- Comprehensive parameter coverage
- High S/N: median S/N per pixel ~106

Why is star formation so inefficient?

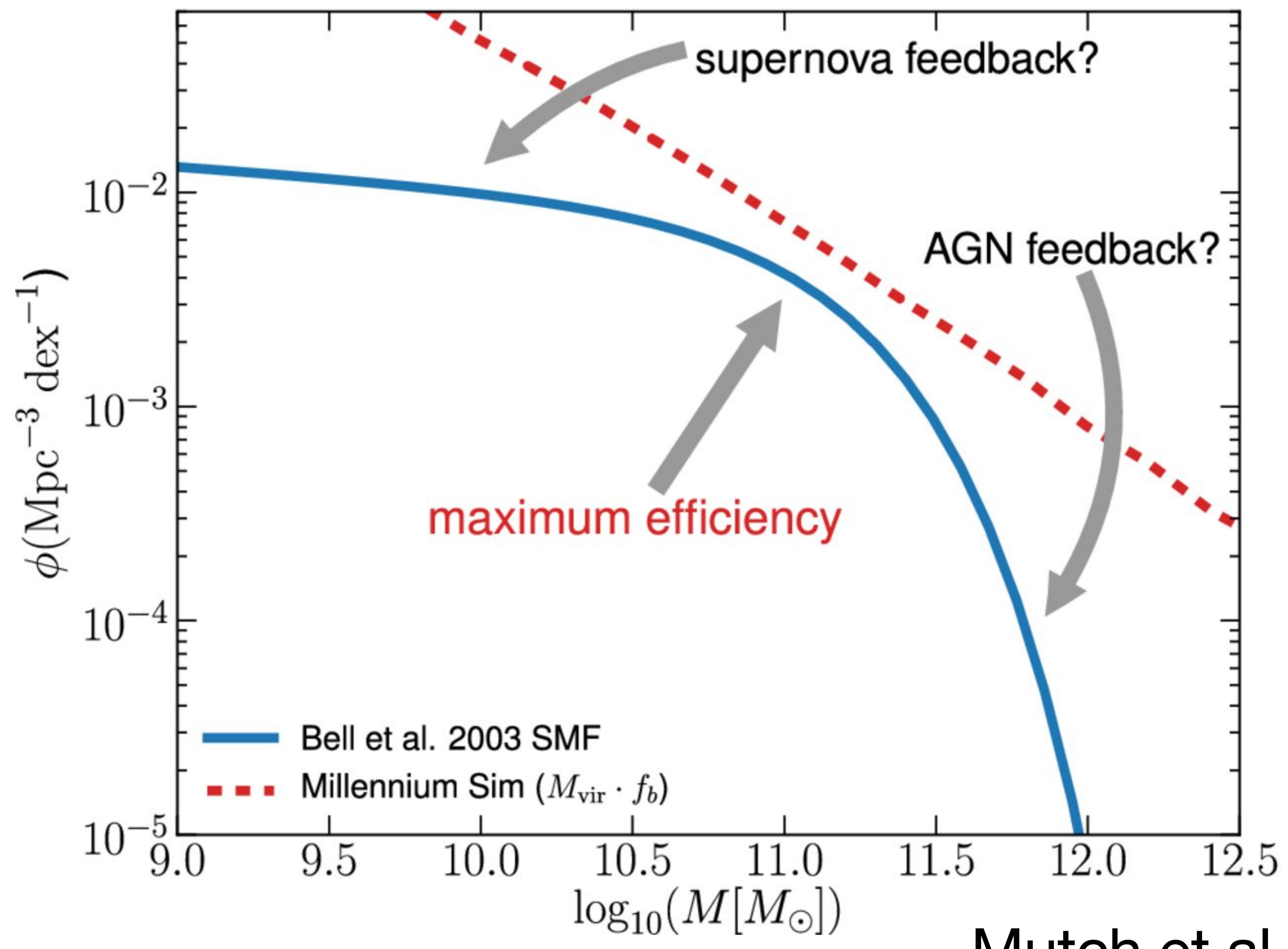

Mutch et al. (2013)

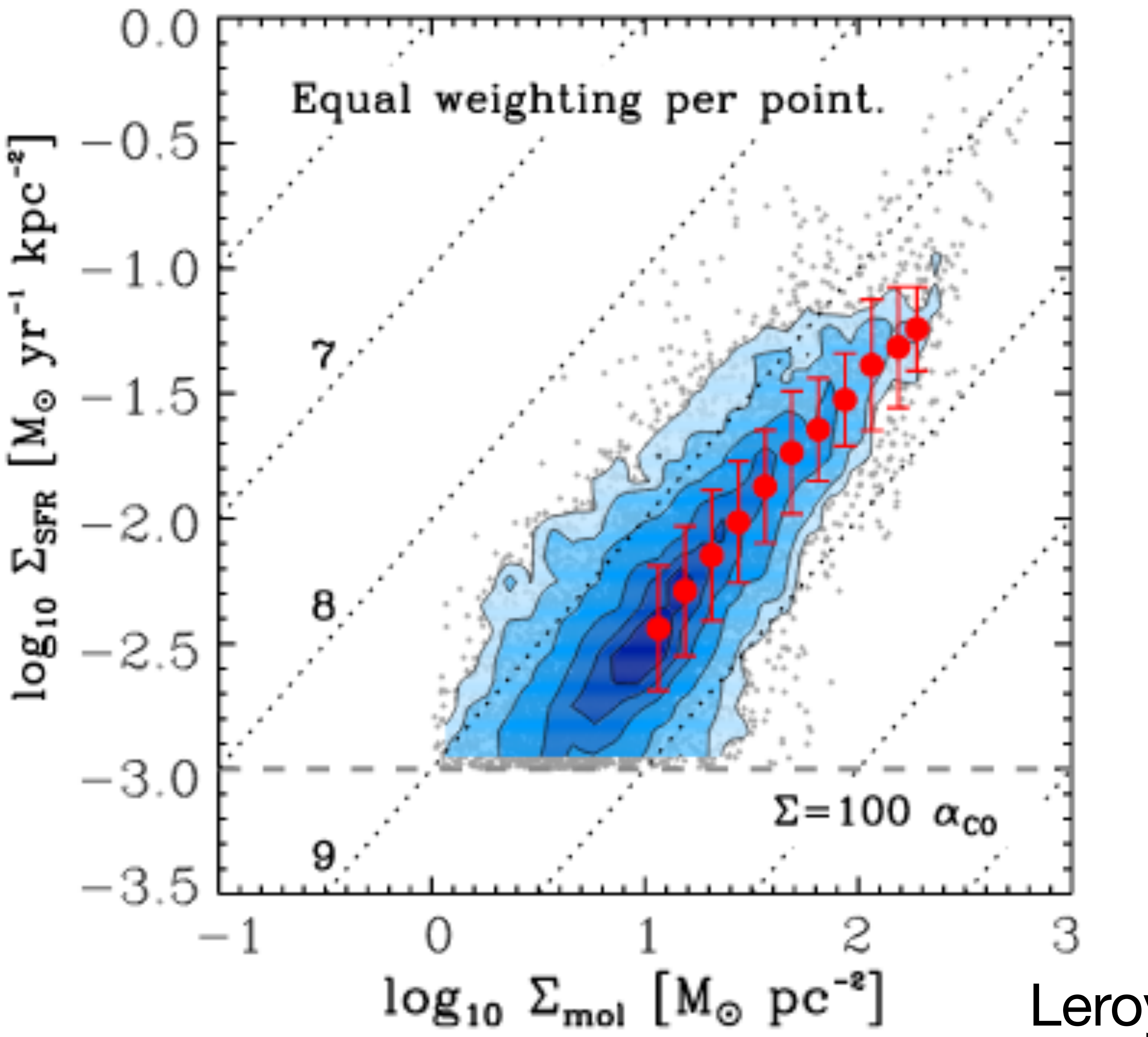

Leroy et al. (2013)

- Both low and high mass galaxies are inefficient at turning baryons to stars.
- Molecular gas depletion time is 100-1000 times longer than the free-fall time of a giant molecular cloud.

Importance of studying the ISM

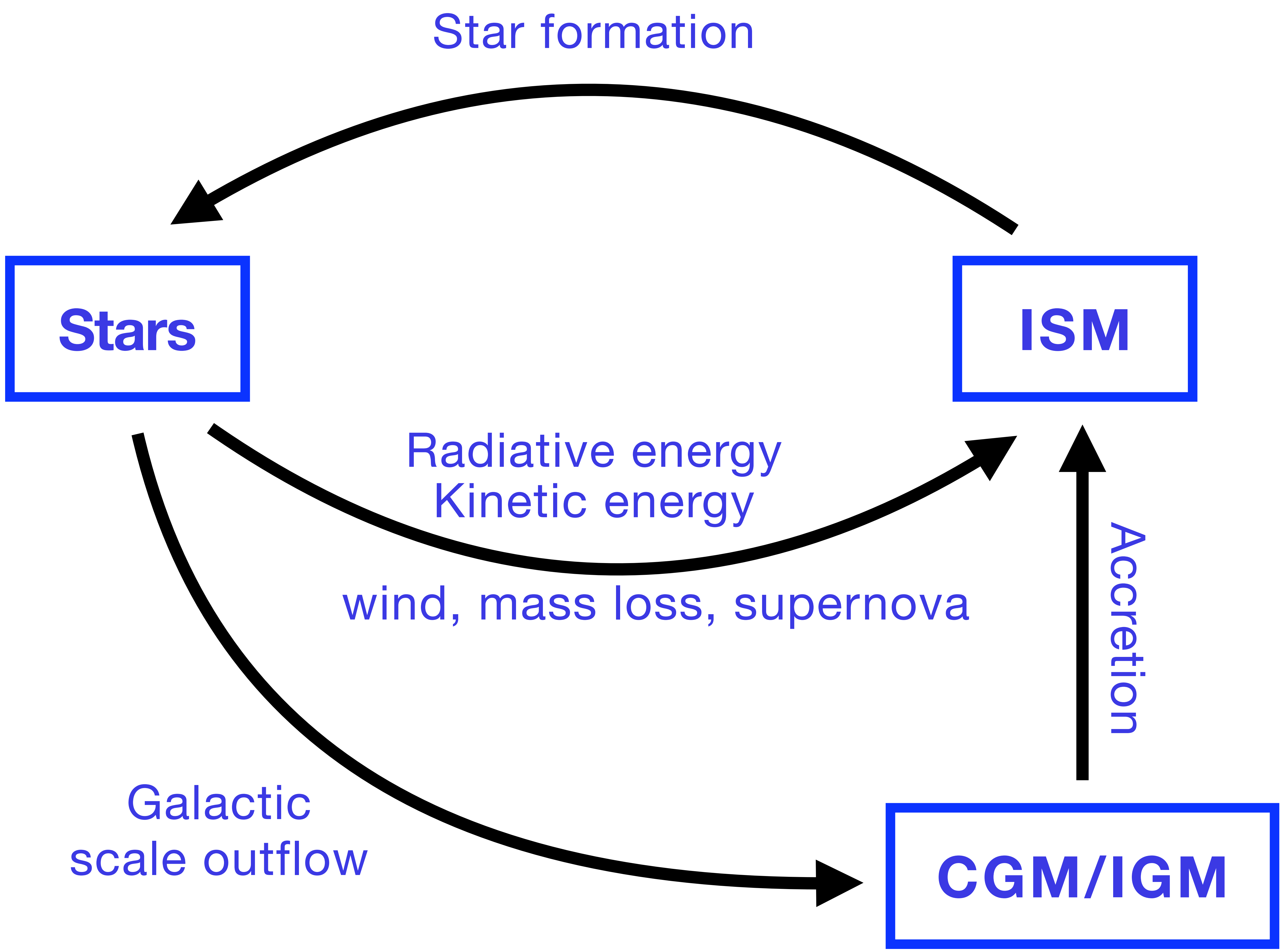

Importance of studying the ISM

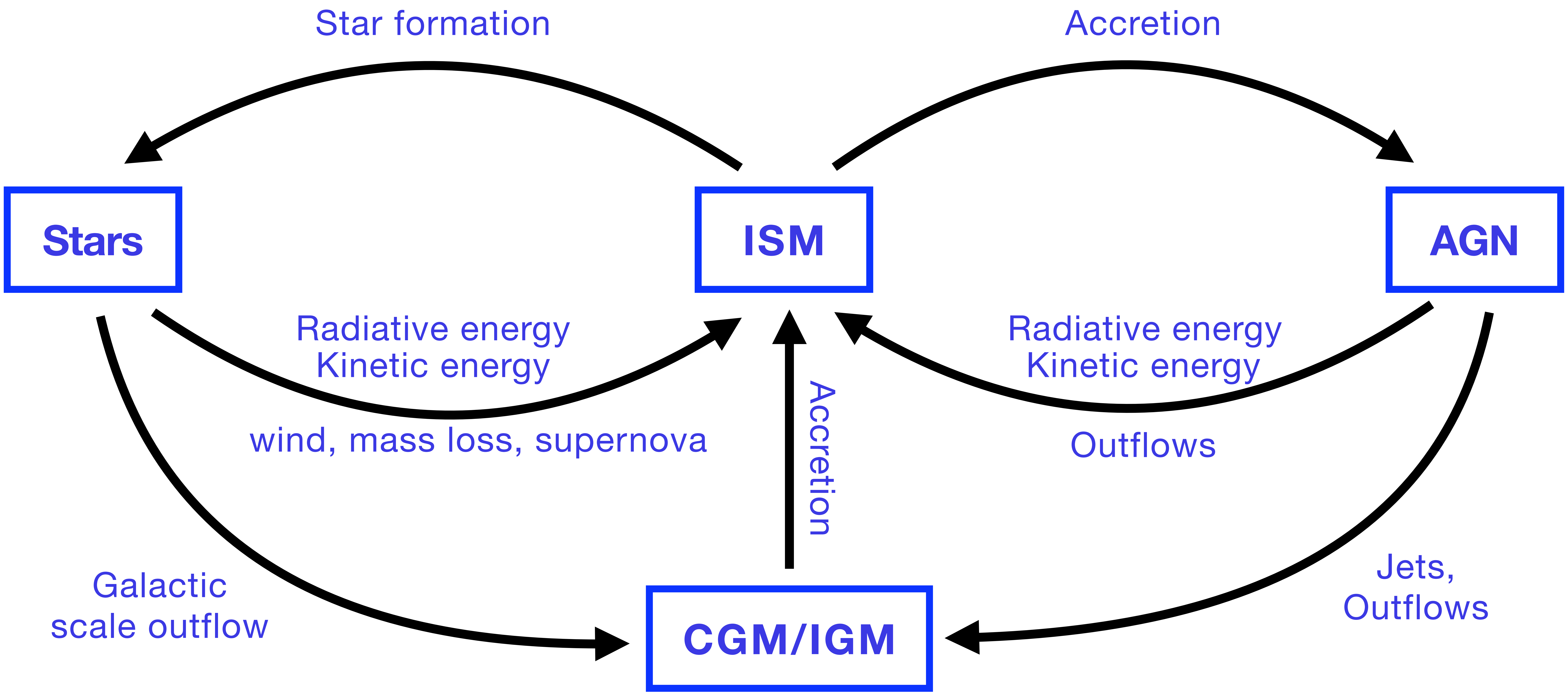

Warm Ionized Gas

http://www.astro.wisc.edu/wham-site/

WHAM

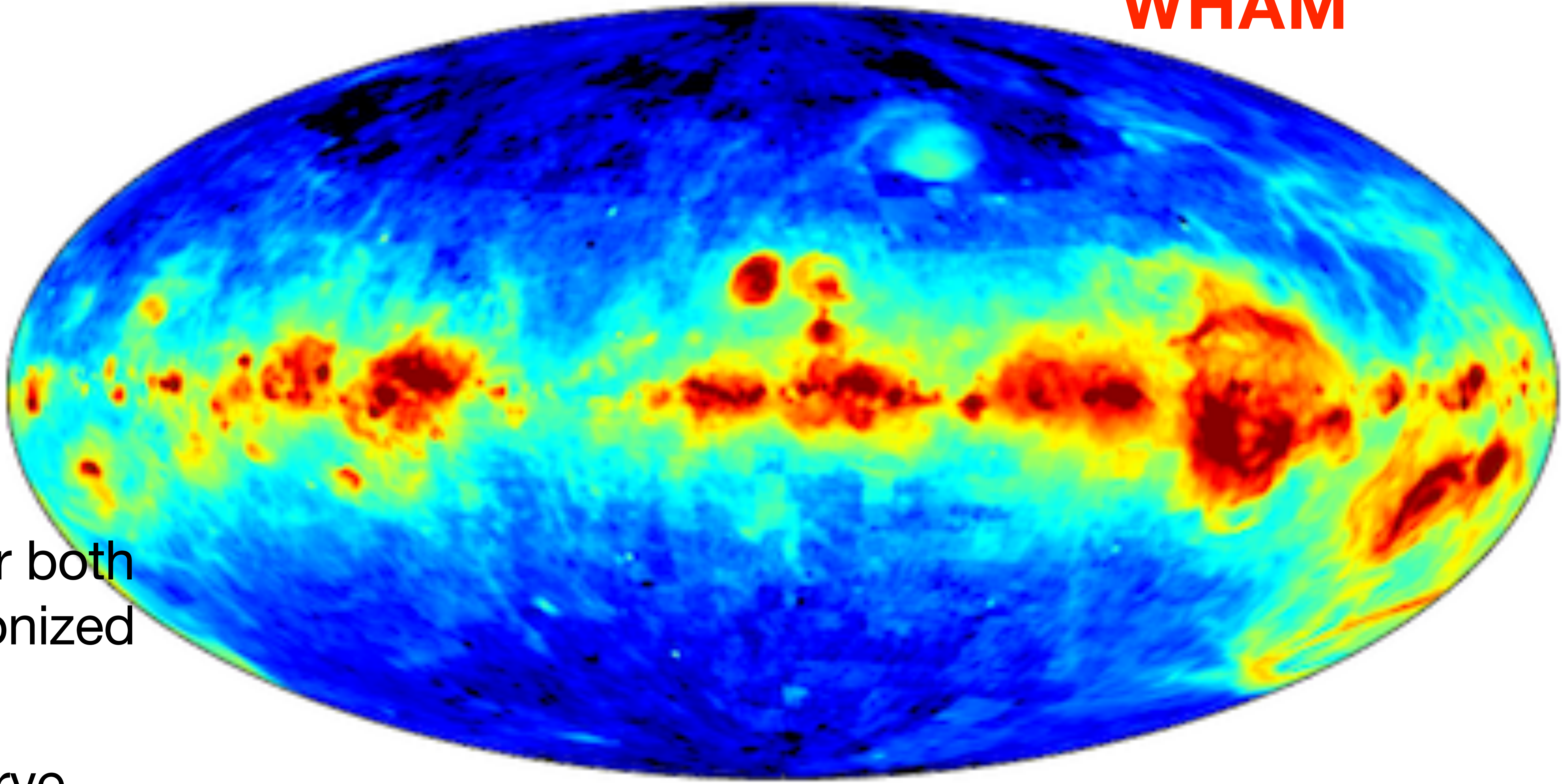

- A stable phase of the ISM under both photoionized and collisionally-ionized conditions
- Near the peak of the cooling curve
- Relatively easy to observe through optical spectroscopy
- Well-developed line ratio diagnostics

However,
mysteries and discrepancies abound!

Two classes of commonly-found, but poorly-understood warm ionized gas

Two classes of commonly-found, but poorly-understood warm ionized gas

- **Diffuse Ionized Gas (DIG) in star-forming disk galaxies**
  - responsible for 50% of the Halpha emission (Oey+2007)

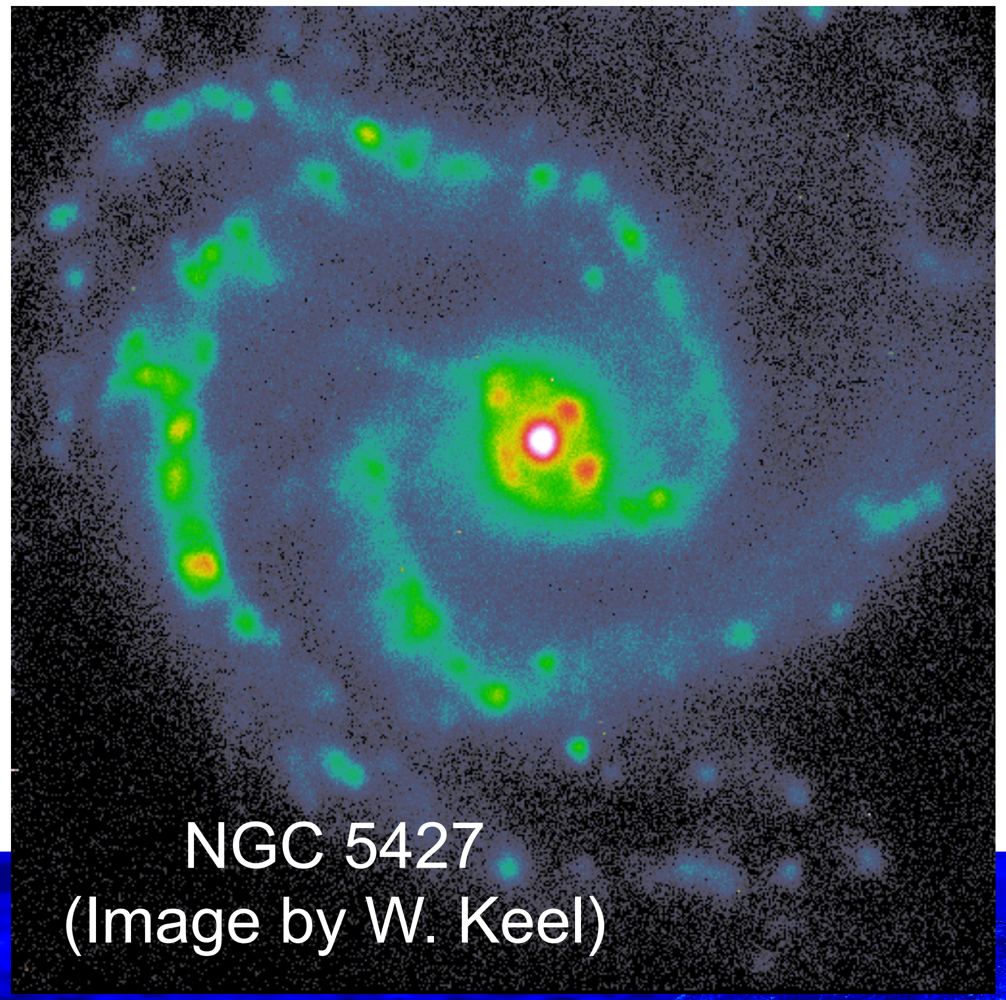

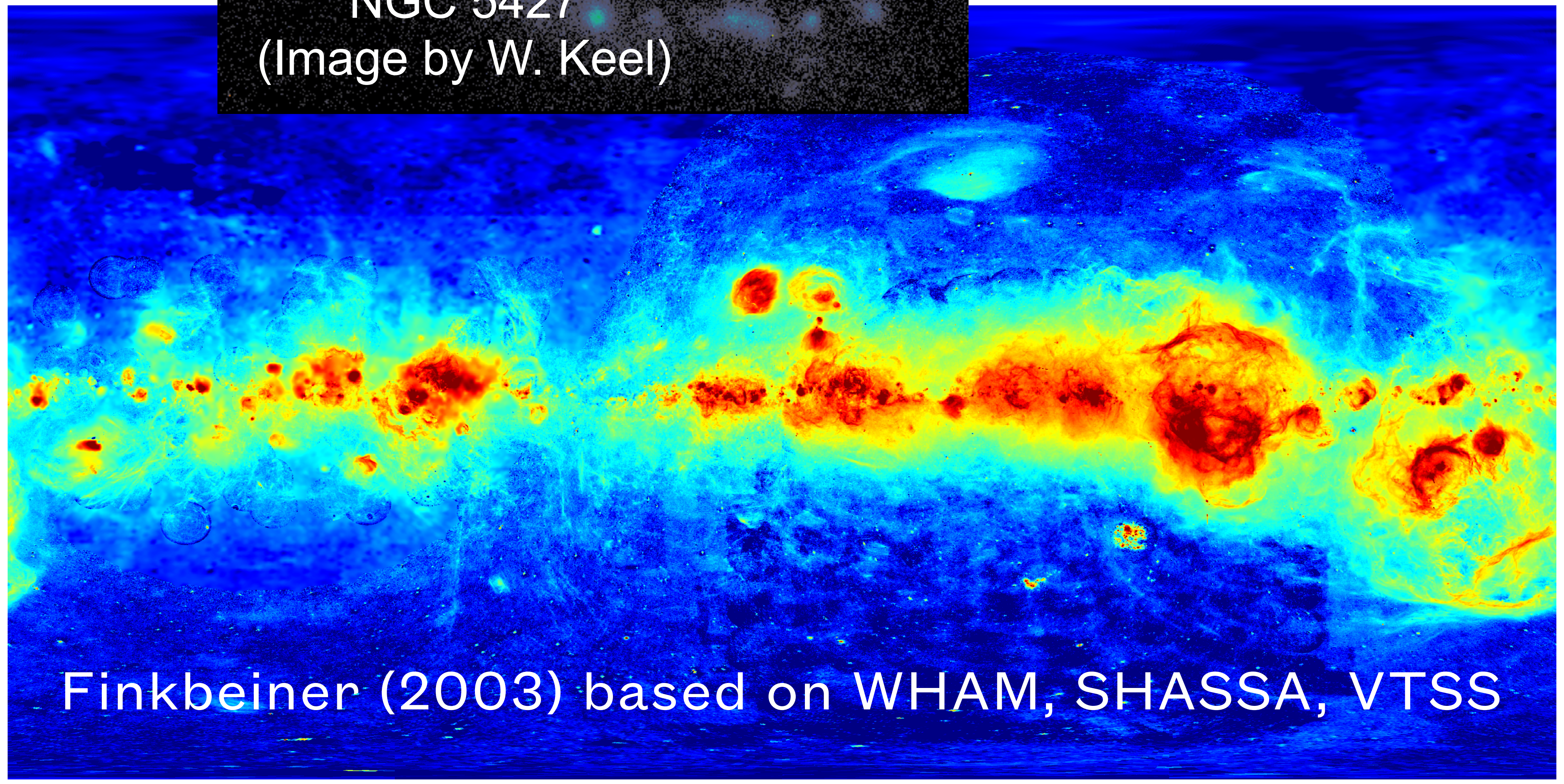

Two classes of commonly-found, but poorly-understood warm ionized gas

- **Diffuse Ionized Gas (DIG) in star-forming disk galaxies**
  - responsible for 50% of the Halpha emission (Oey+2007)
- **Low ionization gas in elliptical and lenticular galaxies (LINER-like, LIER)**
  - detected in more than 70% of early-type galaxies (Sarzi+06)

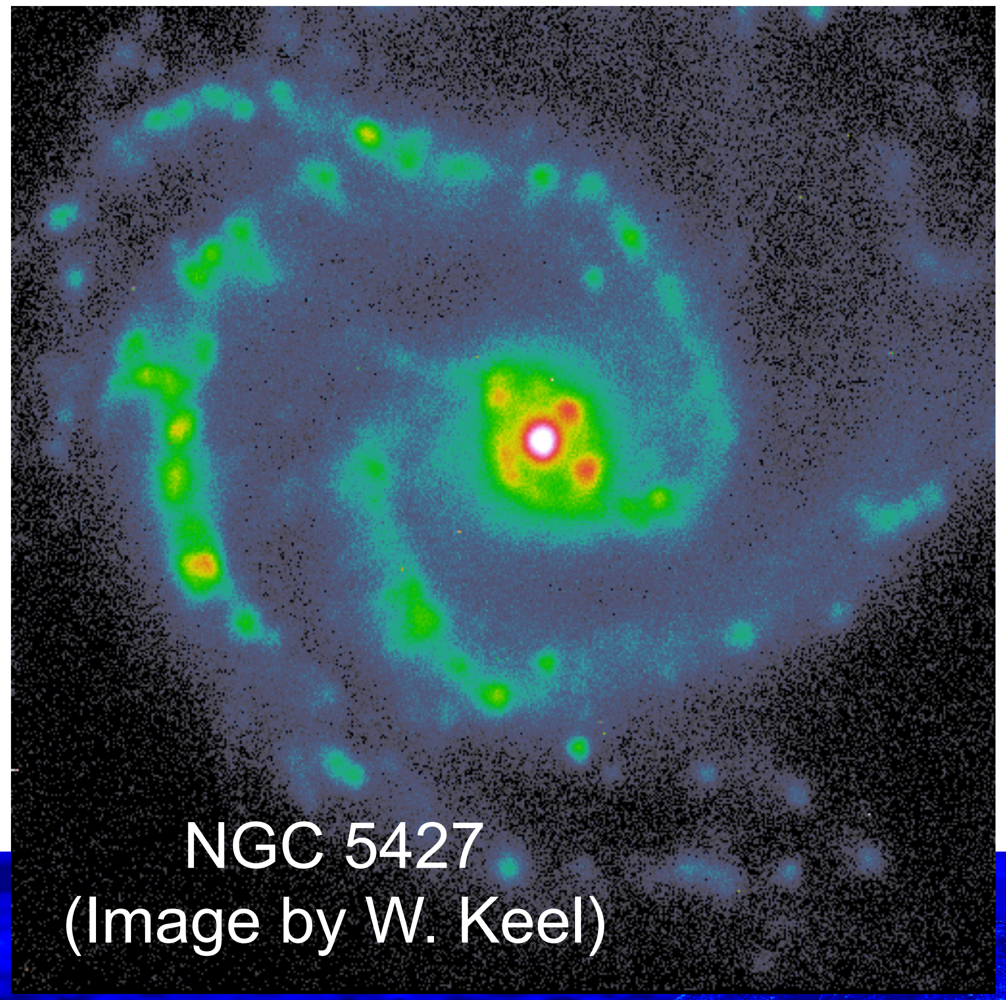

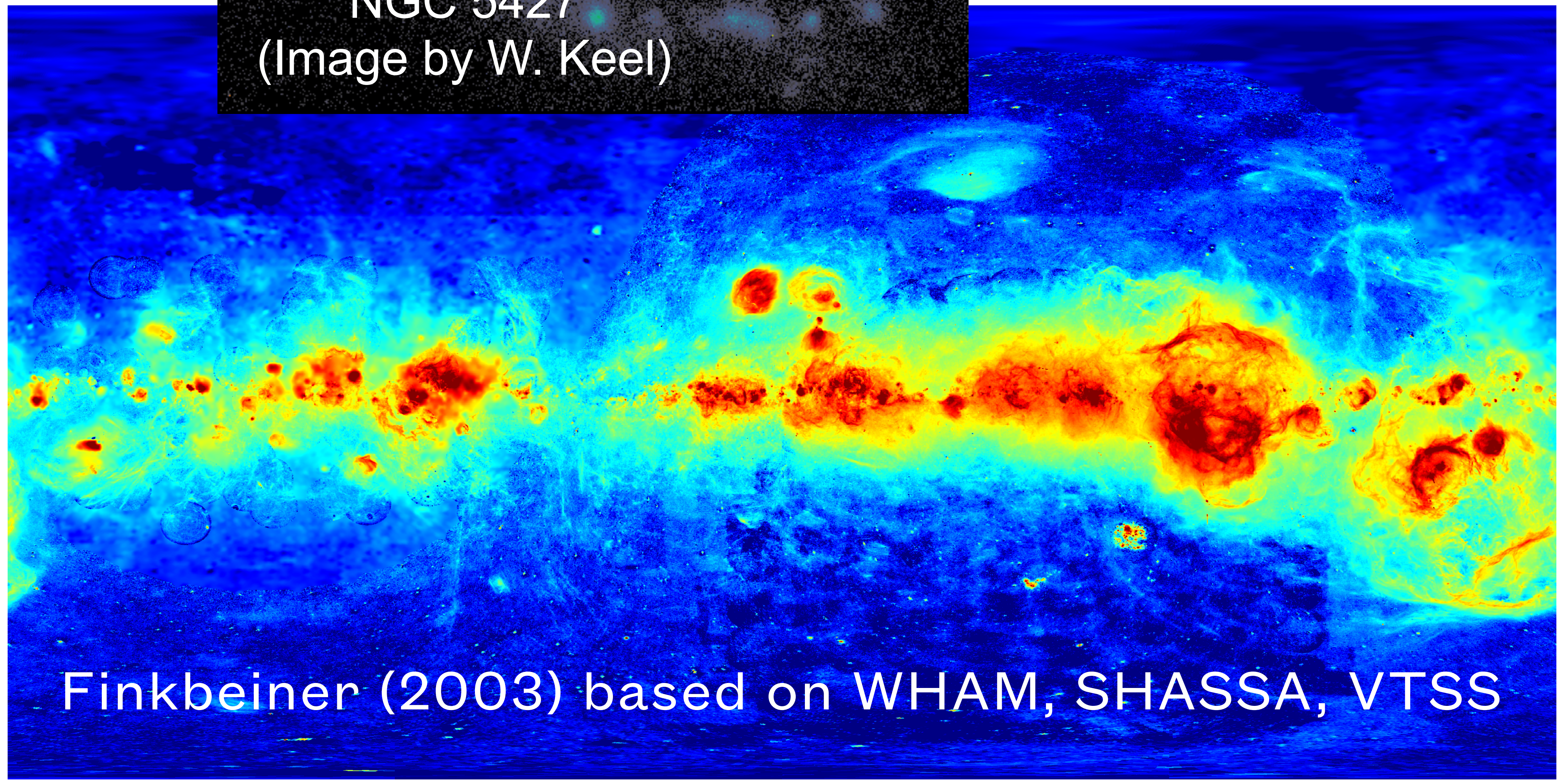

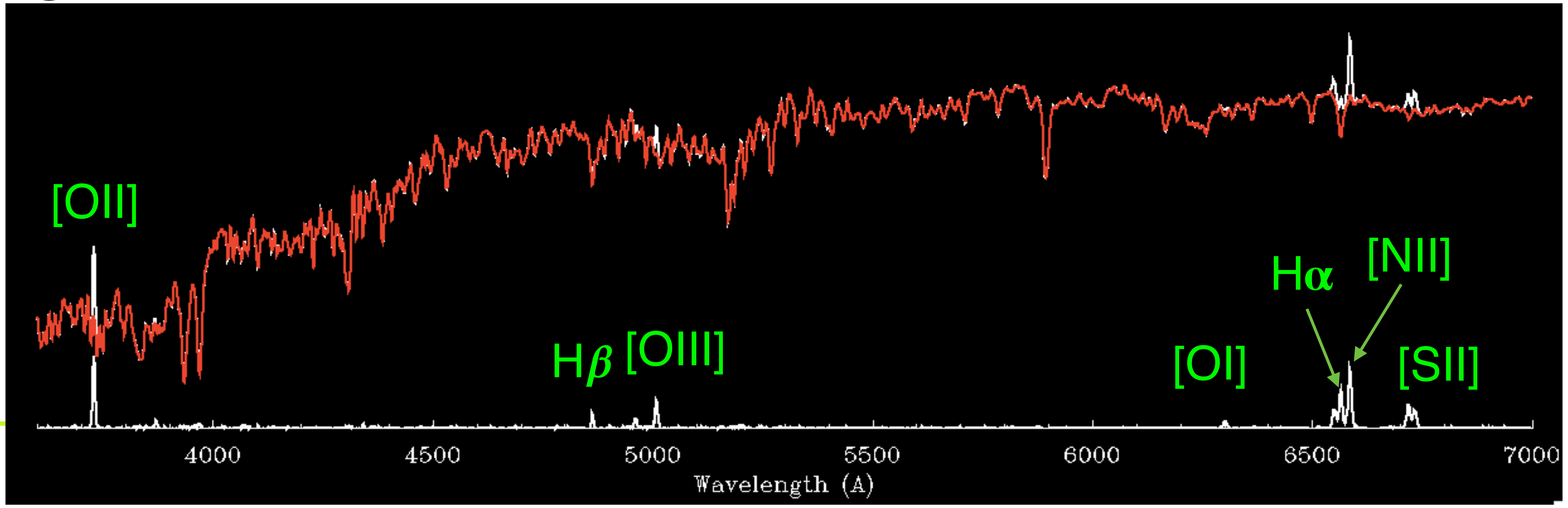

Two classes of commonly-found, but poorly-understood warm ionized gas

- **Diffuse Ionized Gas (DIG) in star-forming disk galaxies**
  - responsible for 50% of the Halpha emission (Oey+2007)
- **Low ionization gas in elliptical and lenticular galaxies (LINER-like, LIER)**
  - detected in more than 70% of early-type galaxies (Sarzi+06)

(Yan et al. 2006, 2012, 2018a, b, Belfiore et al. 2016, Cheung et al. 2016, Roy et al. 2018 & in prep)

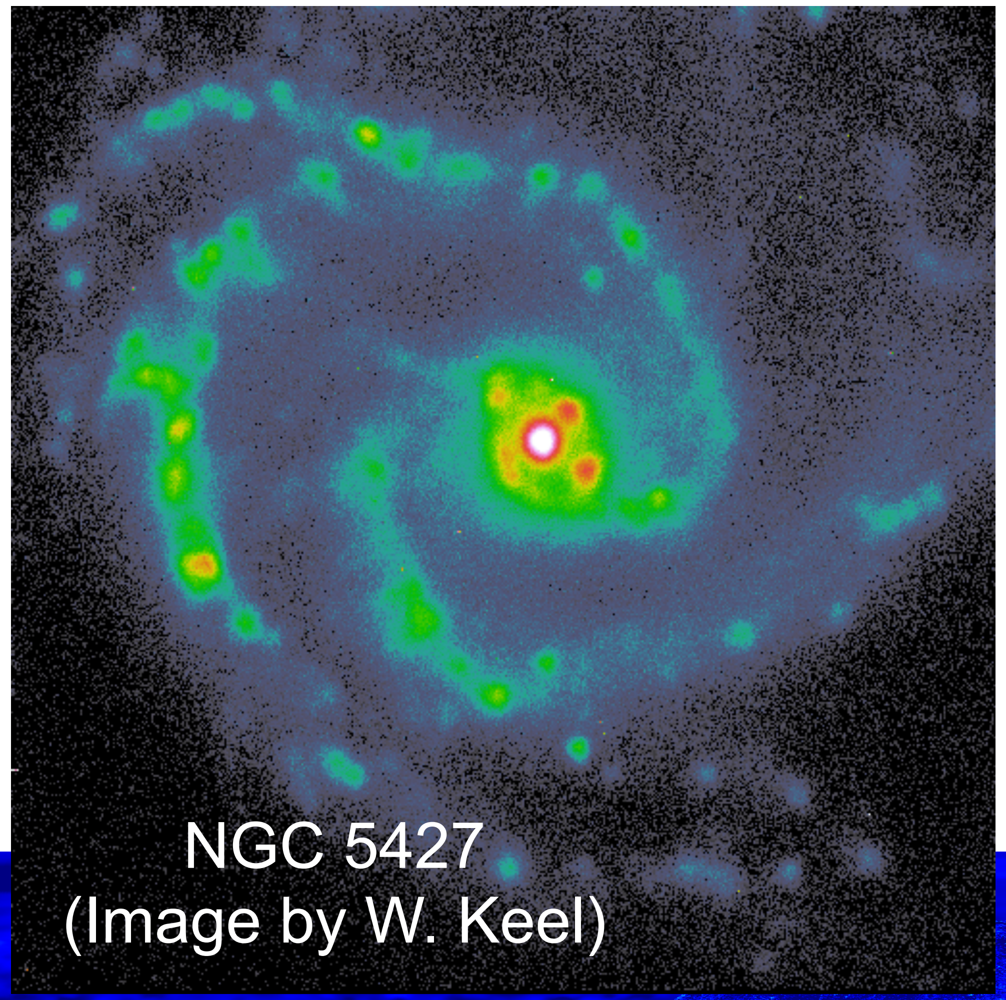

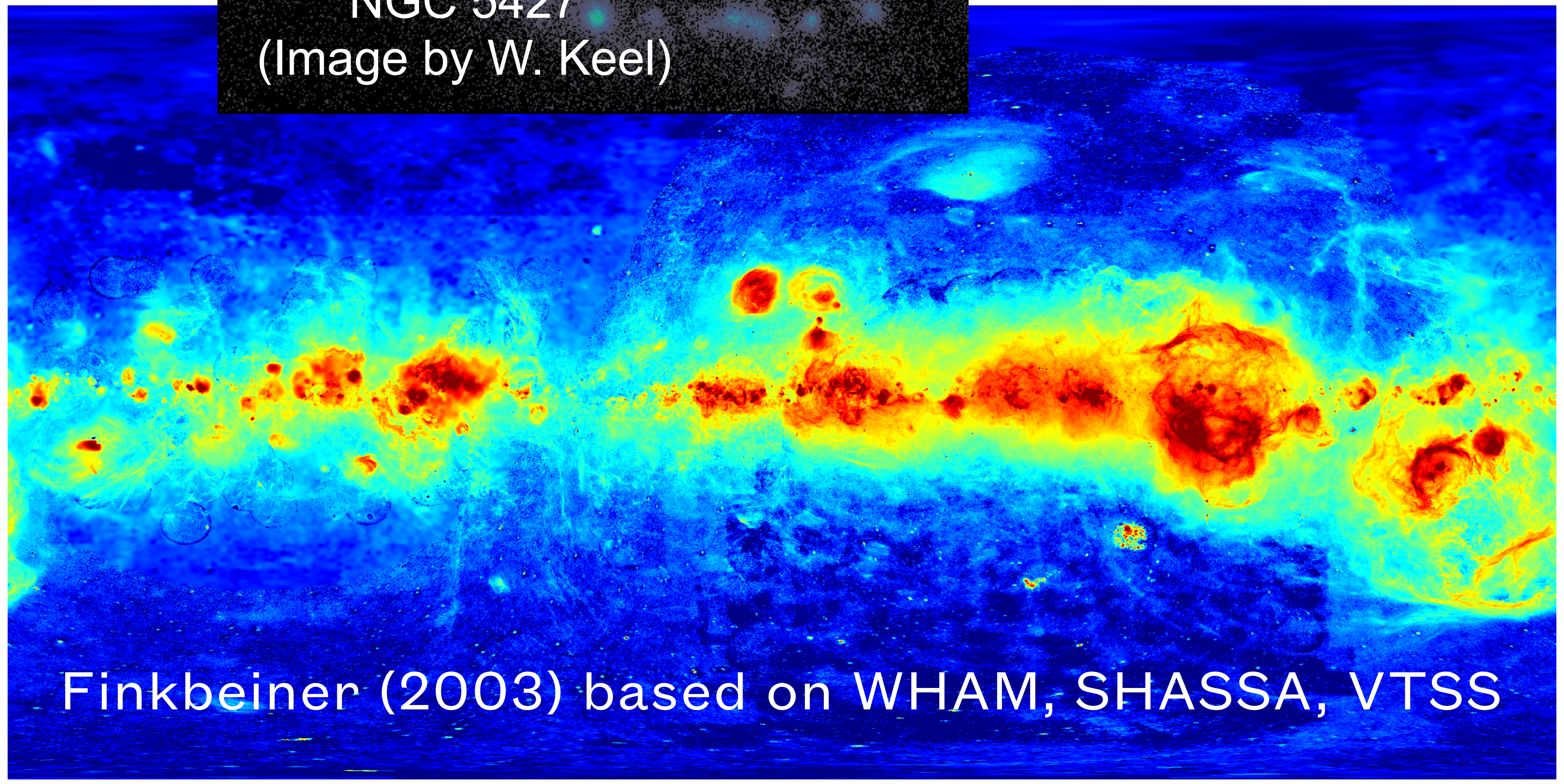

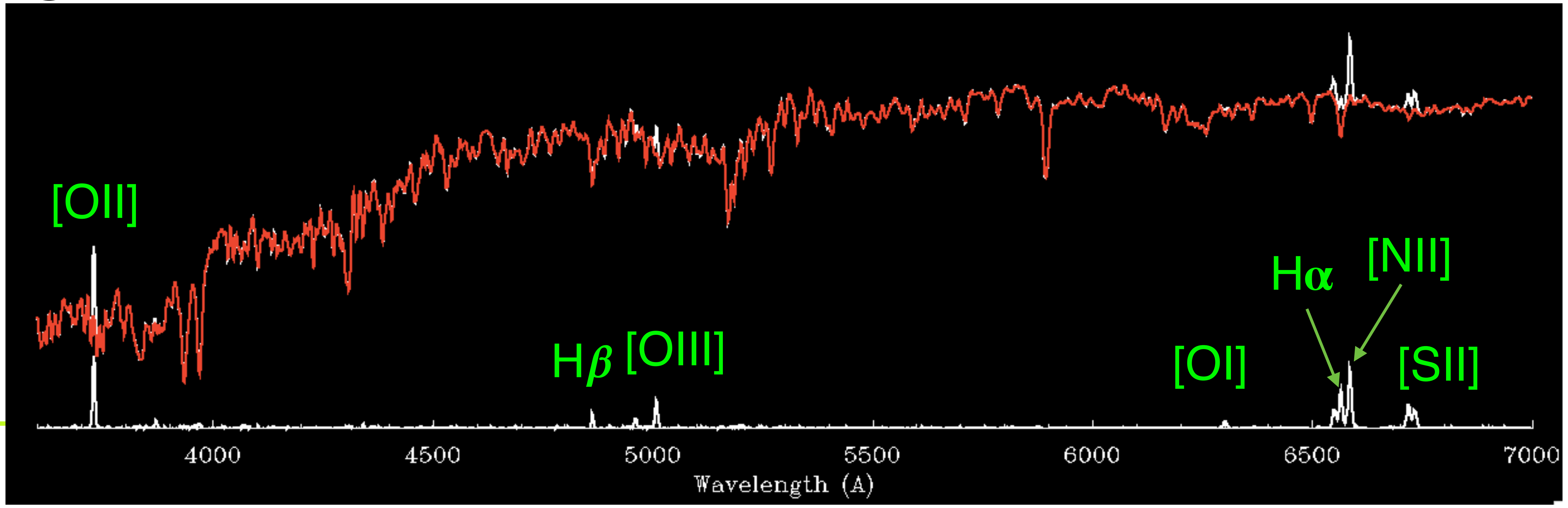

Two classes of commonly-found, but poorly-understood warm ionized gas

- **Diffuse Ionized Gas (DIG) in star-forming disk galaxies** (Zhang et al. 2017)
  - responsible for 50% of the Halpha emission (Oey+2007)
- **Low ionization gas in elliptical and lenticular galaxies (LINER-like, LIER)**
  - detected in more than 70% of early-type galaxies (Sarzi+06)

(Yan et al. 2006, 2012, 2018a, b, Belfiore et al. 2016, Cheung et al. 2016, Roy et al. 2018 & in prep)

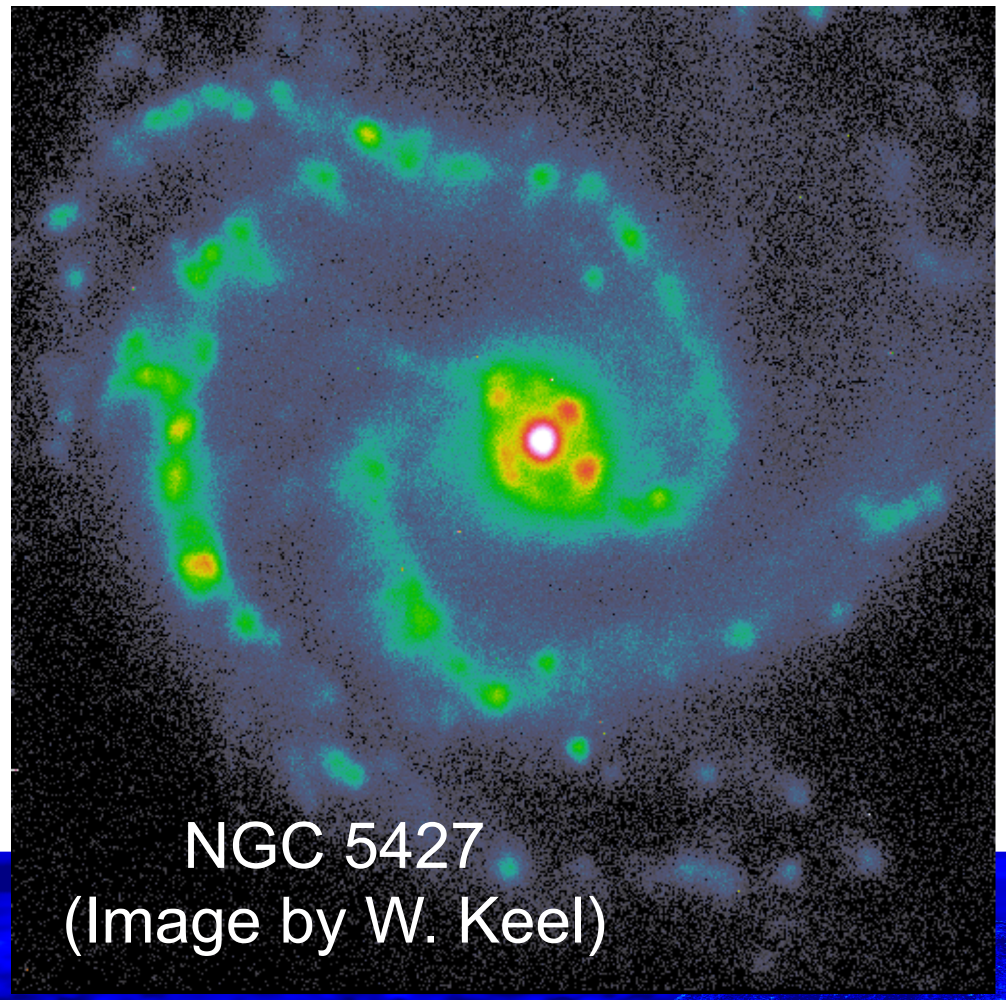

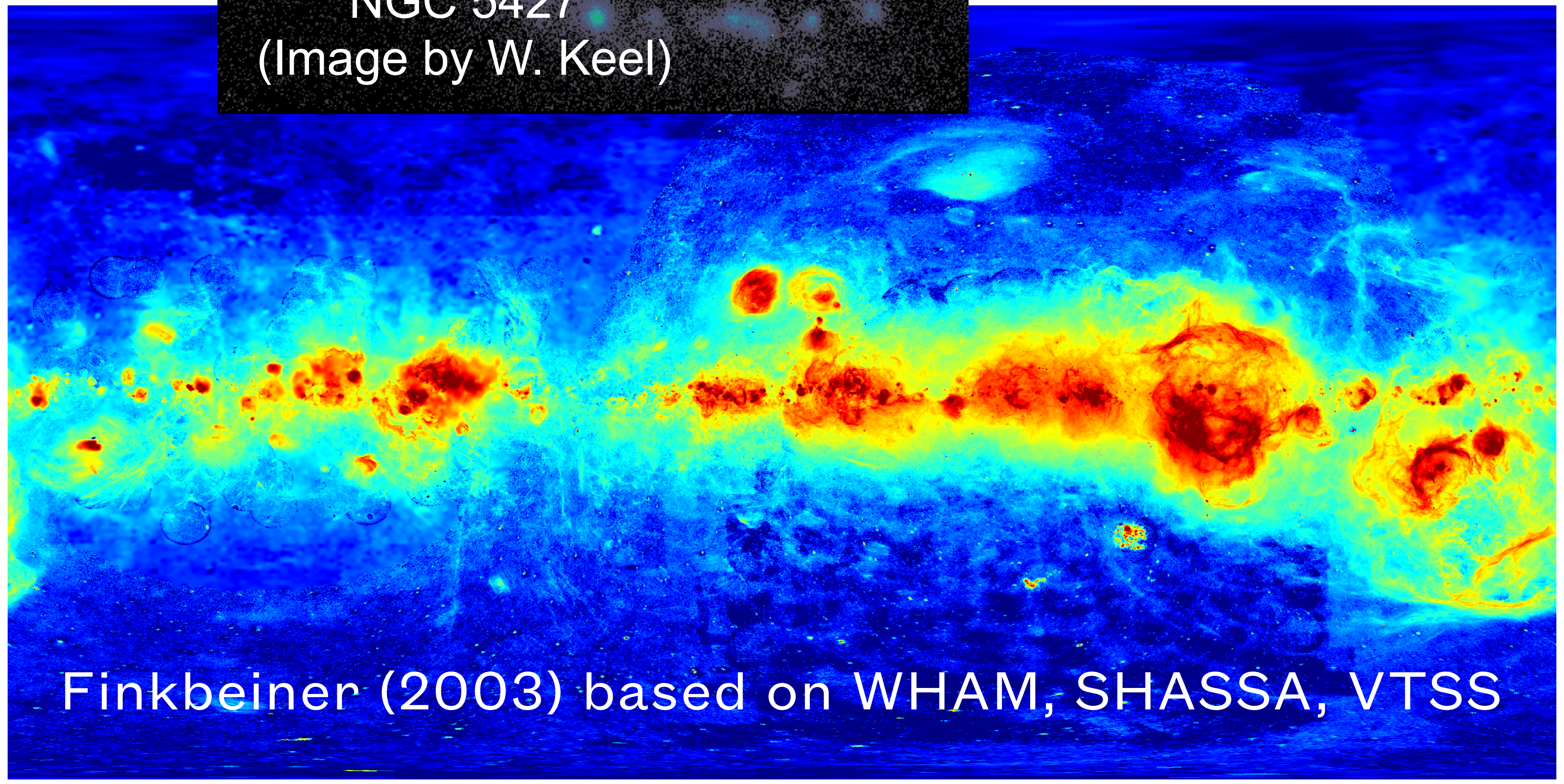

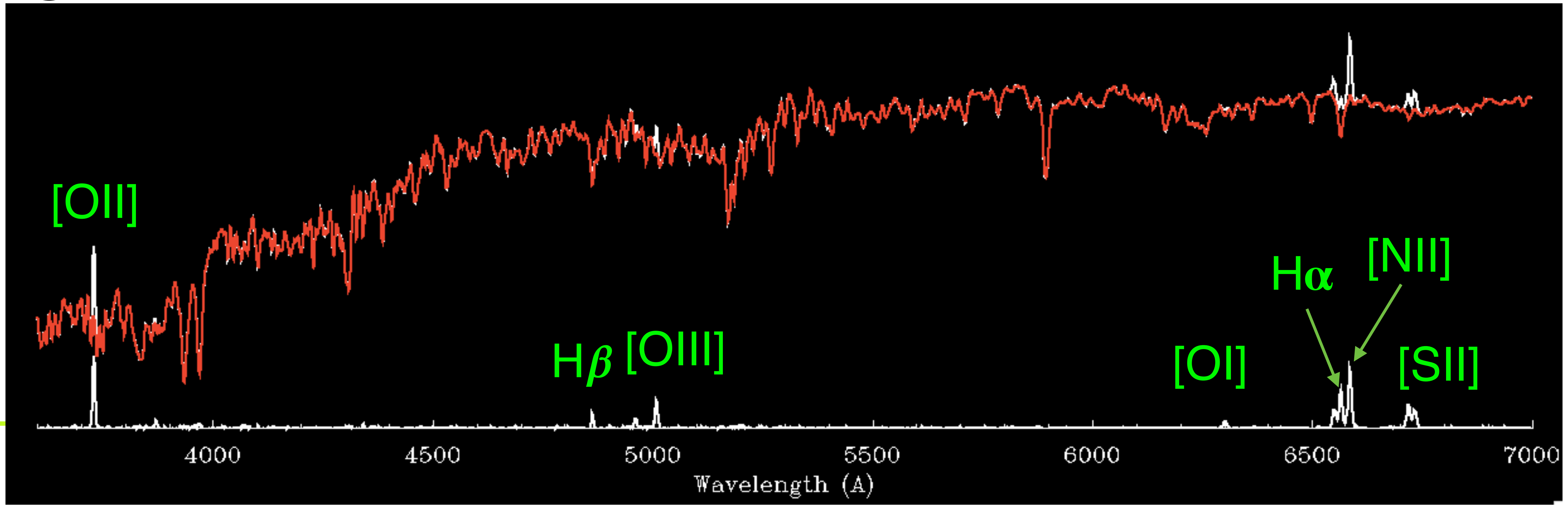

Discrepancies about WIM in star-forming regions

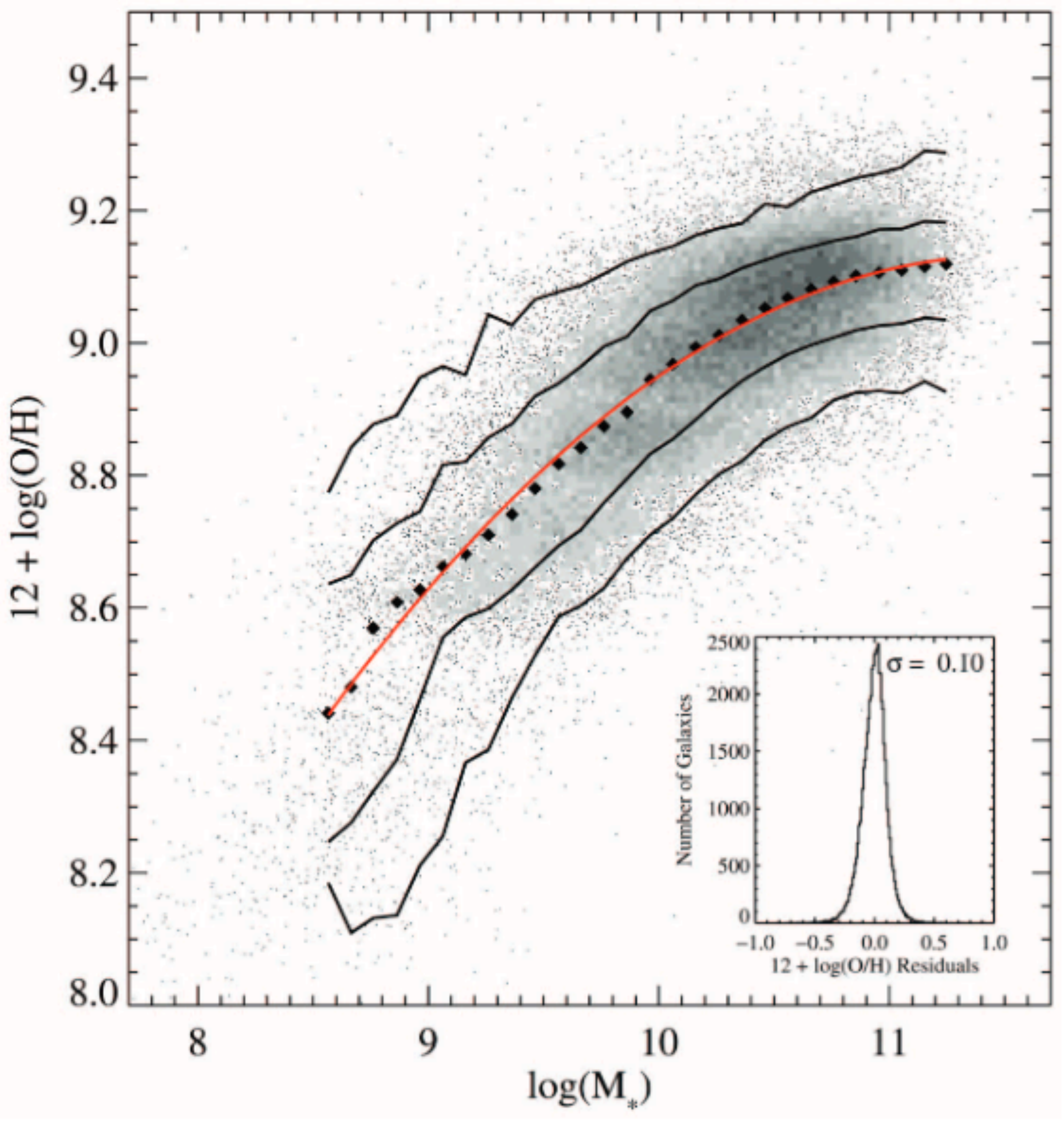

Tremonti et al. (2004)

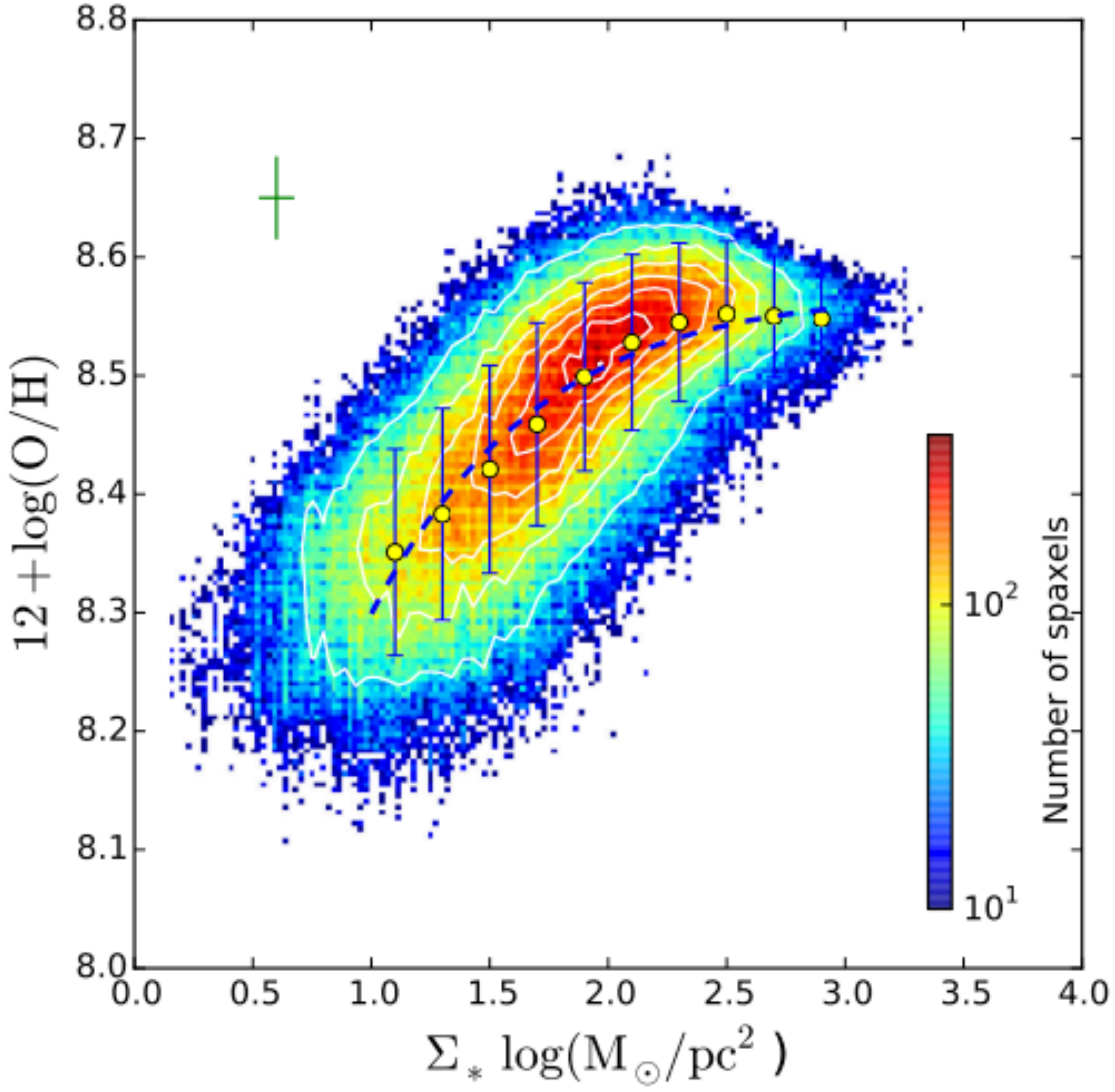

Barrera-Ballesteros et al. (2016)

Discrepancies about WIM in star-forming regions

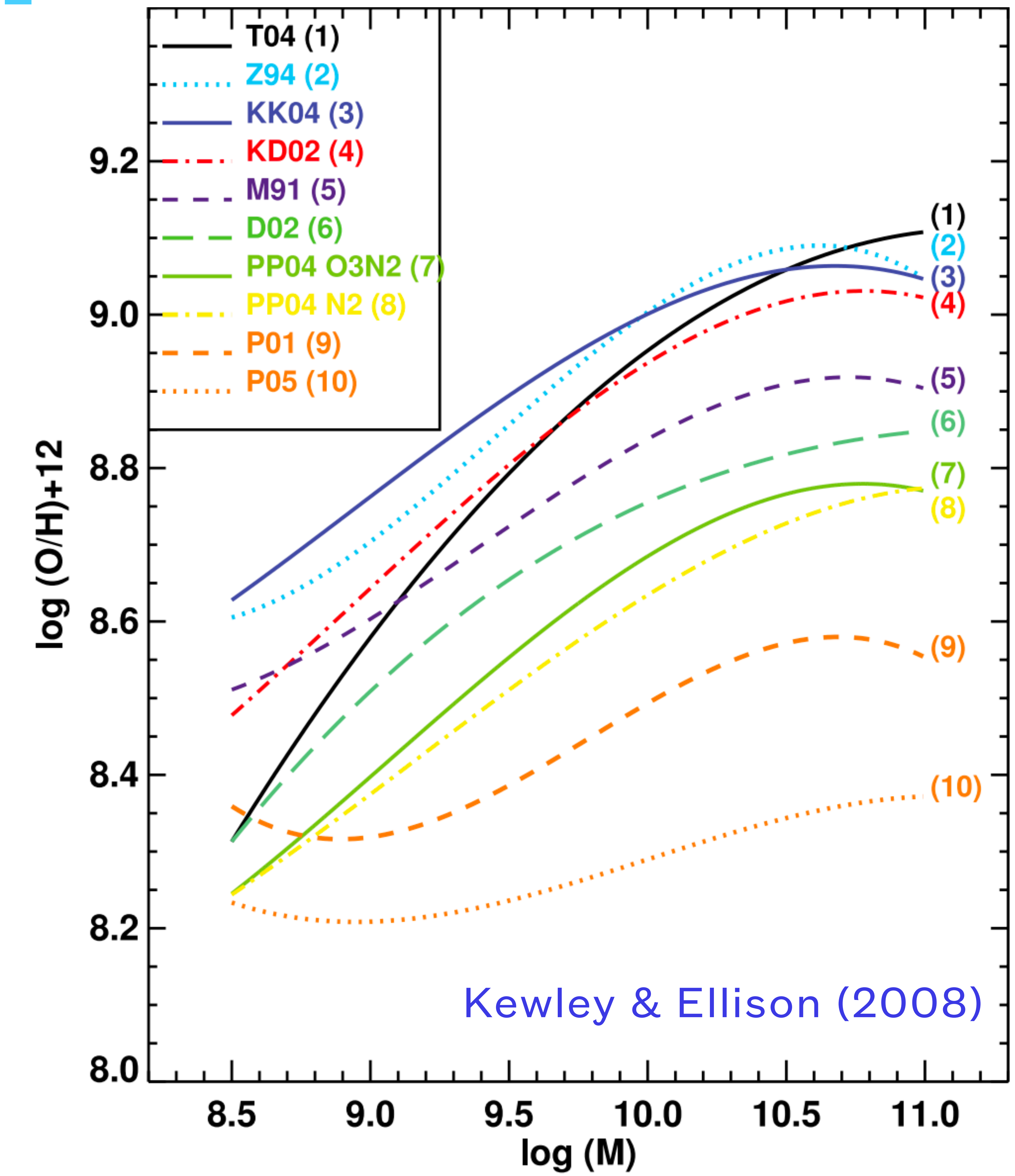

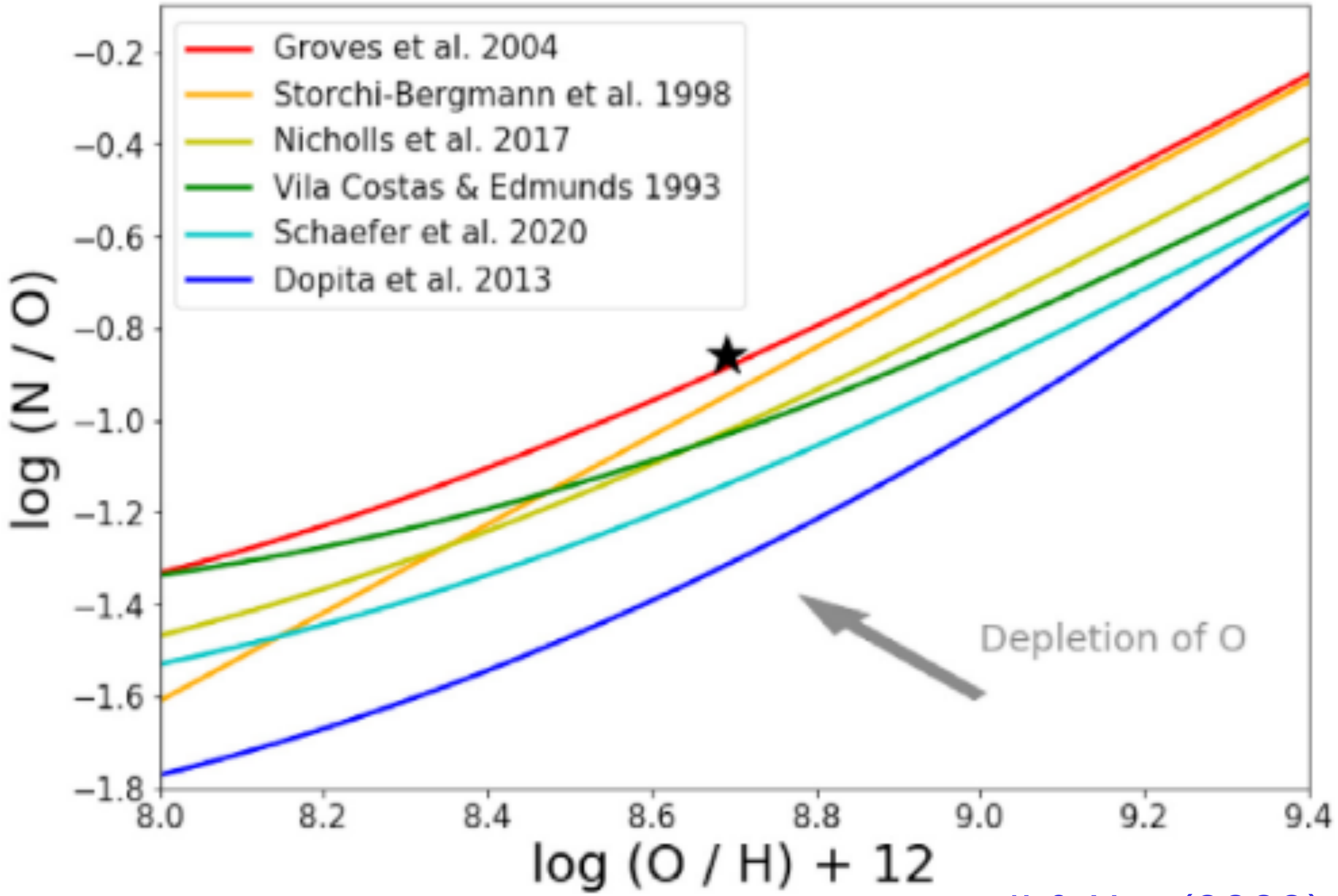

Ji & Yan (2020)

Under-tested Assumptions in Photoionization Models

- Input ionizing SED
  - Starburst99, PEGASE, FSPS, BPASS
  - SFH and age of HII regions
- Elemental abundance pattern
- Secondary elements prescription (N, C)
- Dust depletion pattern
- Geometry, density, pressure of cloud

Classical BPT diagrams

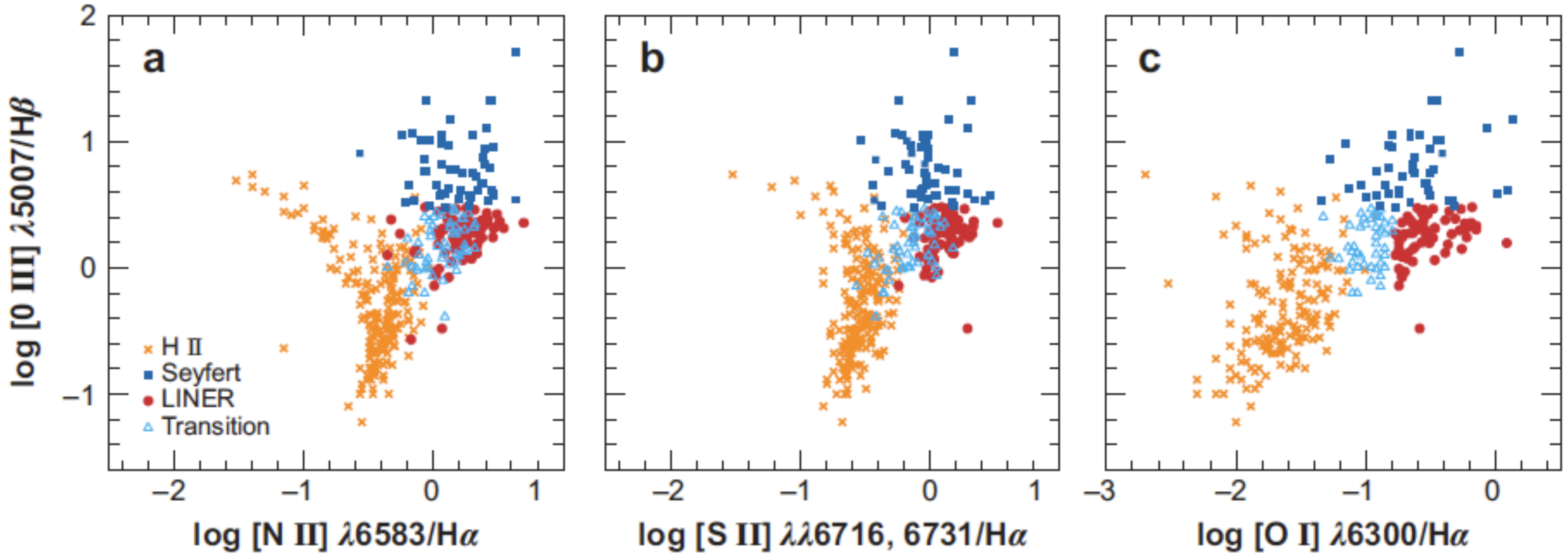

Ho et al. (2008)

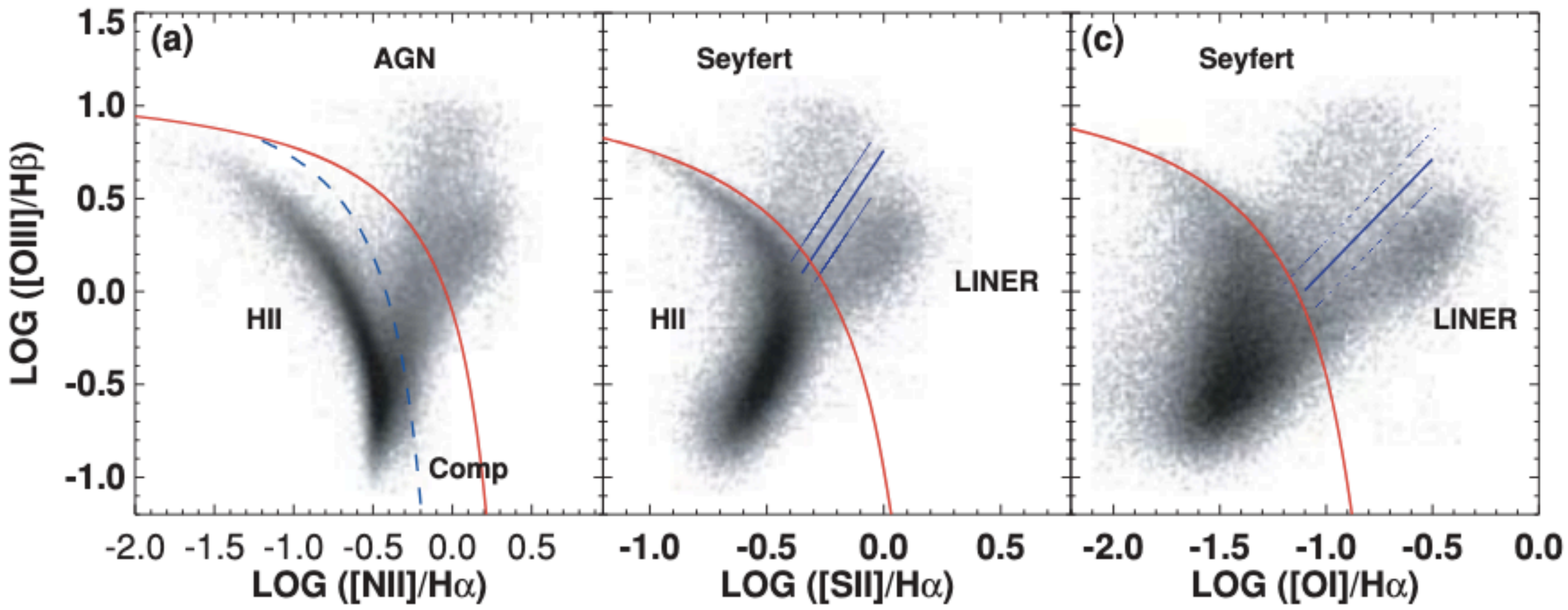

Baldwin, Phillips, & Terlevich (1981)
Veilleux & Osterbrock (1987)
Ho et al. (1995, 1997, 2008)
Kauffmann et al. (2003)
Kewley et al. (2006)
etc.

Kewley et al. (2006)

Drawbacks of the Classical BPT diagrams

- Usage is limited to classifications.

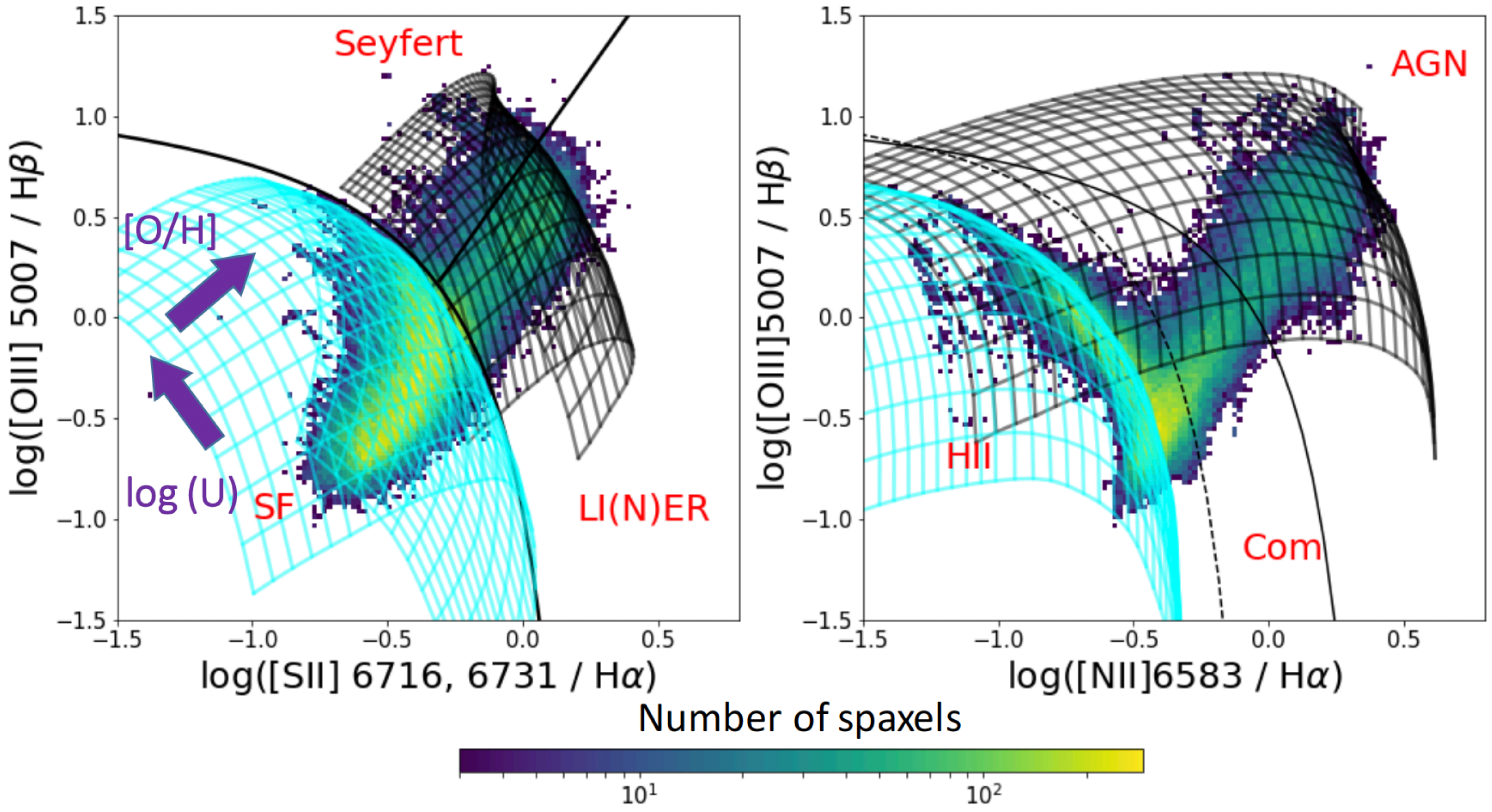

Baldwin, Phillips, & Terlevich (1981), Veilleux & Osterbrock (1987)
Ho et al. (1995, 1997, 2008), Kauffmann et al. (2003), Kewley et al. (2006), etc.

Drawbacks of the Classical BPT diagrams

- Usage is limited to classifications.
- Demarcations are empirical — not well motivated theoretically.

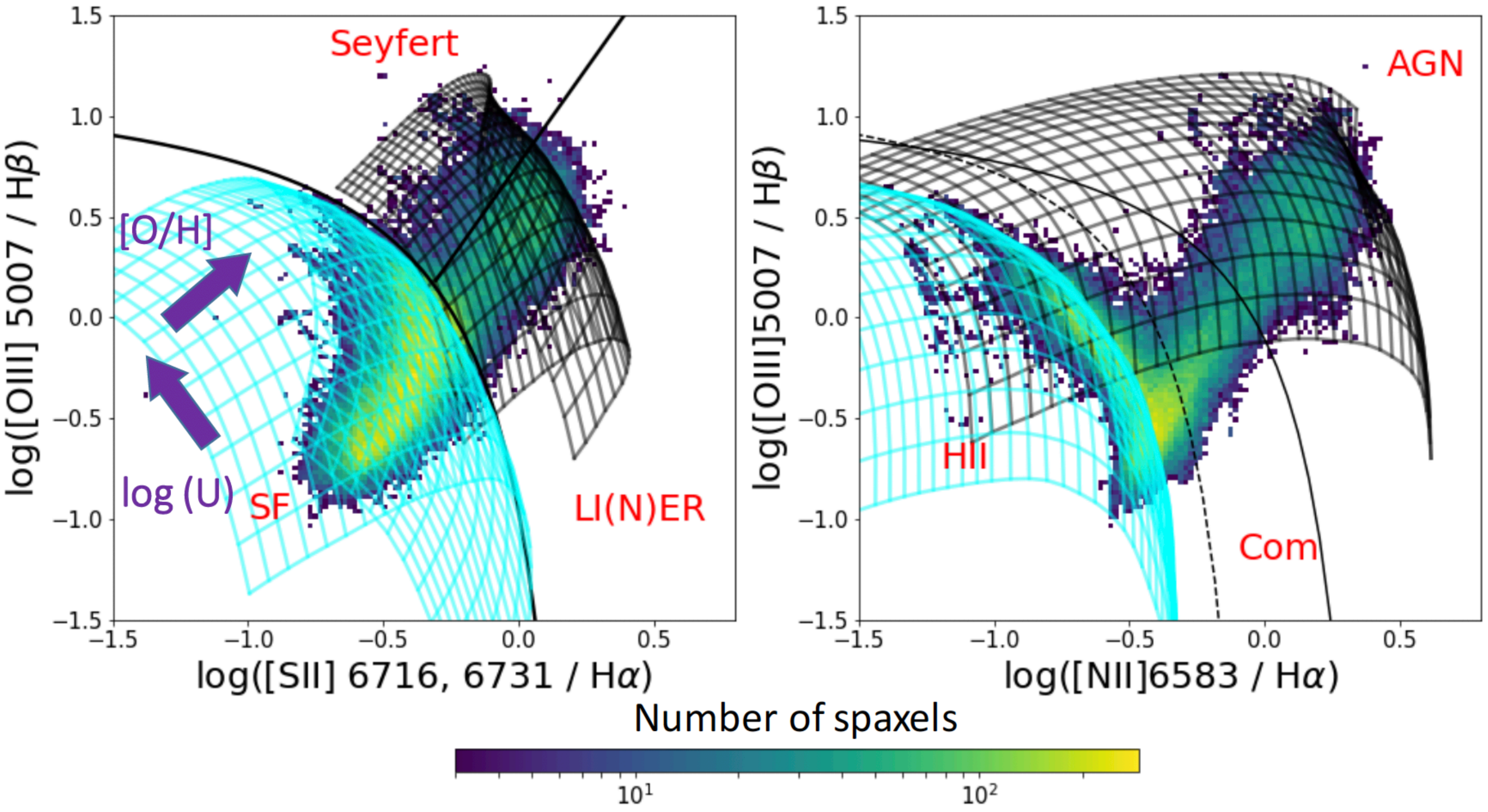

Baldwin, Phillips, & Terlevich (1981), Veilleux & Osterbrock (1987)
Ho et al. (1995, 1997, 2008), Kauffmann et al. (2003), Kewley et al. (2006), etc.

Drawbacks of the Classical BPT diagrams

- Usage is limited to classifications.
- Demarcations are empirical — not well motivated theoretically.
- Classifications can be diagram-dependent, leading to ambiguity.

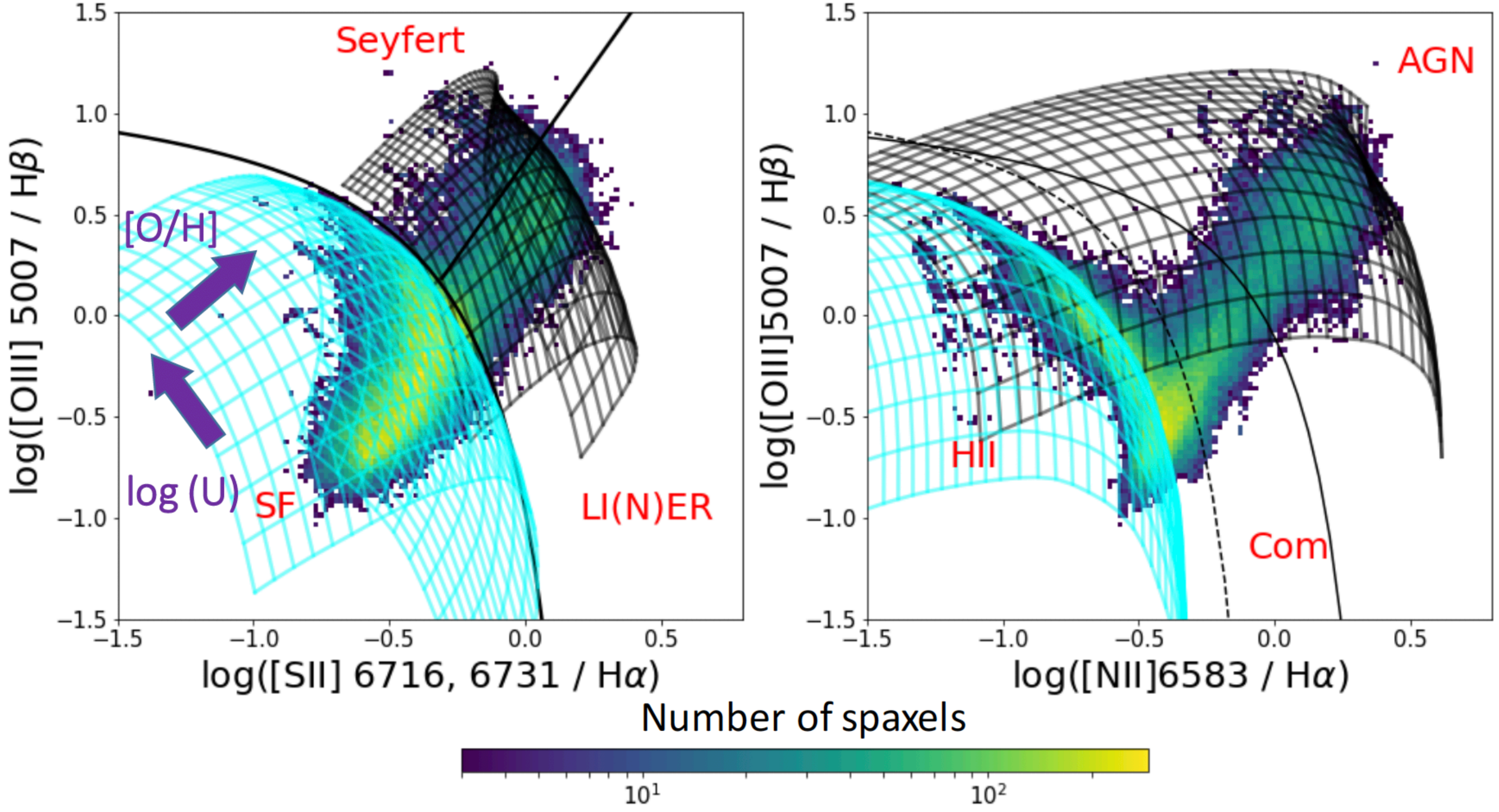

Baldwin, Phillips, & Terlevich (1981), Veilleux & Osterbrock (1987)
Ho et al. (1995, 1997, 2008), Kauffmann et al. (2003), Kewley et al. (2006), etc.

Drawbacks of the Classical BPT diagrams

- Usage is limited to classifications.
- Demarcations are empirical — not well motivated theoretically.
- Classifications can be diagram-dependent, leading to ambiguity.
- Nature of the composite region (aka. mixing sequence, intermediate region) is unclear.

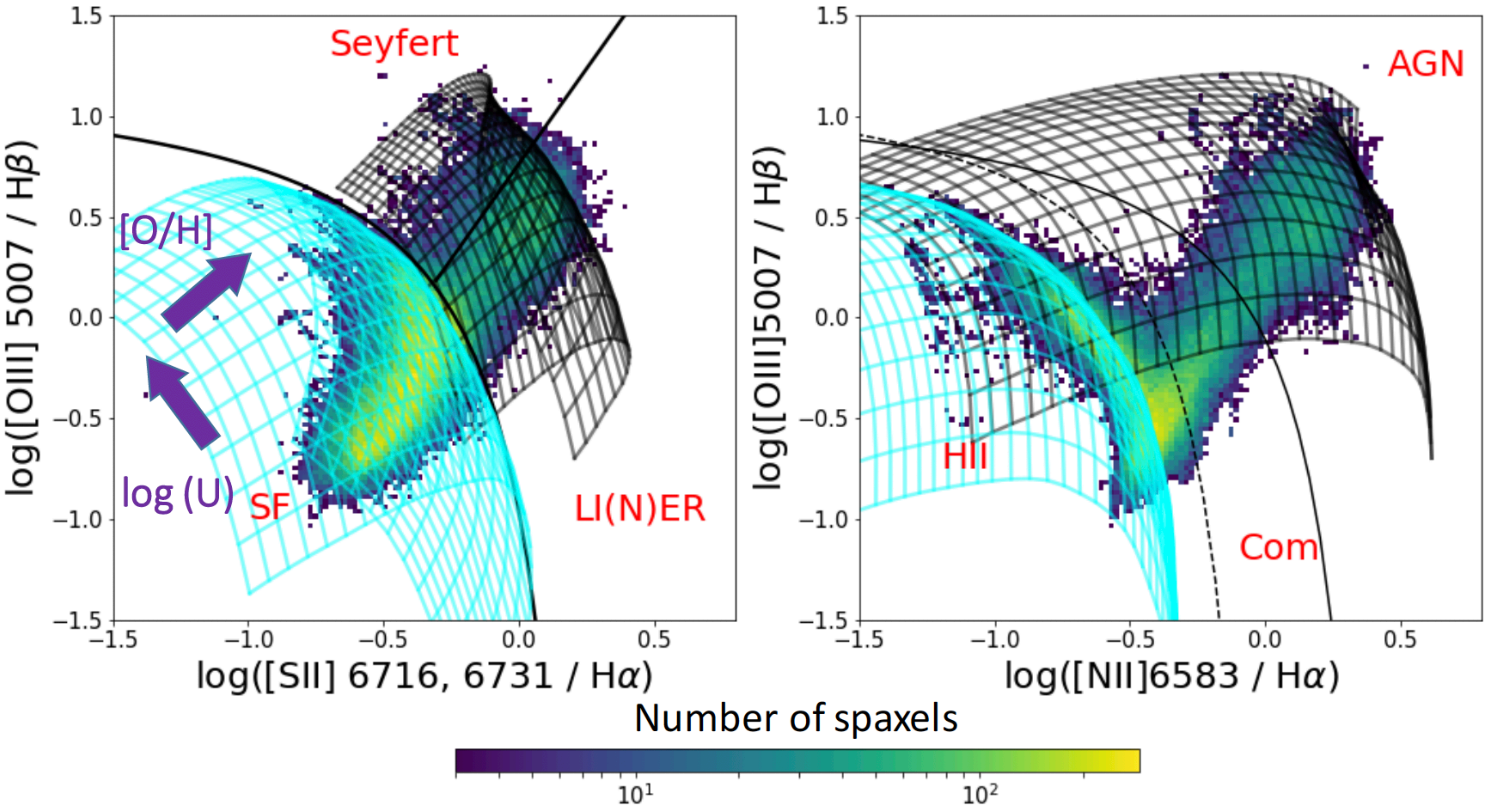

Baldwin, Phillips, & Terlevich (1981), Veilleux & Osterbrock (1987)
Ho et al. (1995, 1997, 2008), Kauffmann et al. (2003), Kewley et al. (2006), etc.

Drawbacks of the Classical BPT diagrams

- Usage is limited to classifications.
- Demarcations are empirical — not well motivated theoretically.
- Classifications can be diagram-dependent, leading to ambiguity.
- Nature of the composite region (aka. mixing sequence, intermediate region) is unclear.
- Decomposition of the composites depends significantly on the chosen starting points.

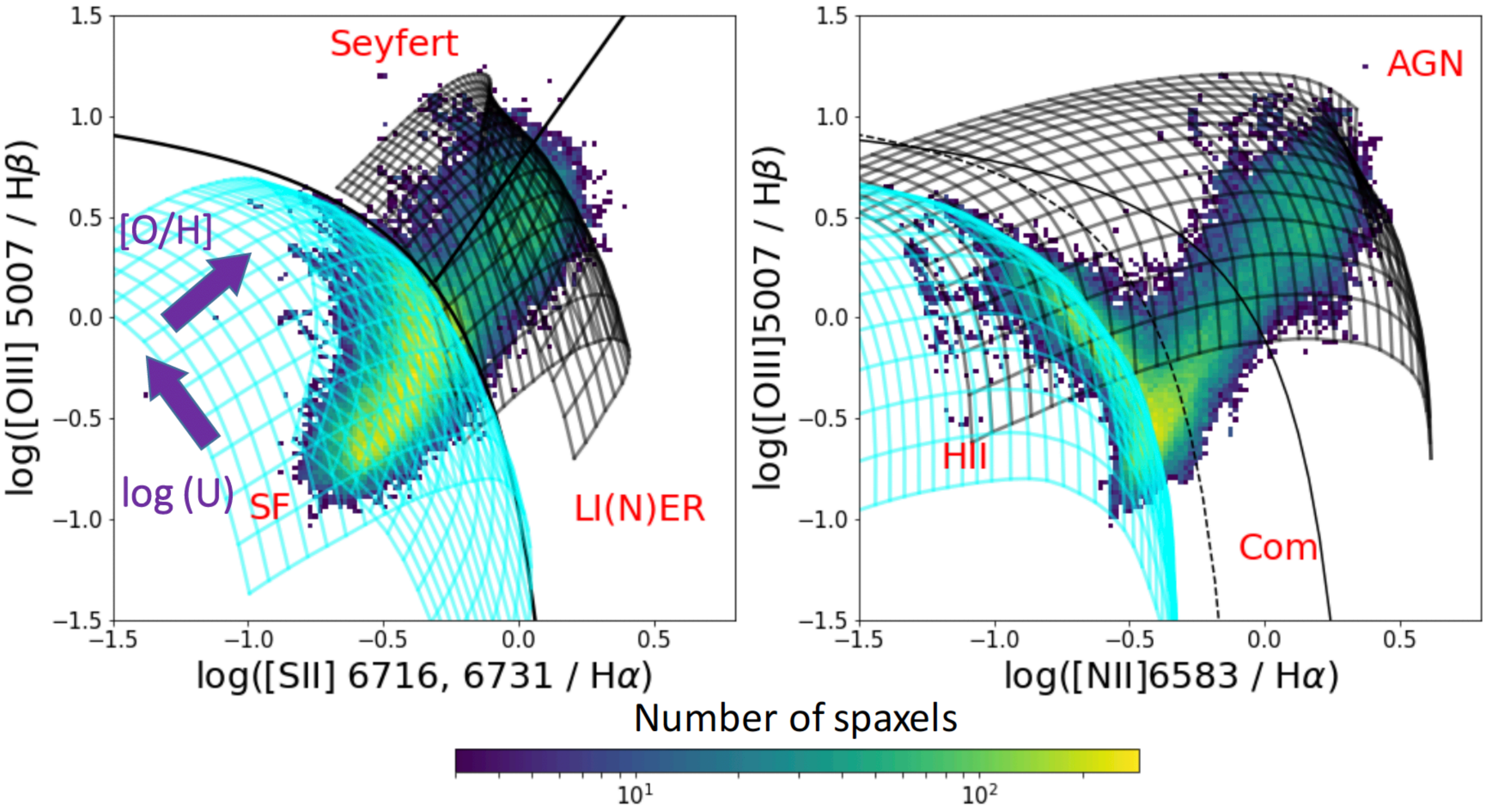

Baldwin, Phillips, & Terlevich (1981), Veilleux & Osterbrock (1987)
Ho et al. (1995, 1997, 2008), Kauffmann et al. (2003), Kewley et al. (2006), etc.

BPT diagram in 3D

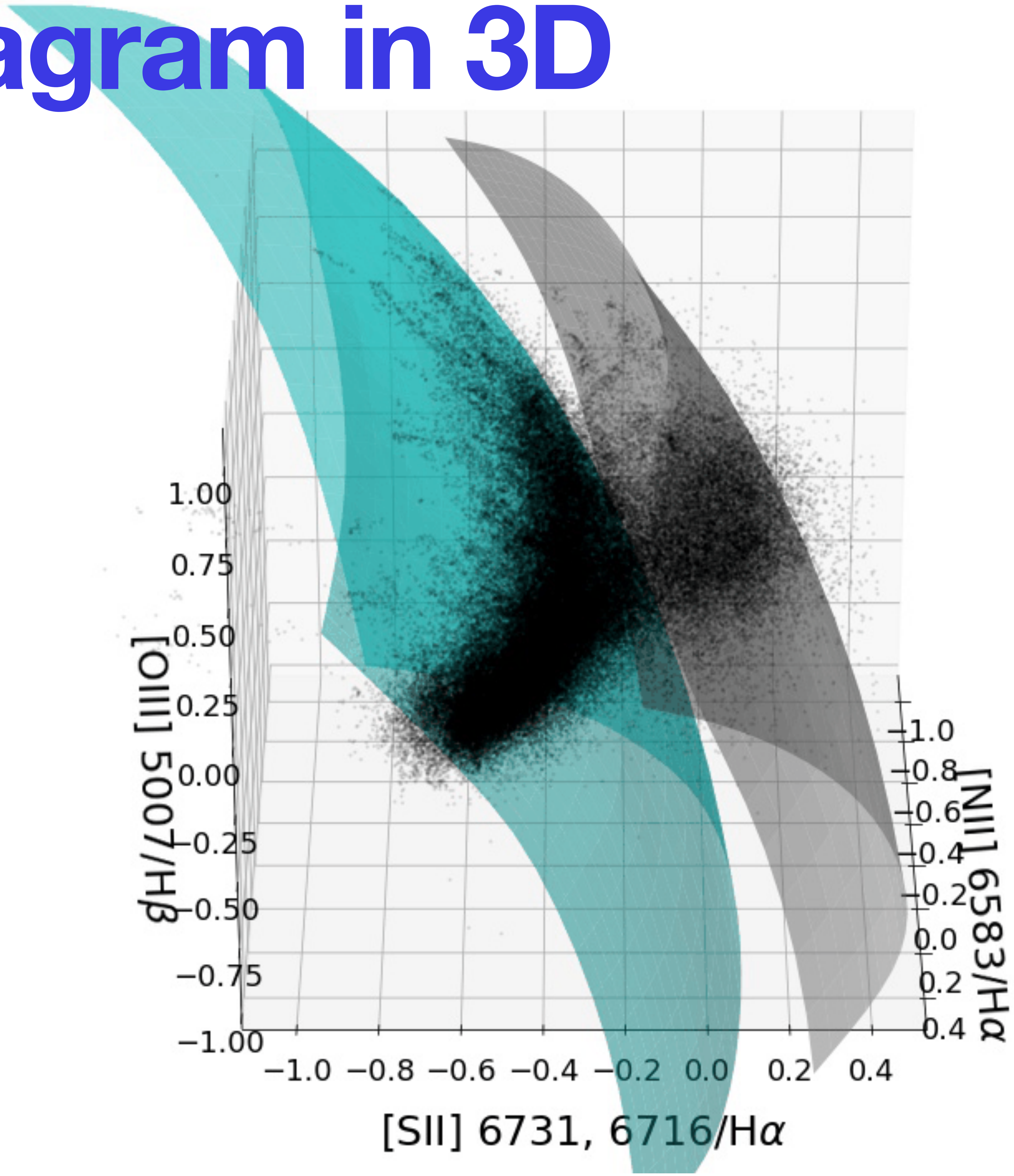

Xihan Ji

- All spaxels within the central 0.3Re of MaNGA galaxies (MPL-7)
- S/N> 3 in all lines
- SF and AGN model surfaces from CLOUDY

Ji & Yan (2020)

BPT diagram in 3D

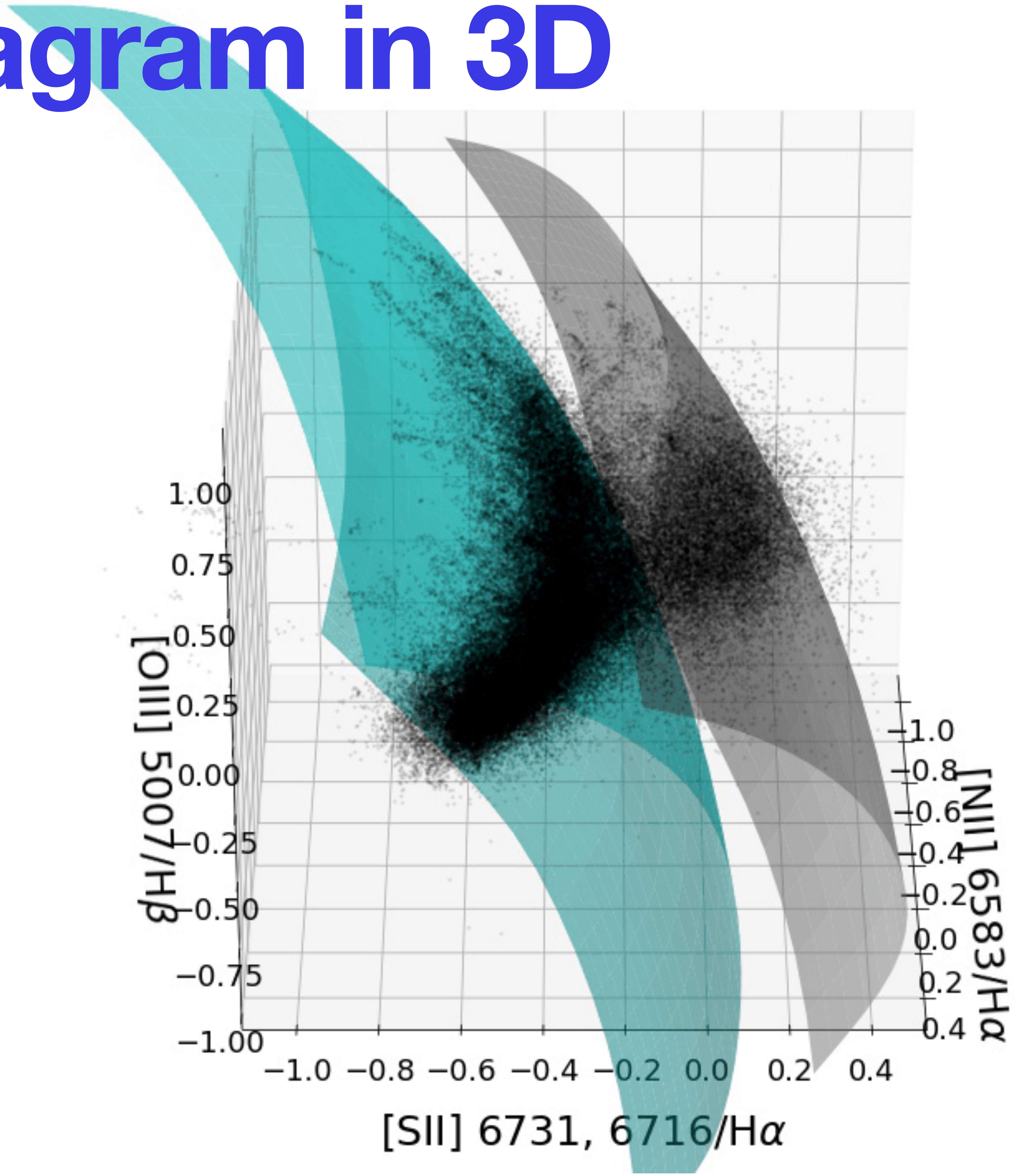

Xihan Ji

- All spaxels within the central 0.3Re of MaNGA galaxies (MPL-7)
- S/N> 3 in all lines
- SF and AGN model surfaces from CLOUDY

Ji & Yan (2020)

Find the edge-on viewing angle

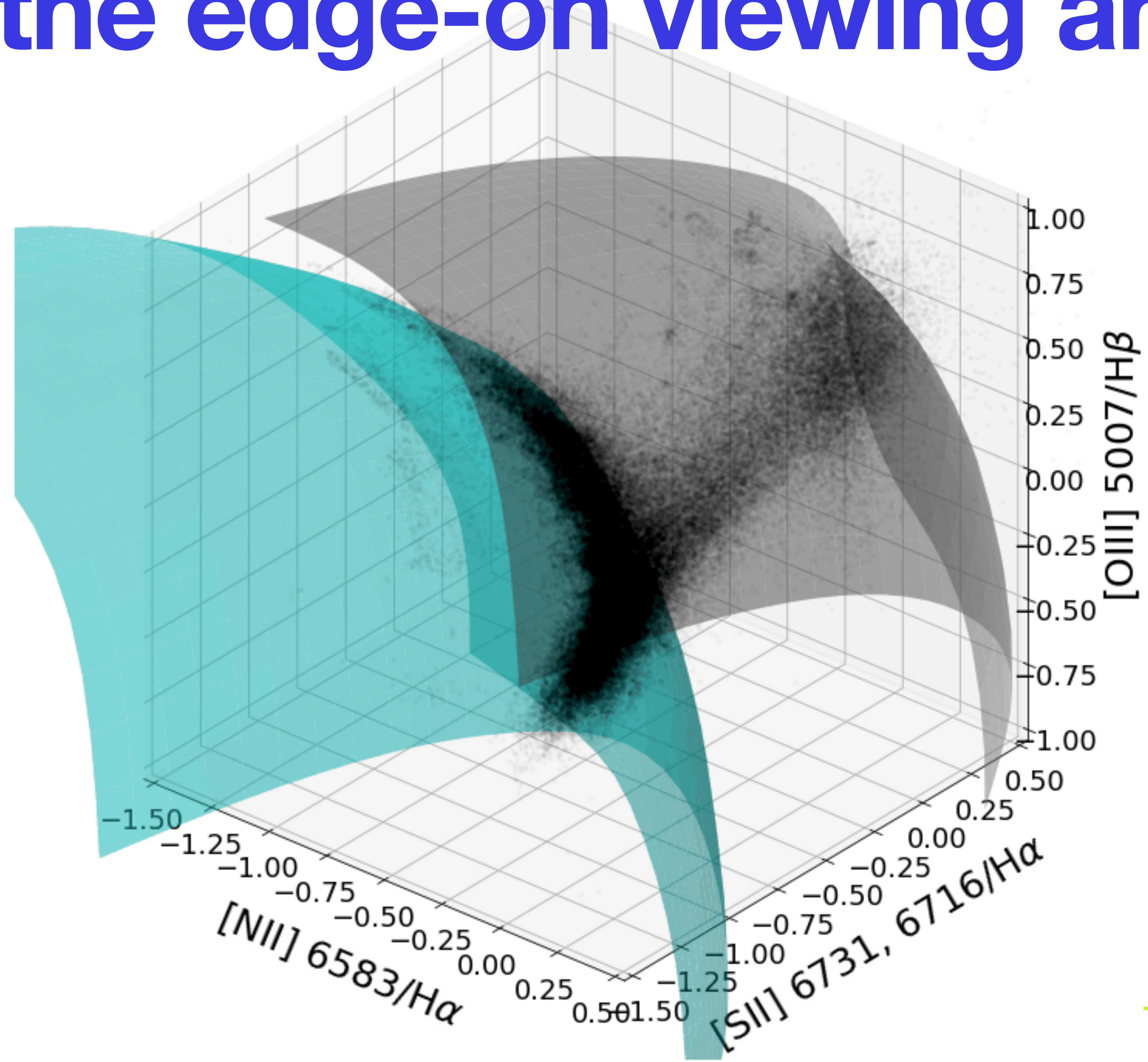

Find the edge-on viewing angle

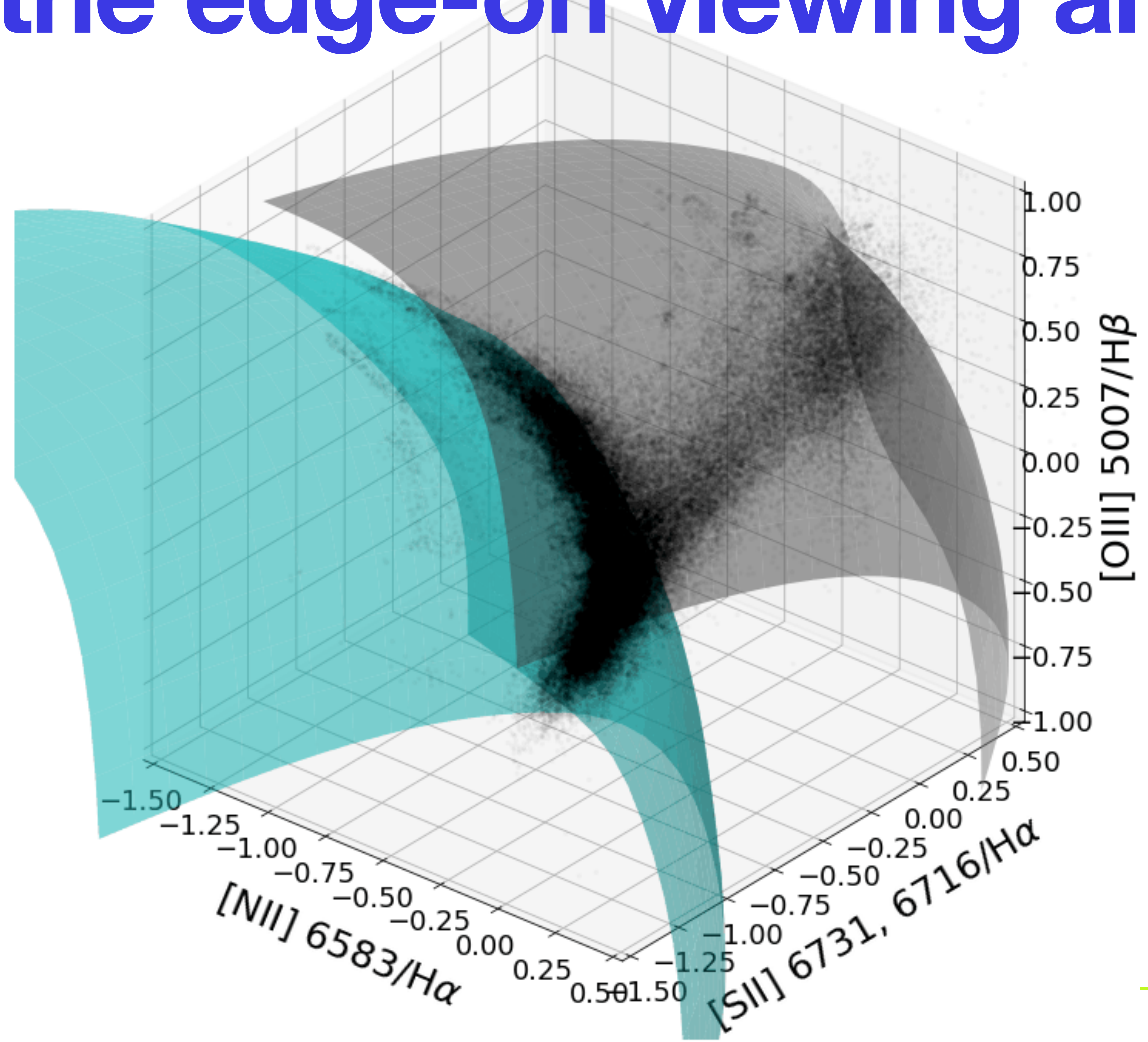

Reproject to 2D

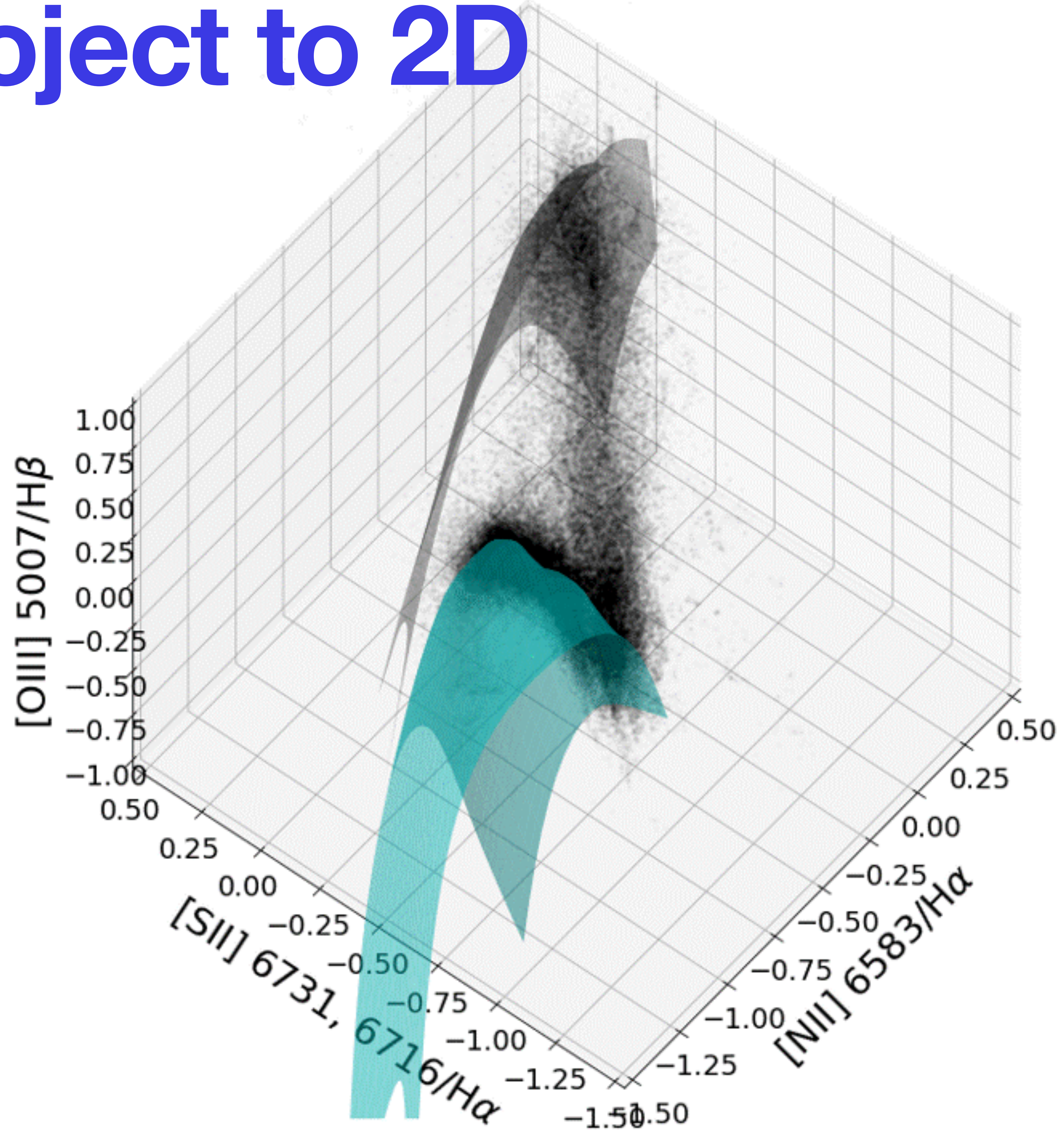

Reproject to 2D

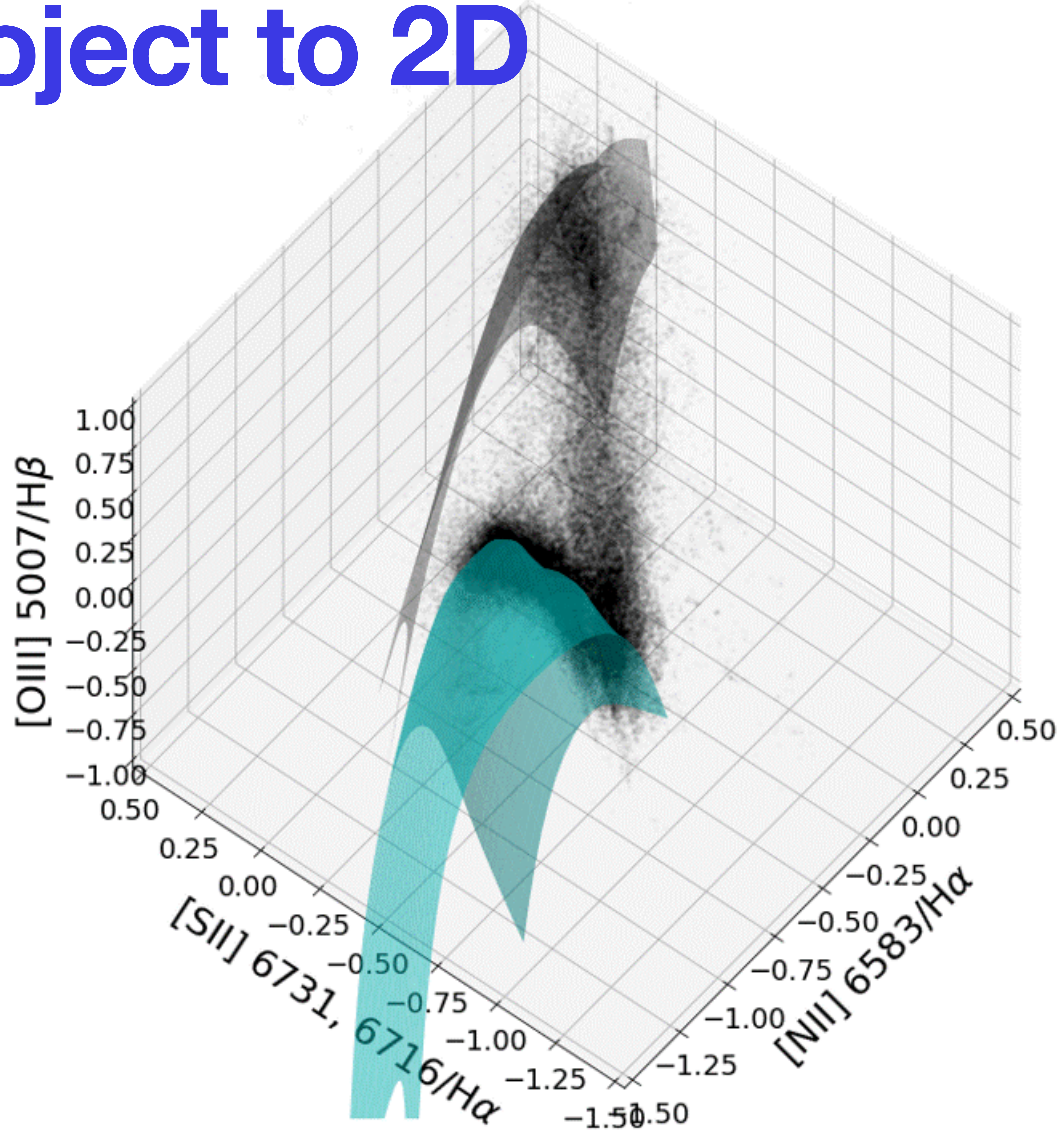

Reproject to 2D

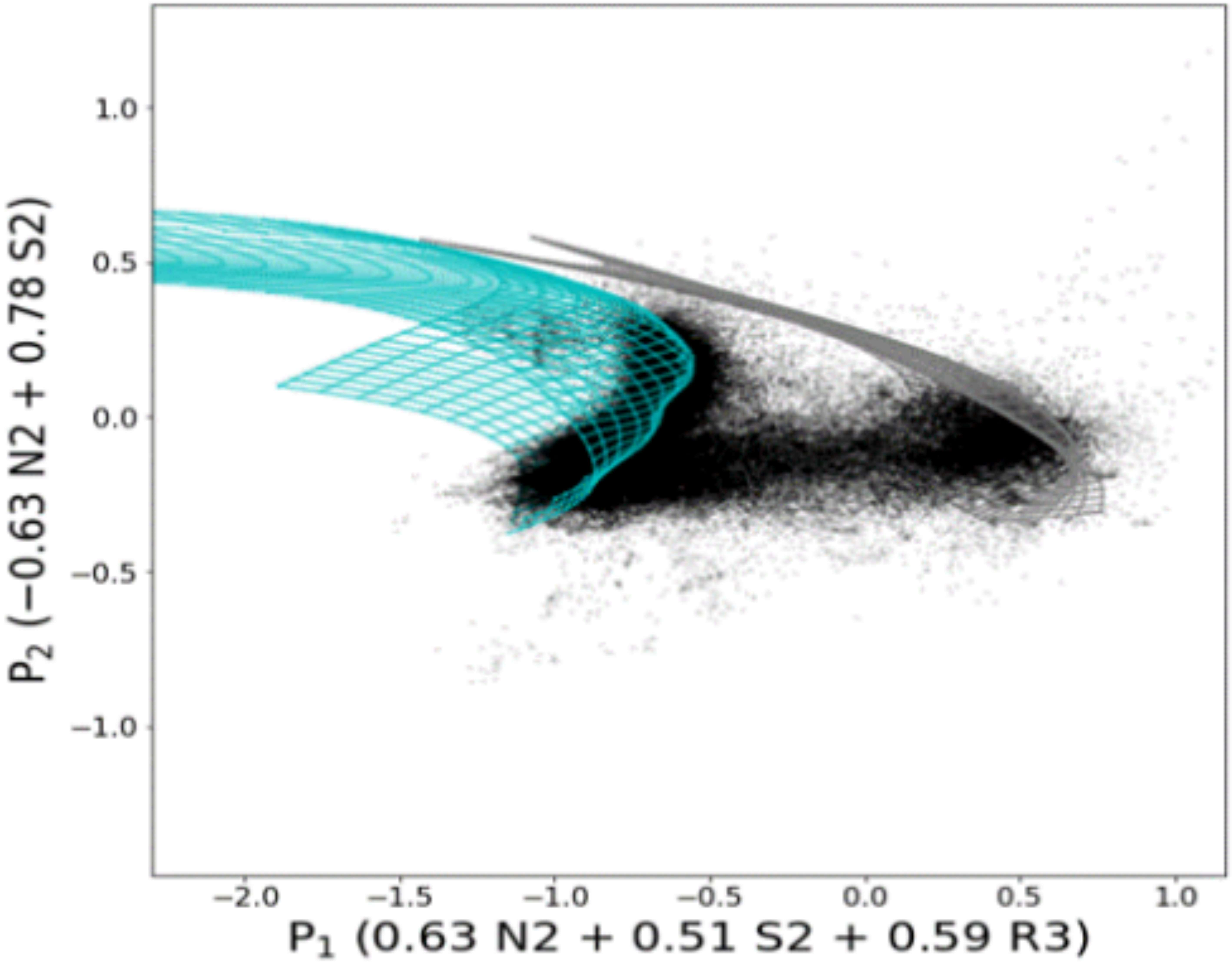

$$N2 \equiv \log \frac{[\mathrm{NII}]\ \lambda 6583\mathrm{A}}{\mathrm{H}\alpha}$$

$$S2 \equiv \log \frac{[\mathrm{SII}]\ \lambda\lambda 6716{,}6731\mathrm{AA}}{\mathrm{H}\alpha}$$

$$R3 \equiv \log \frac{[\mathrm{OIII}]\ \lambda 5007\mathrm{A}}{\mathrm{H}\beta}$$

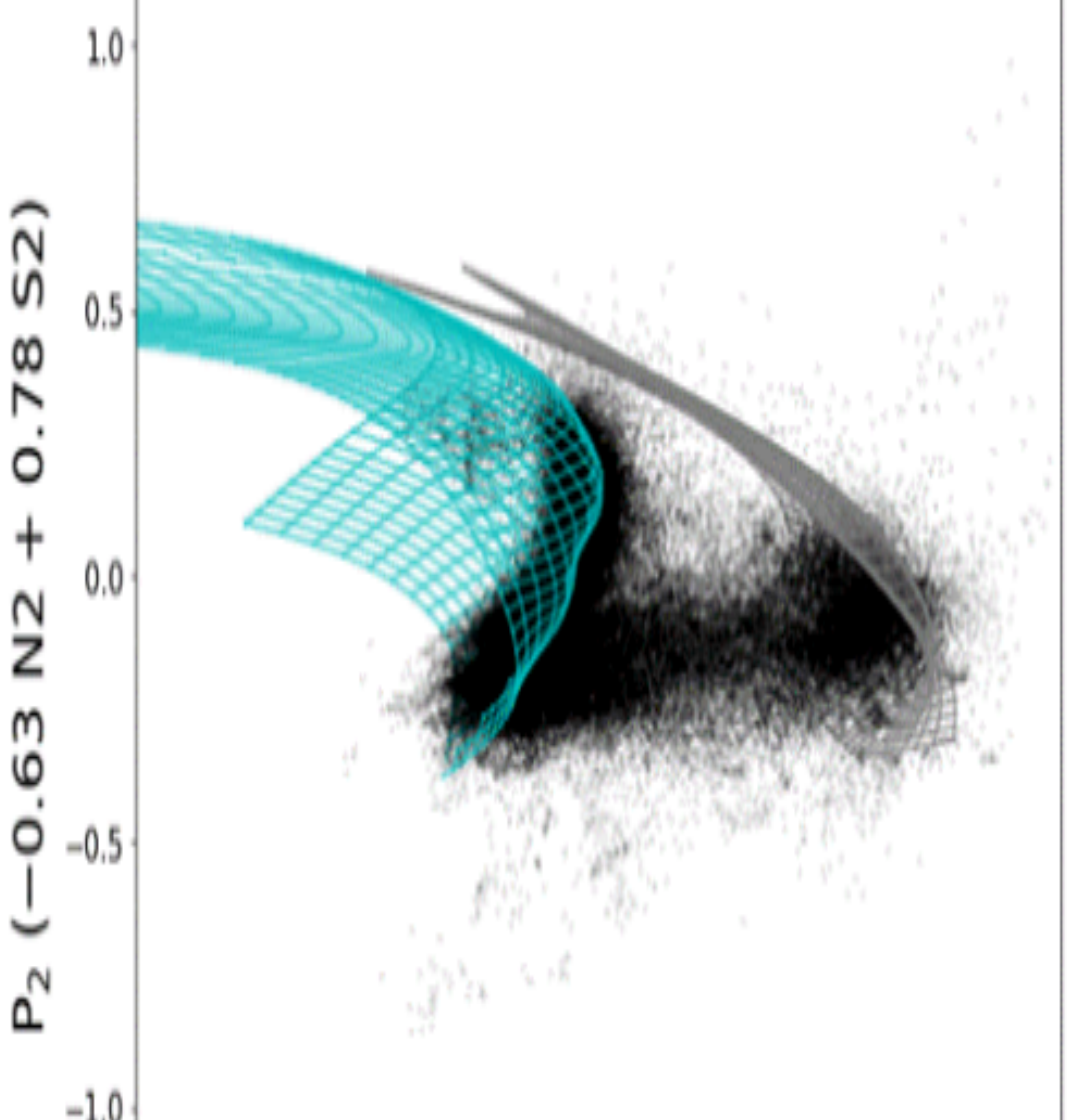

All spaxels within the central 0.3Re of MaNGA galaxies (MPL-7)

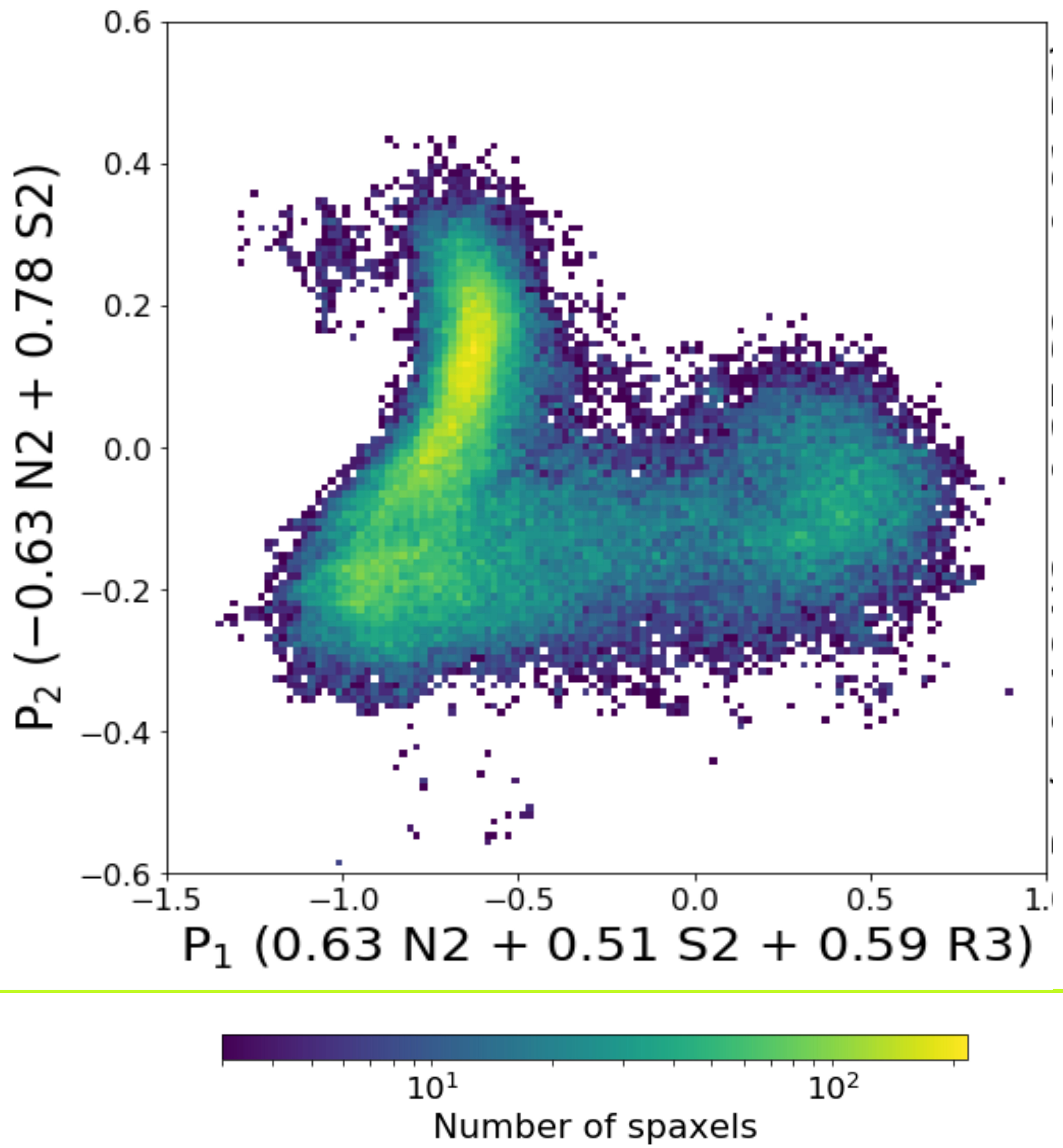

All spaxels within the central 0.3Re of MaNGA galaxies (MPL-7)

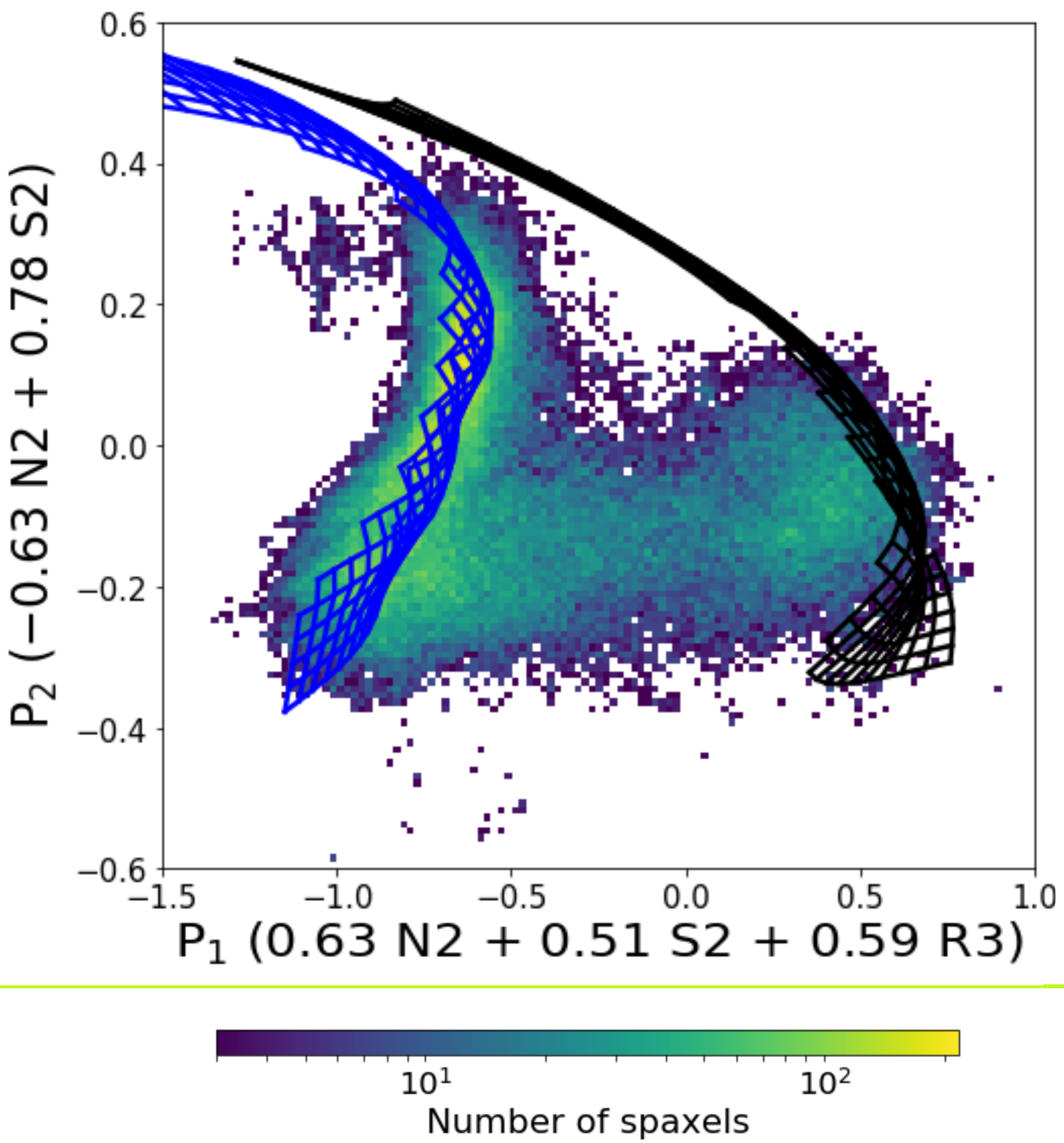

All spaxels within the central 0.3Re of MaNGA galaxies (MPL-7)

Reprojected BPT diagrams

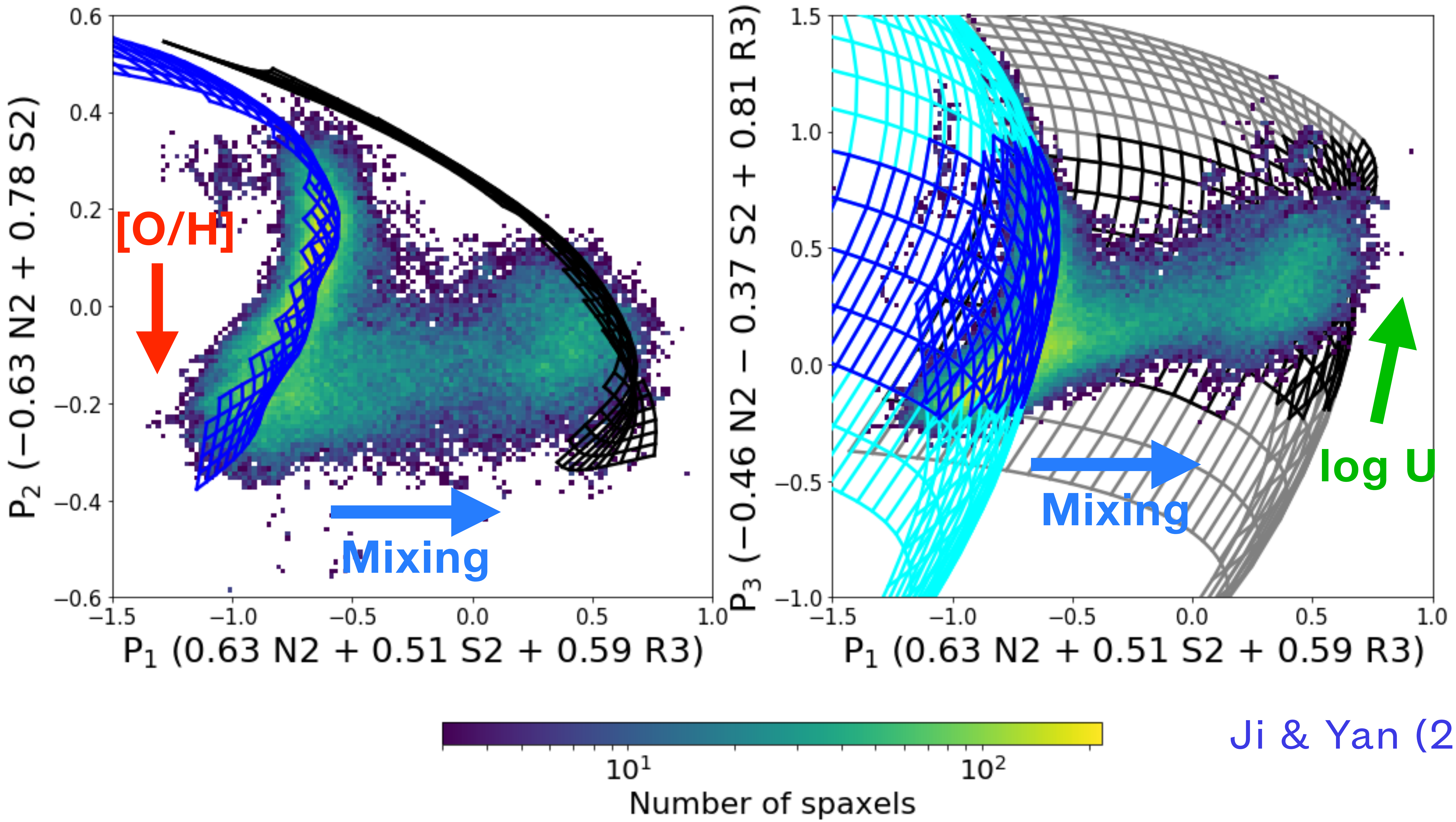

Ji & Yan (2020)

Constraining the N/O prescription

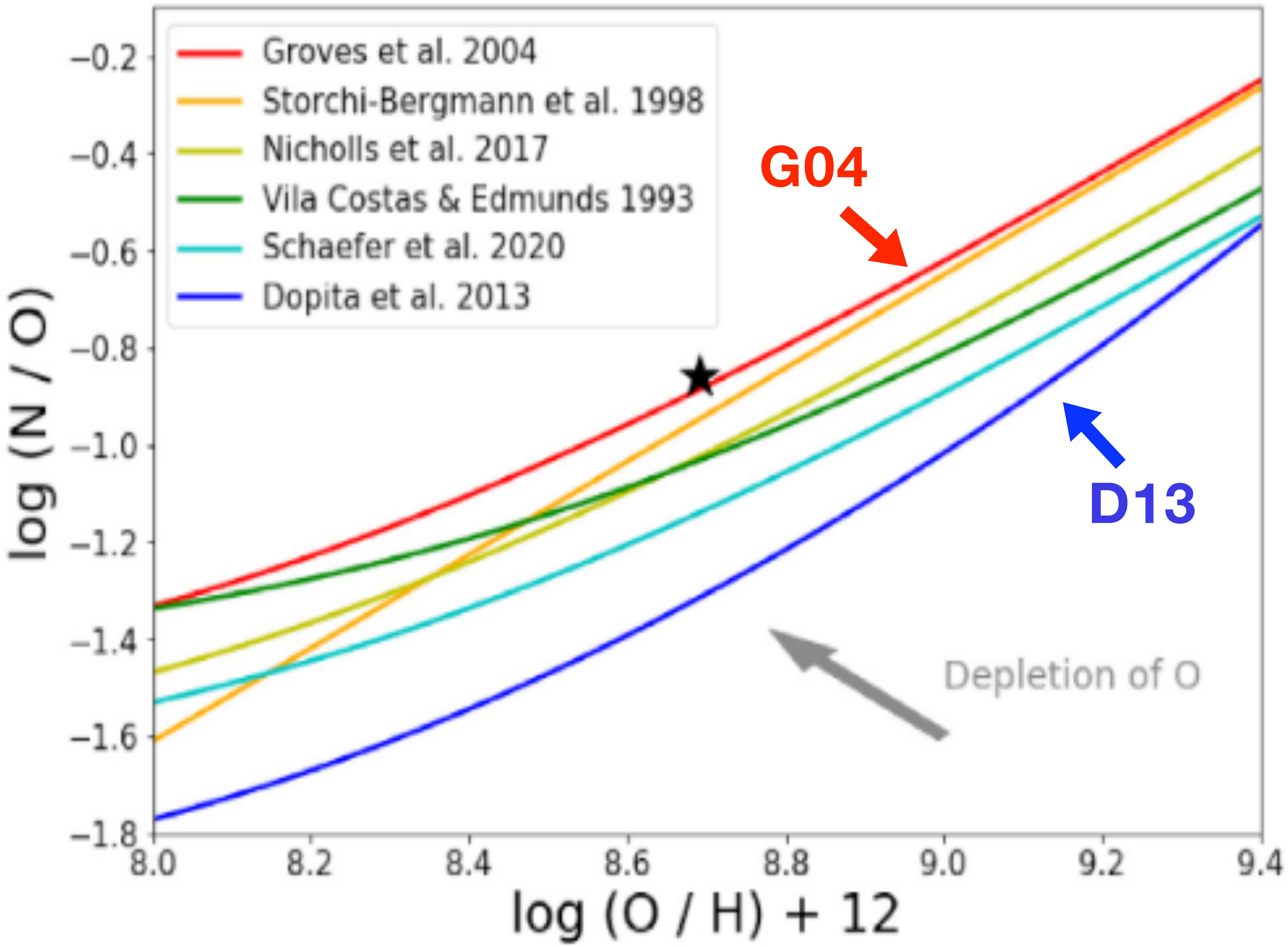

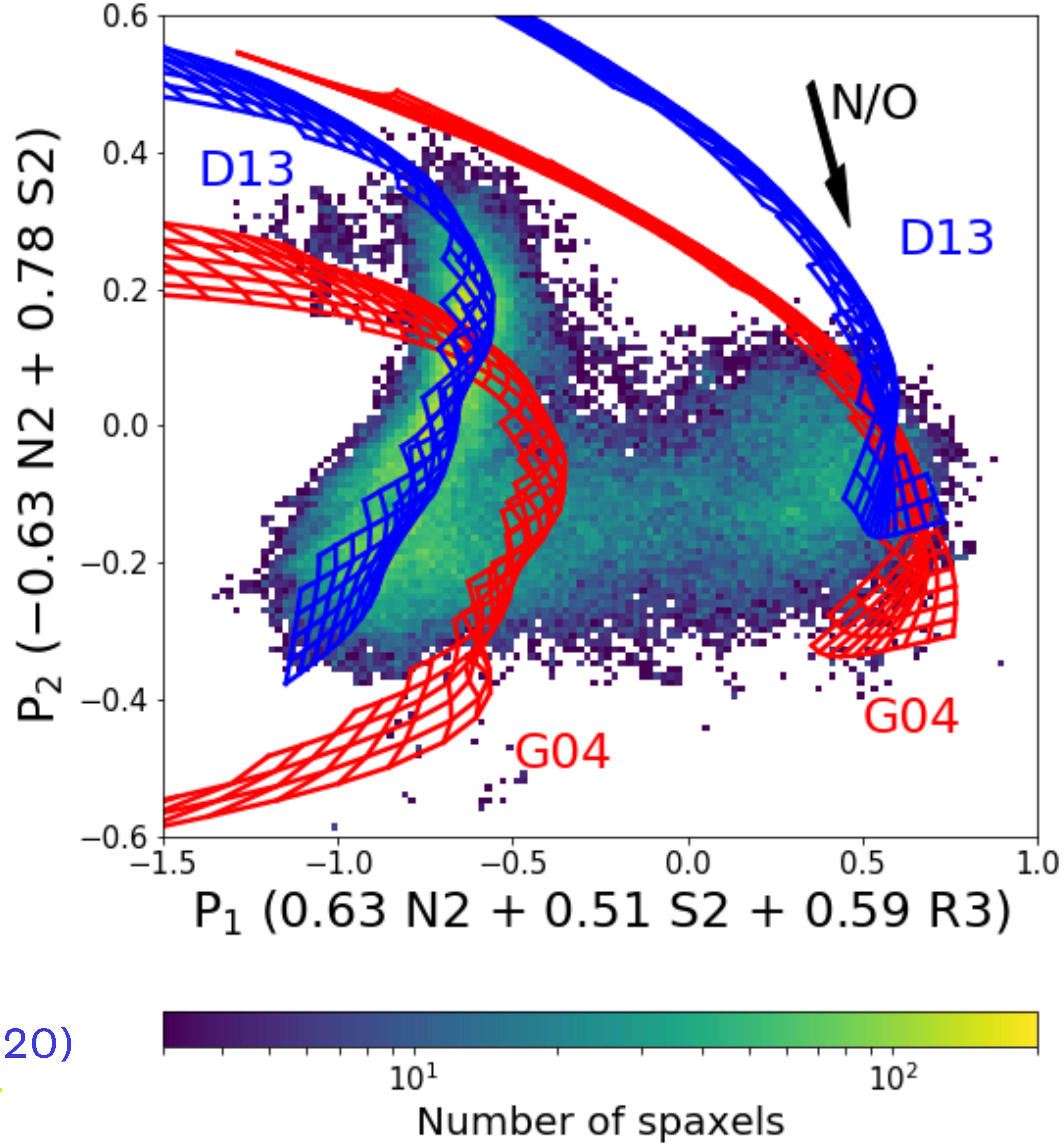

Ji & Yan (2020)

Constraining the input SED

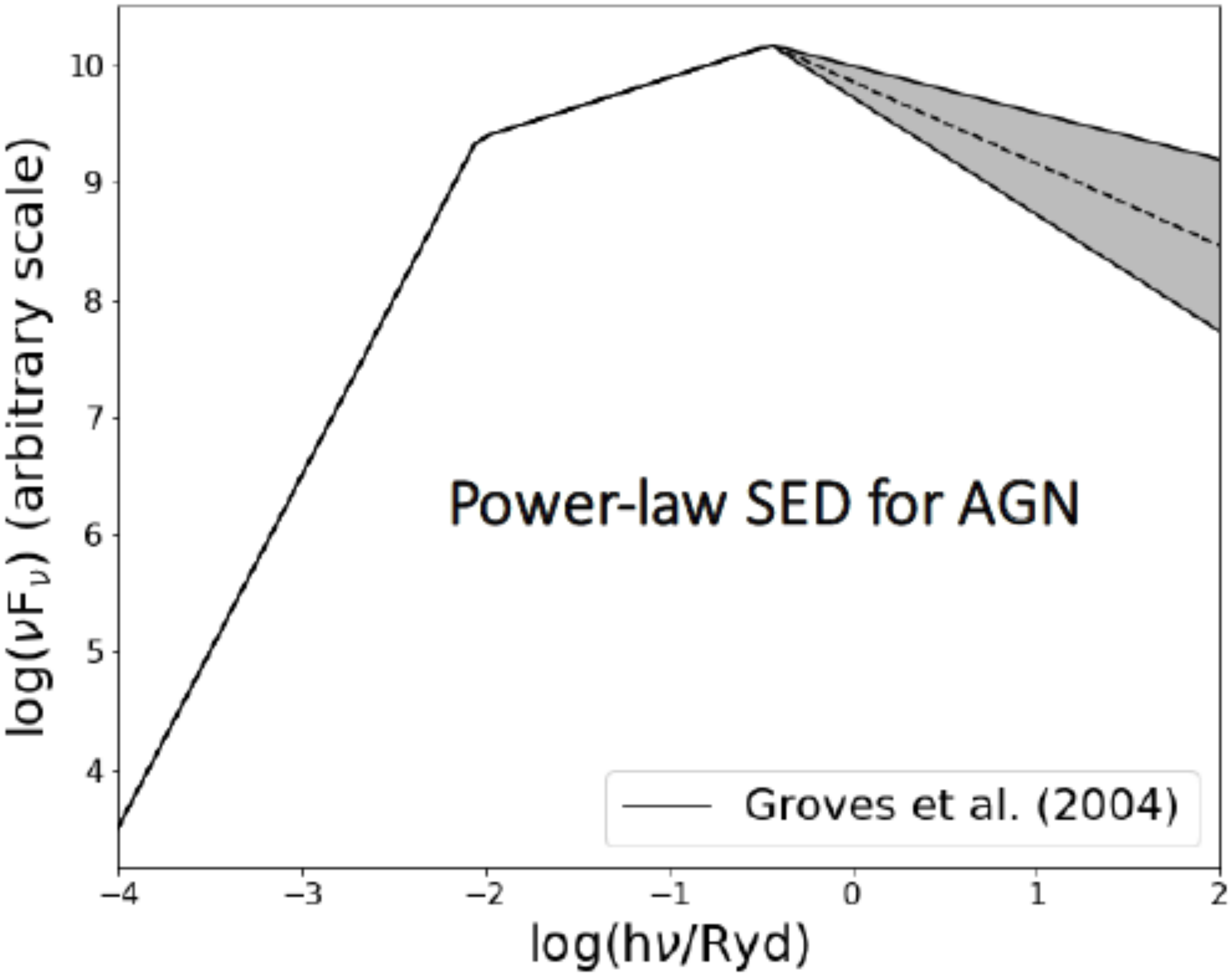

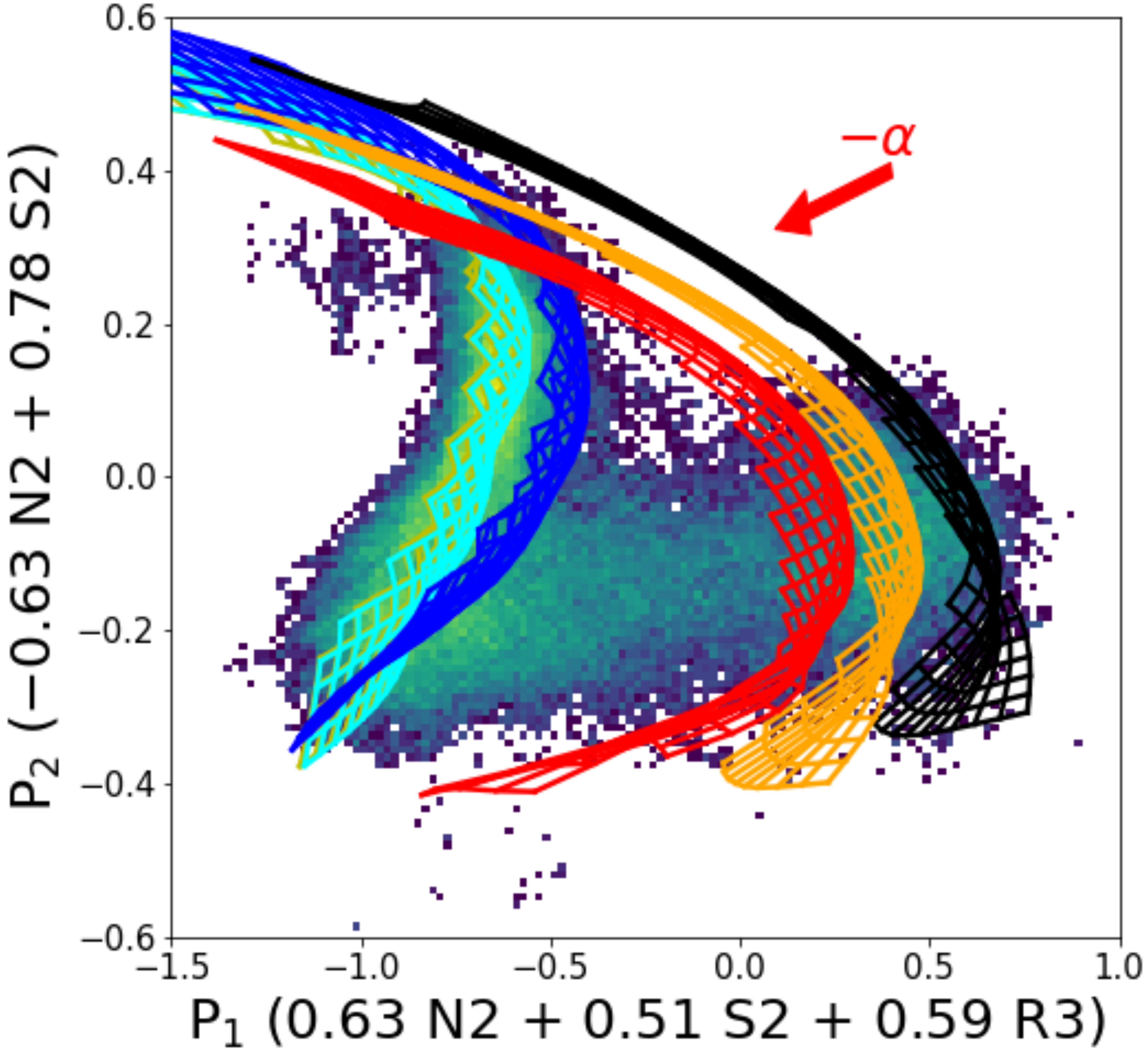

Ji & Yan (2020)

Consistency with other line ratios

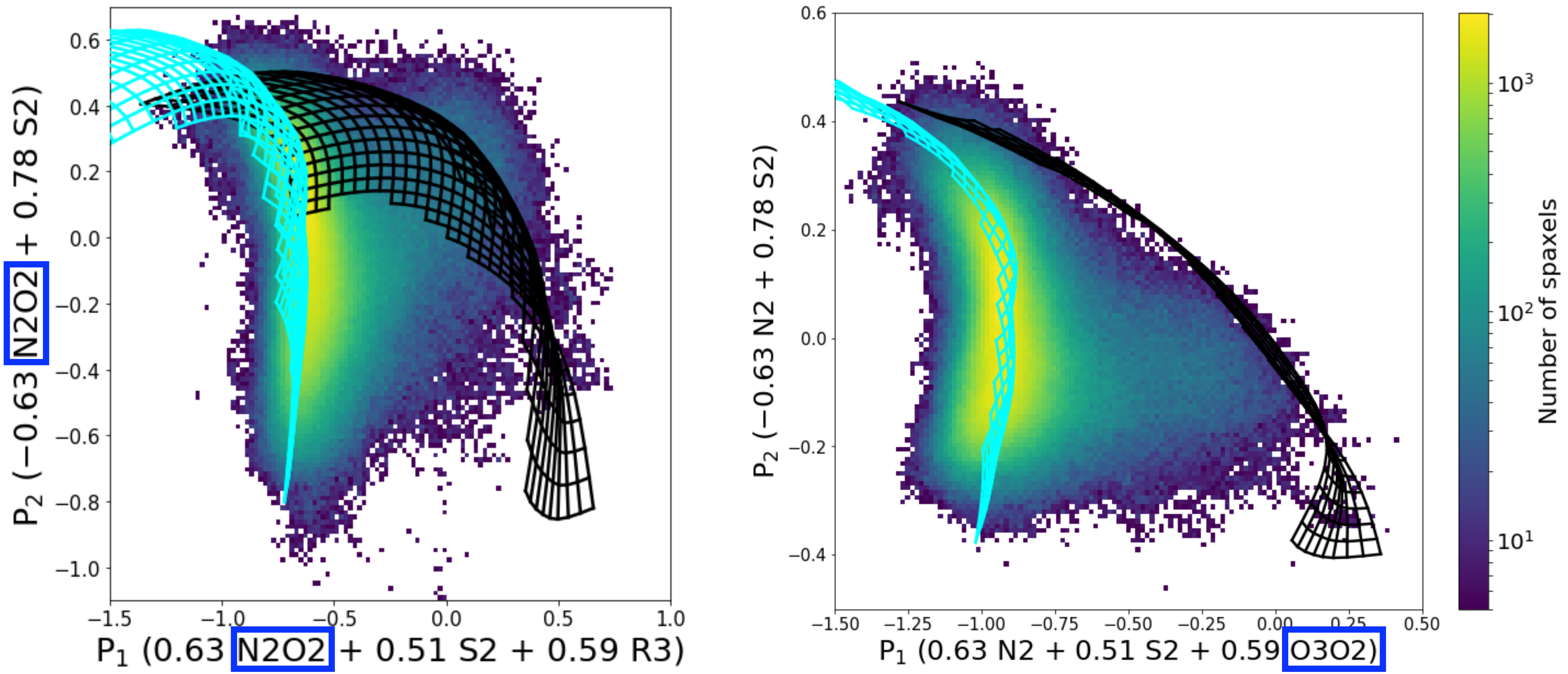

Not all models in the literature are consistent with the data

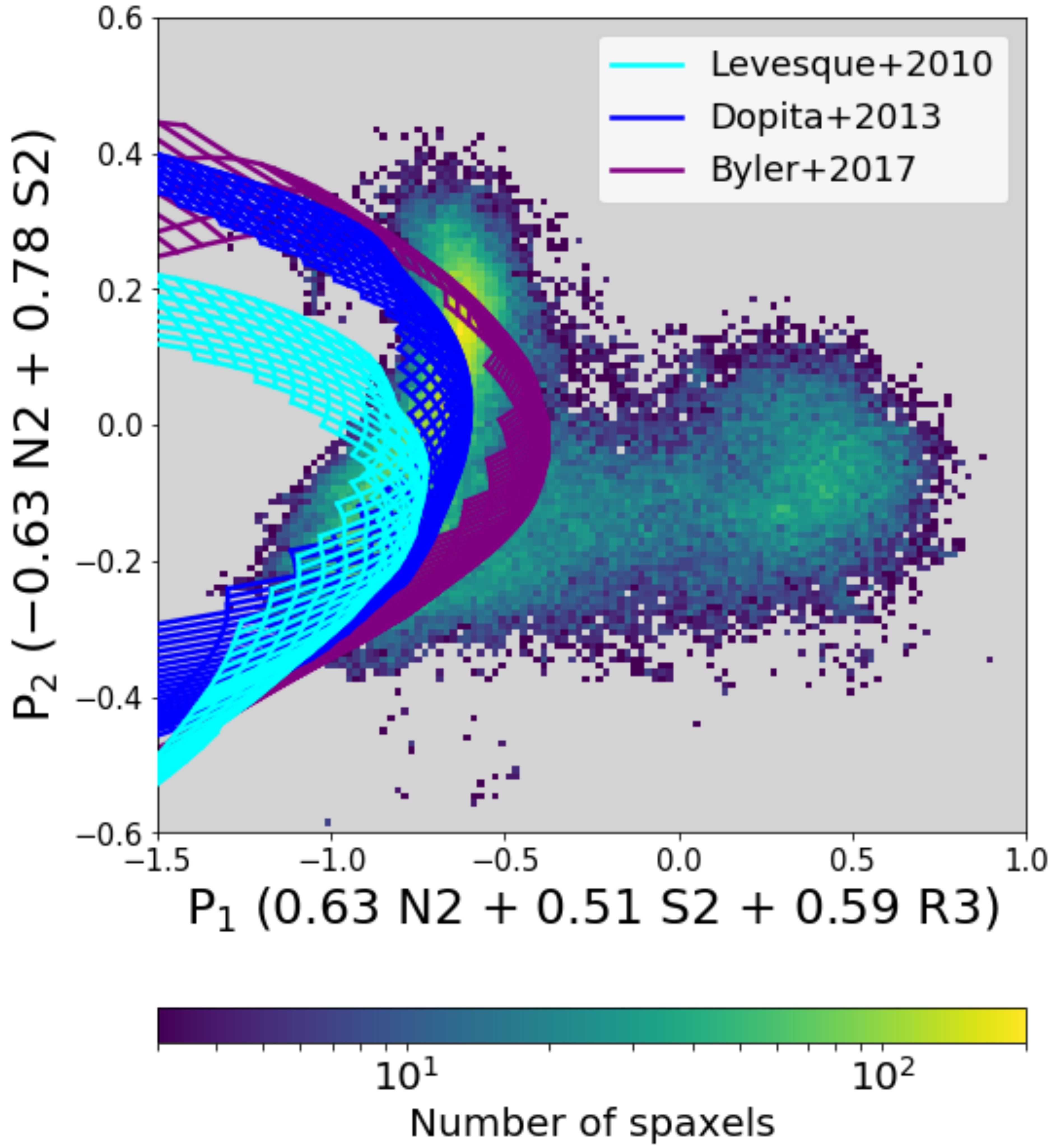

Models that appear to be consistent with the data in the BPT diagrams are not always consistent with the data in 3D.

Incorrect models lead to discrepancies among different methods

- Using Dopita (2013) models to constrain metallicity and ionization parameter
- Slightly harder input SED than our default SF model, and different dust depletion pattern.

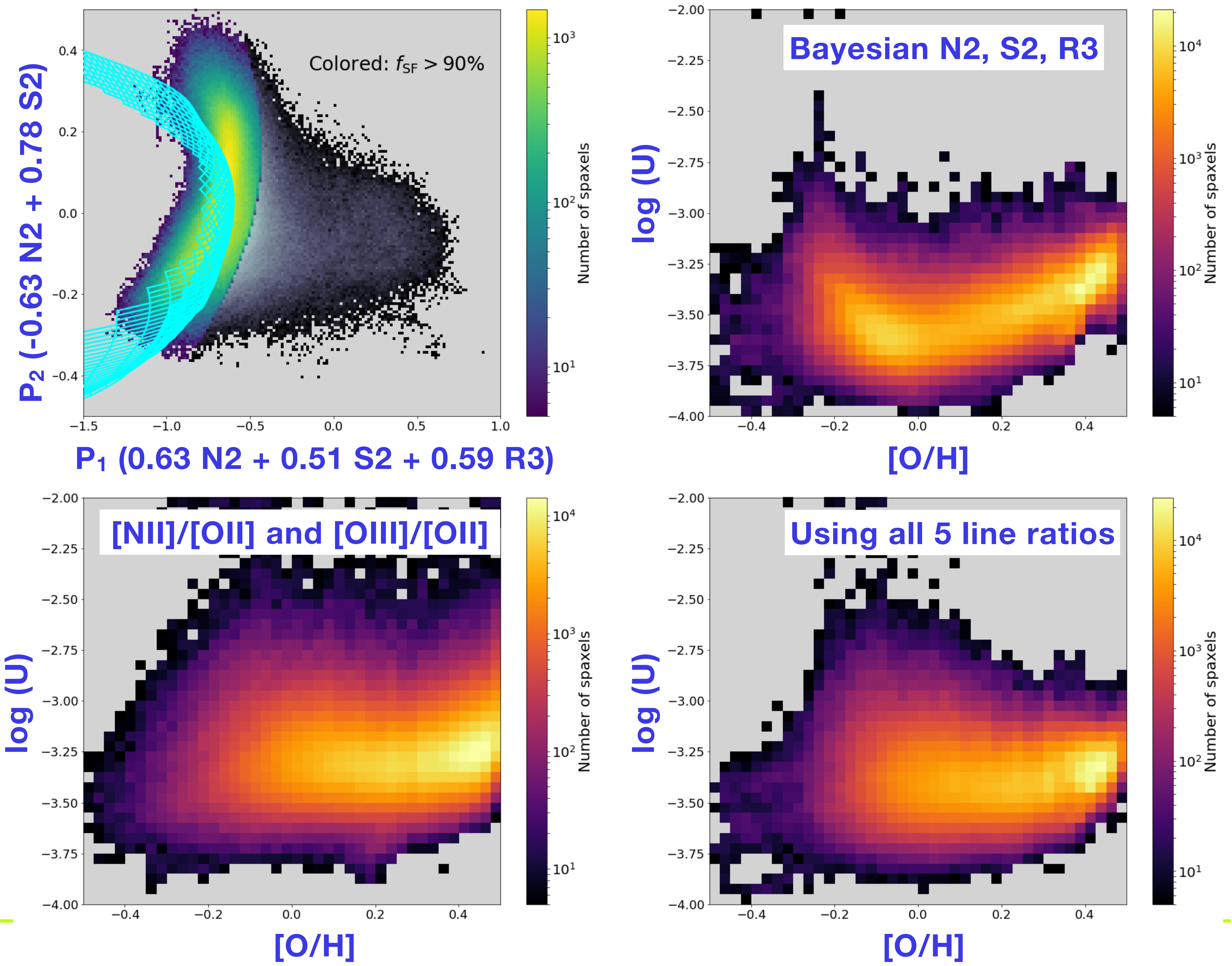

Ji & Yan, in prep

Incorrect models lead to discrepancies among different methods

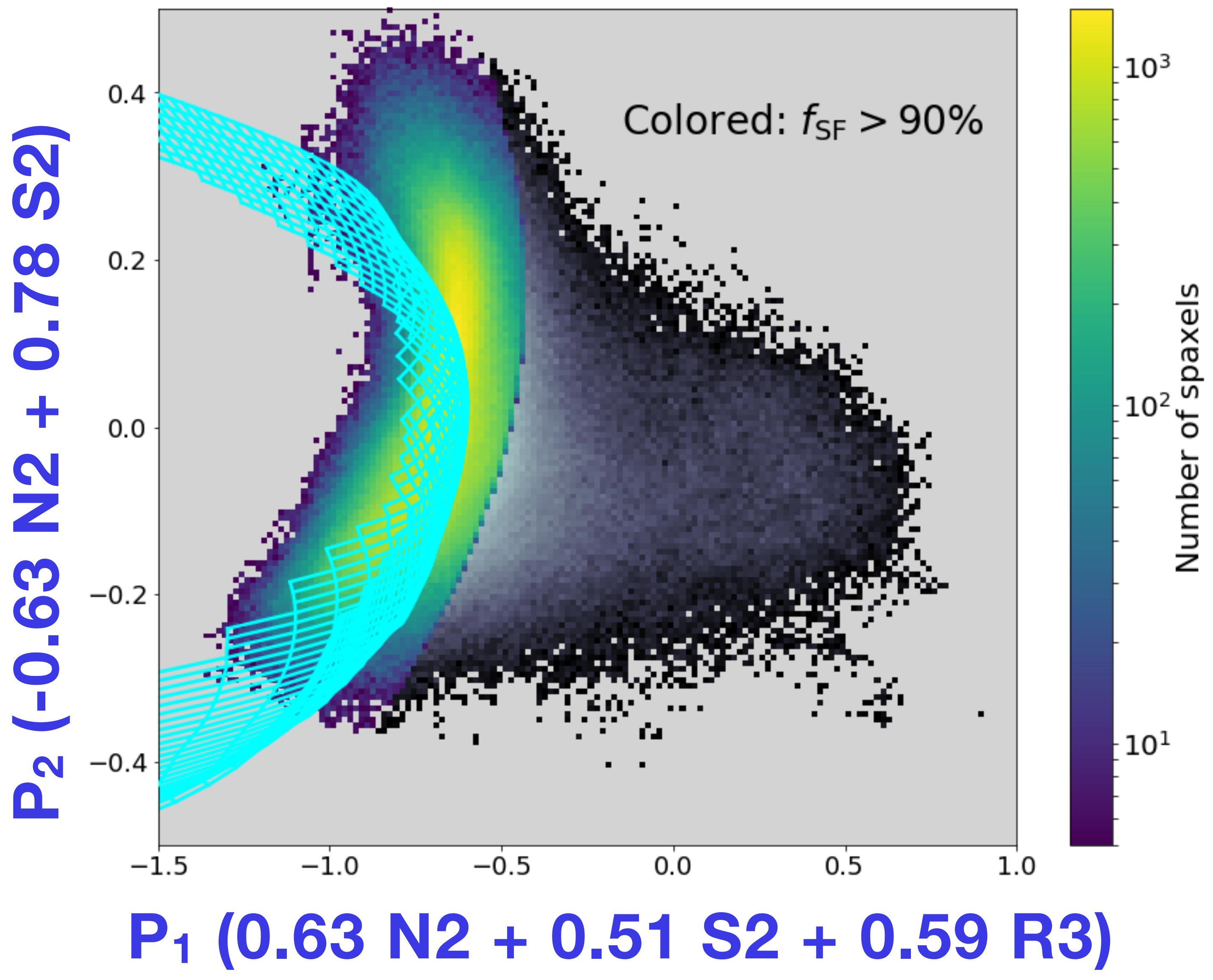

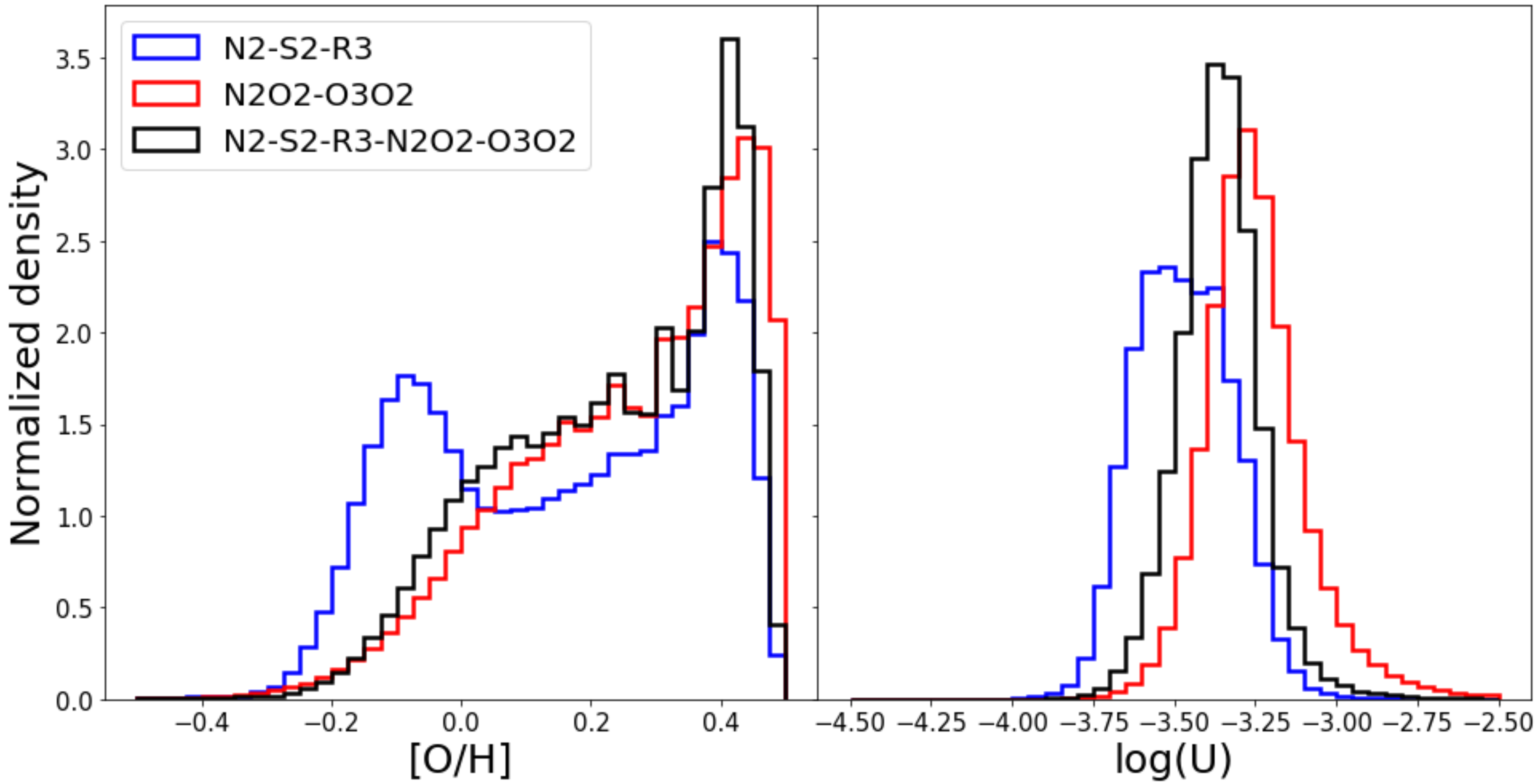

Ji & Yan, in prep

Correct models lead to consistent results among different methods

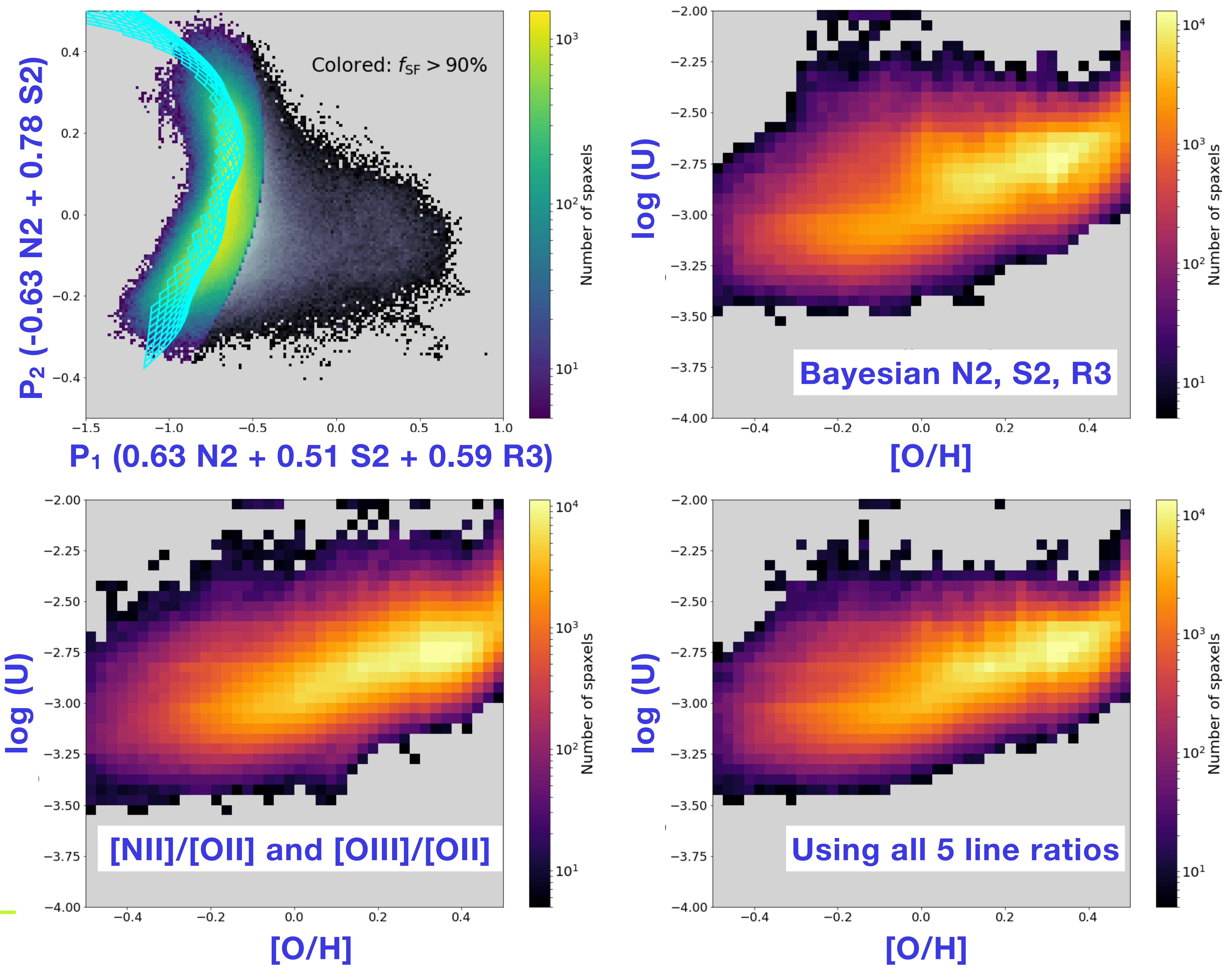

Ji & Yan, in prep

Correct models lead to consistent results among different methods

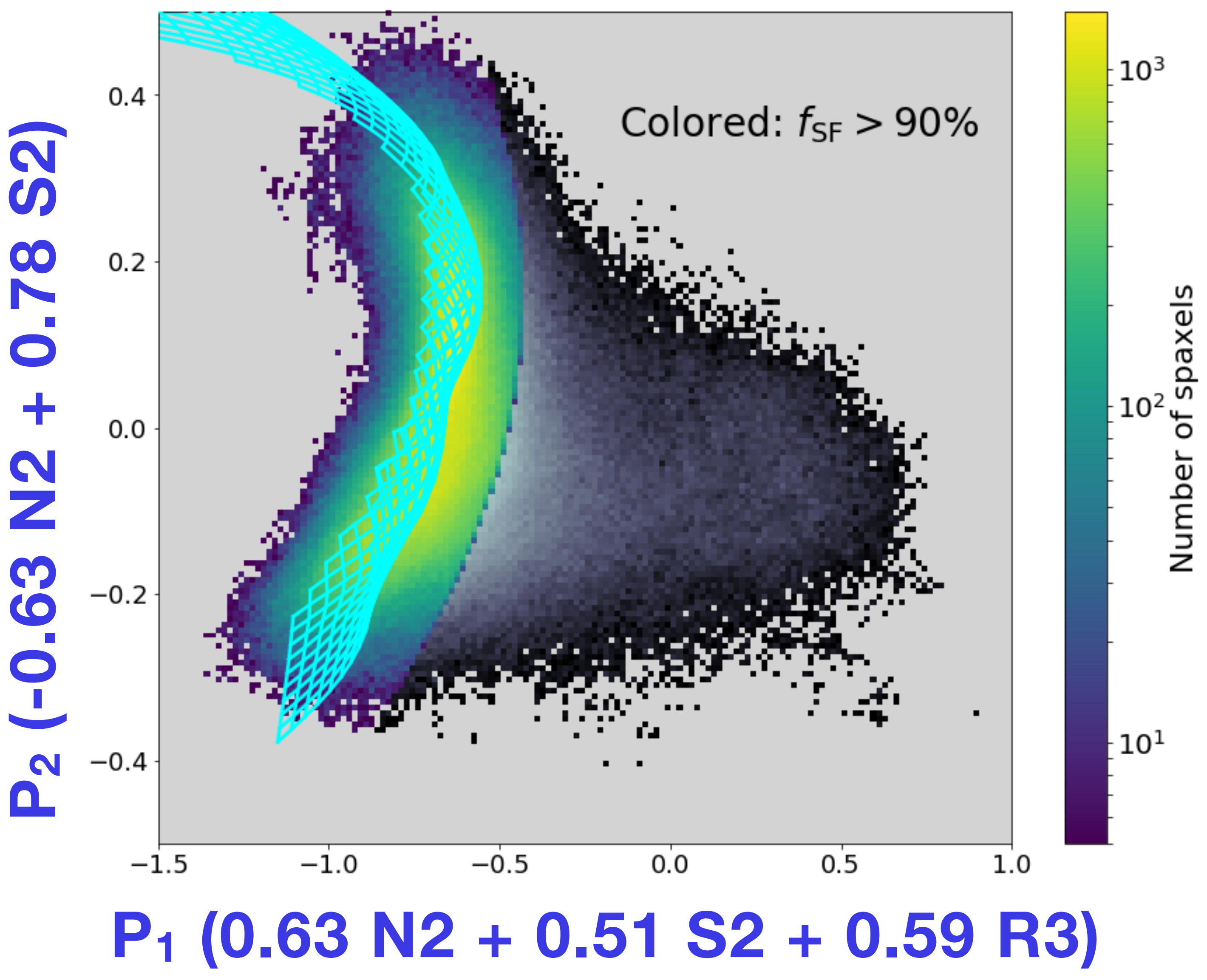

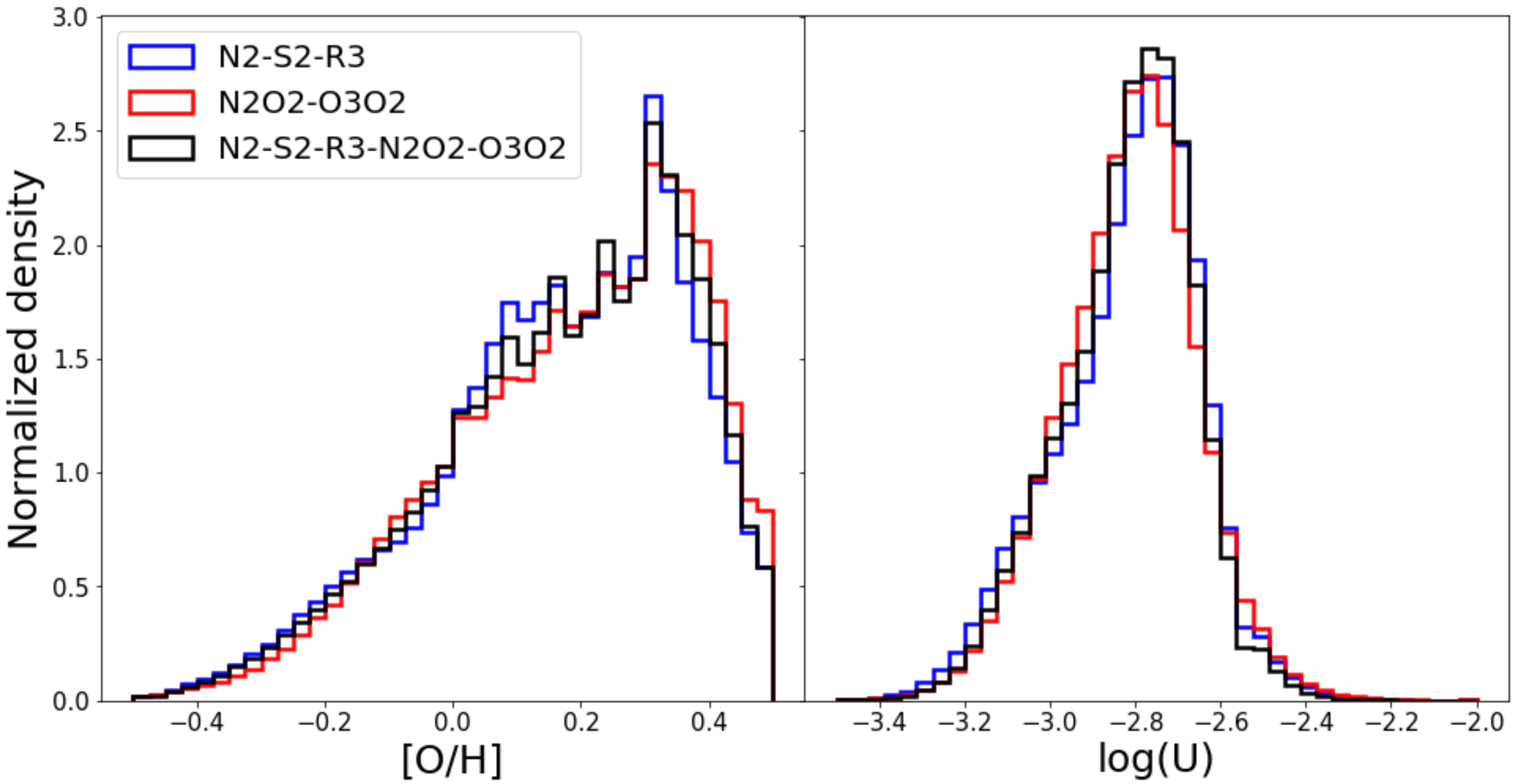

Ji & Yan, in prep

Inconsistent Lines: [OI] and [SIII]

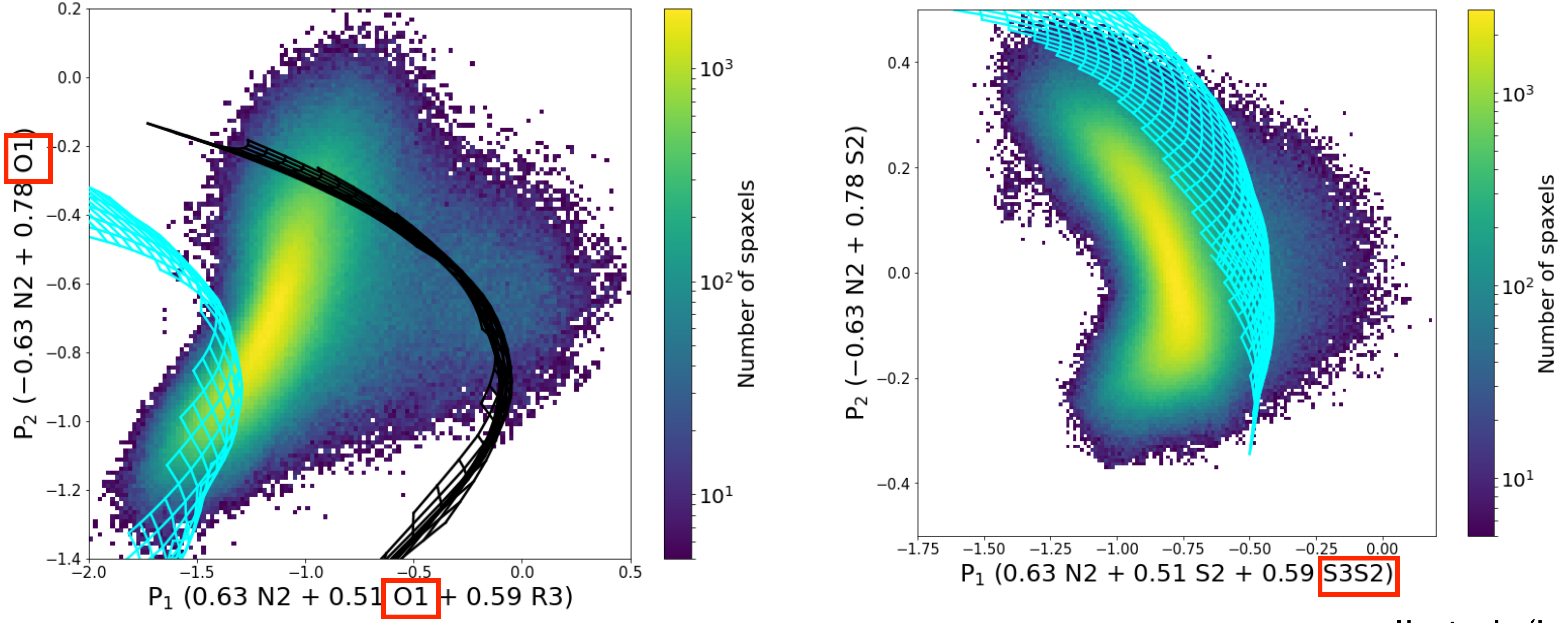

Ji et al. (in prep)

- [OI] is under-predicted by 0.15-0.5 dex; [SIII] is over-predicted by 0.5 dex.

Precision gas astrophysics
in the same style as precision cosmology

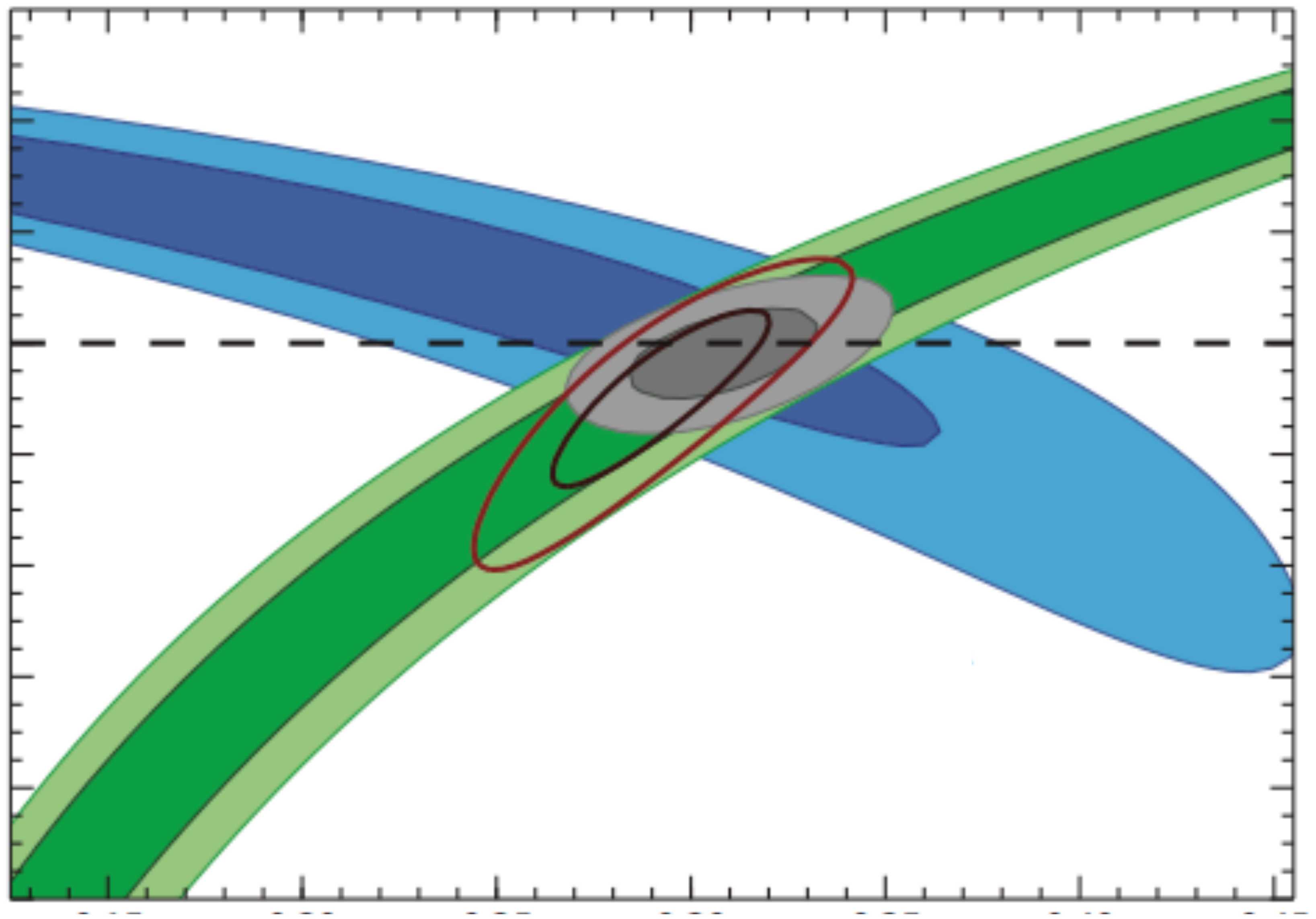

A roadmap:

Precision gas astrophysics in the same style as precision cosmology

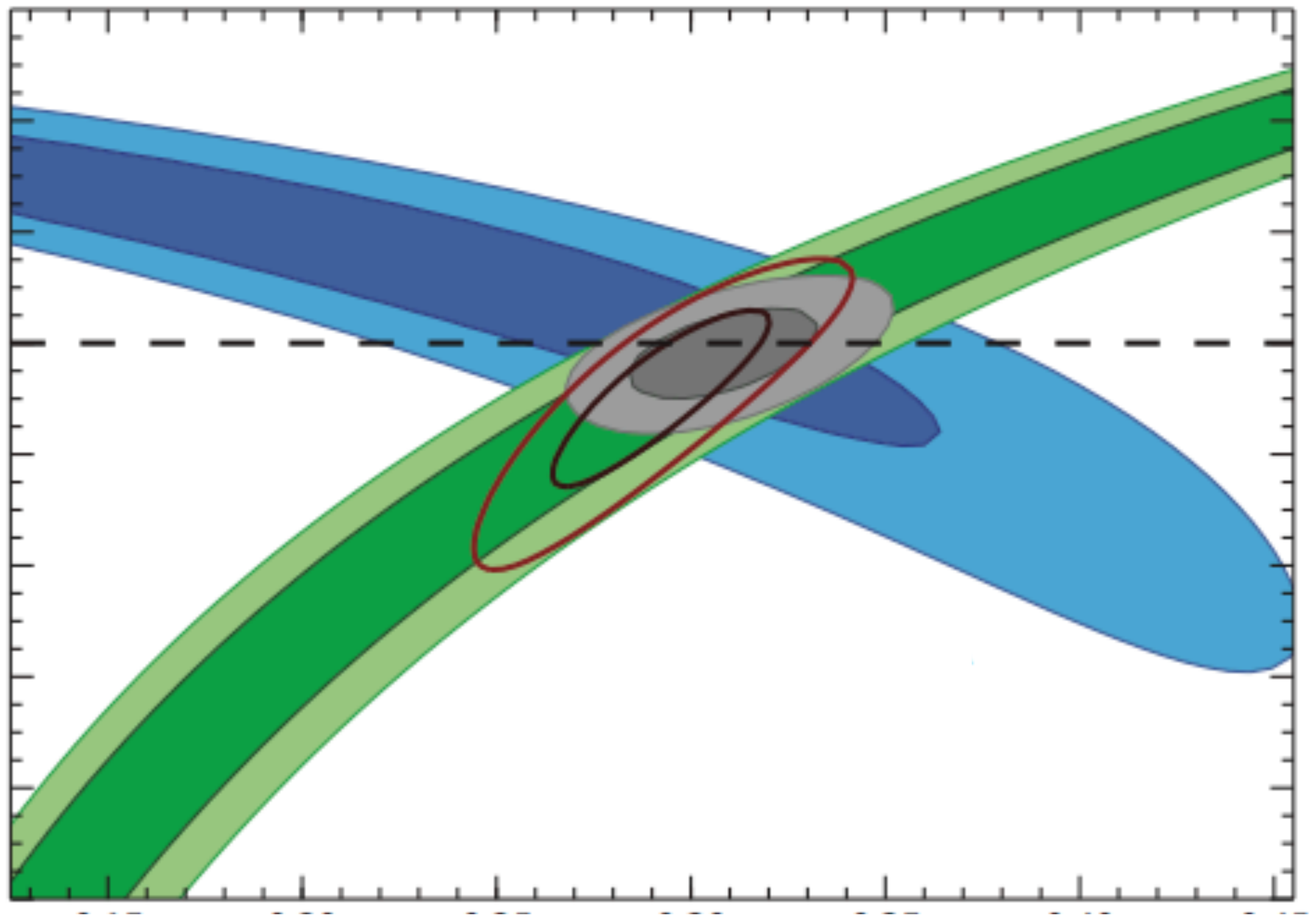

A roadmap:

- Identify and fix the problematic lines.

Precision gas astrophysics in the same style as precision cosmology

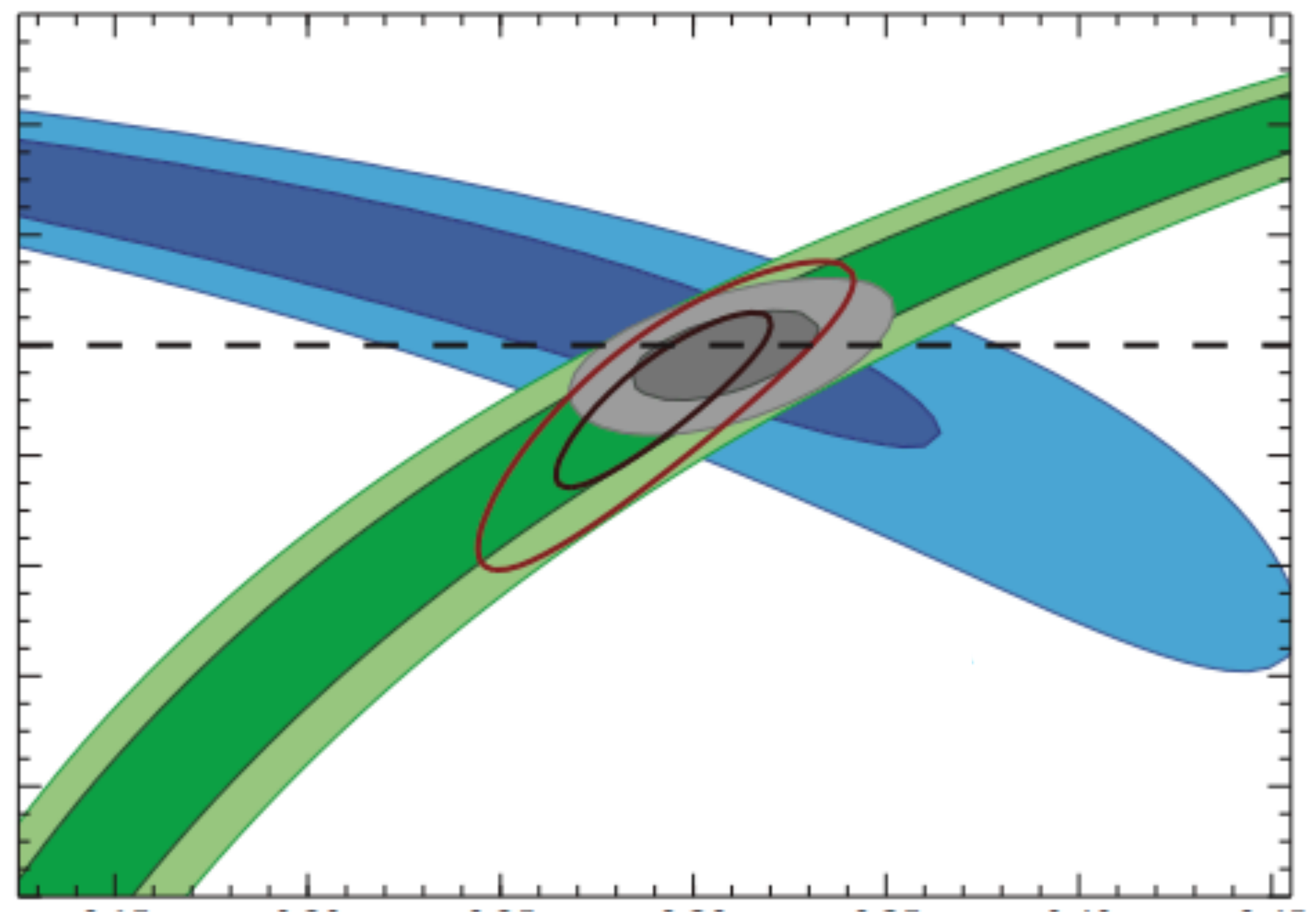

A roadmap:

- Identify and fix the problematic lines.
- Establish a metric to quantify the consistency between data and model surface in higher dimensions.

Precision gas astrophysics in the same style as precision cosmology

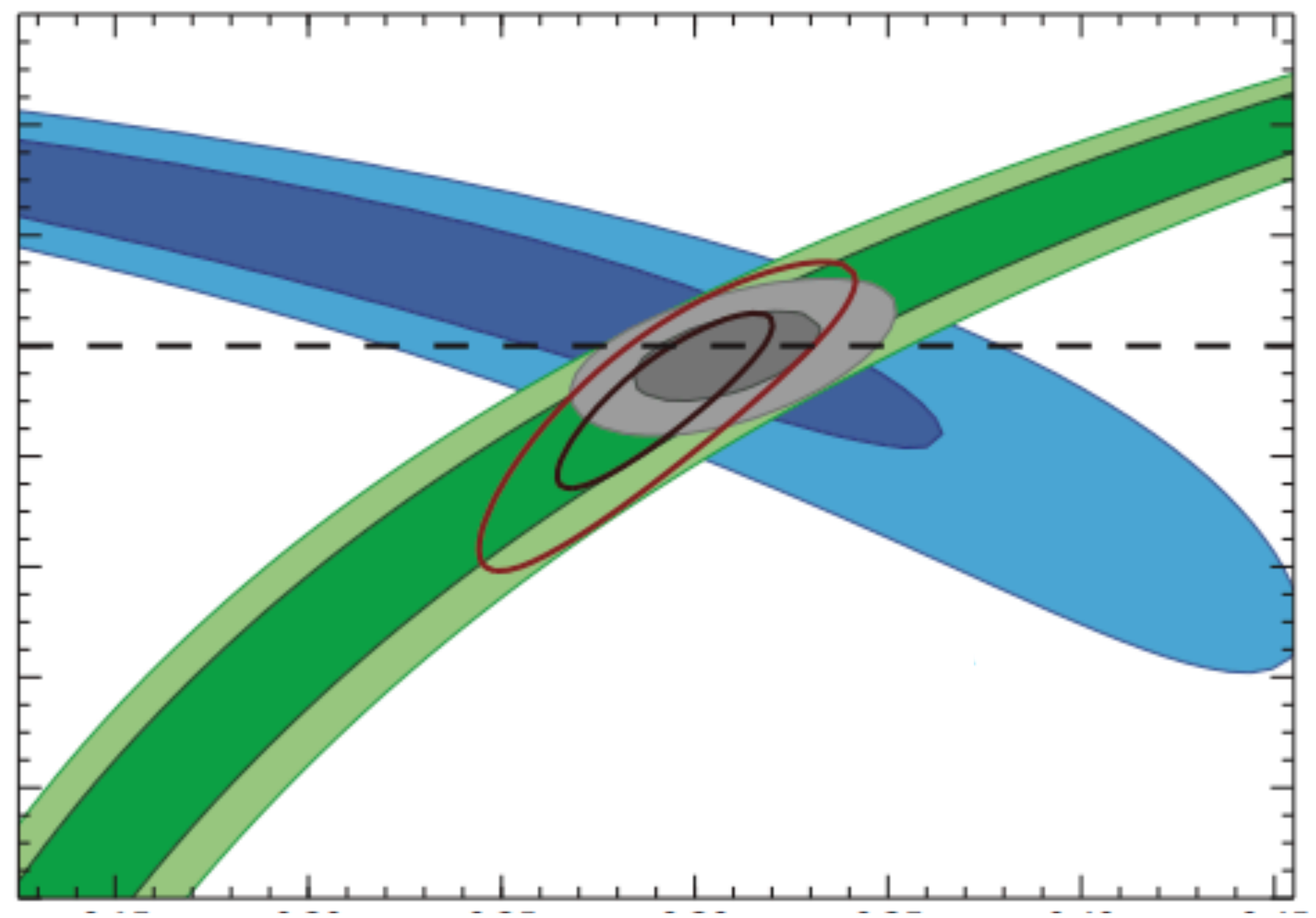

A roadmap:

- Identify and fix the problematic lines.
- Establish a metric to quantify the consistency between data and model surface in higher dimensions.
- Parameterize the input assumptions: SED, N/O prescription, dust depletion pattern.

Precision gas astrophysics in the same style as precision cosmology

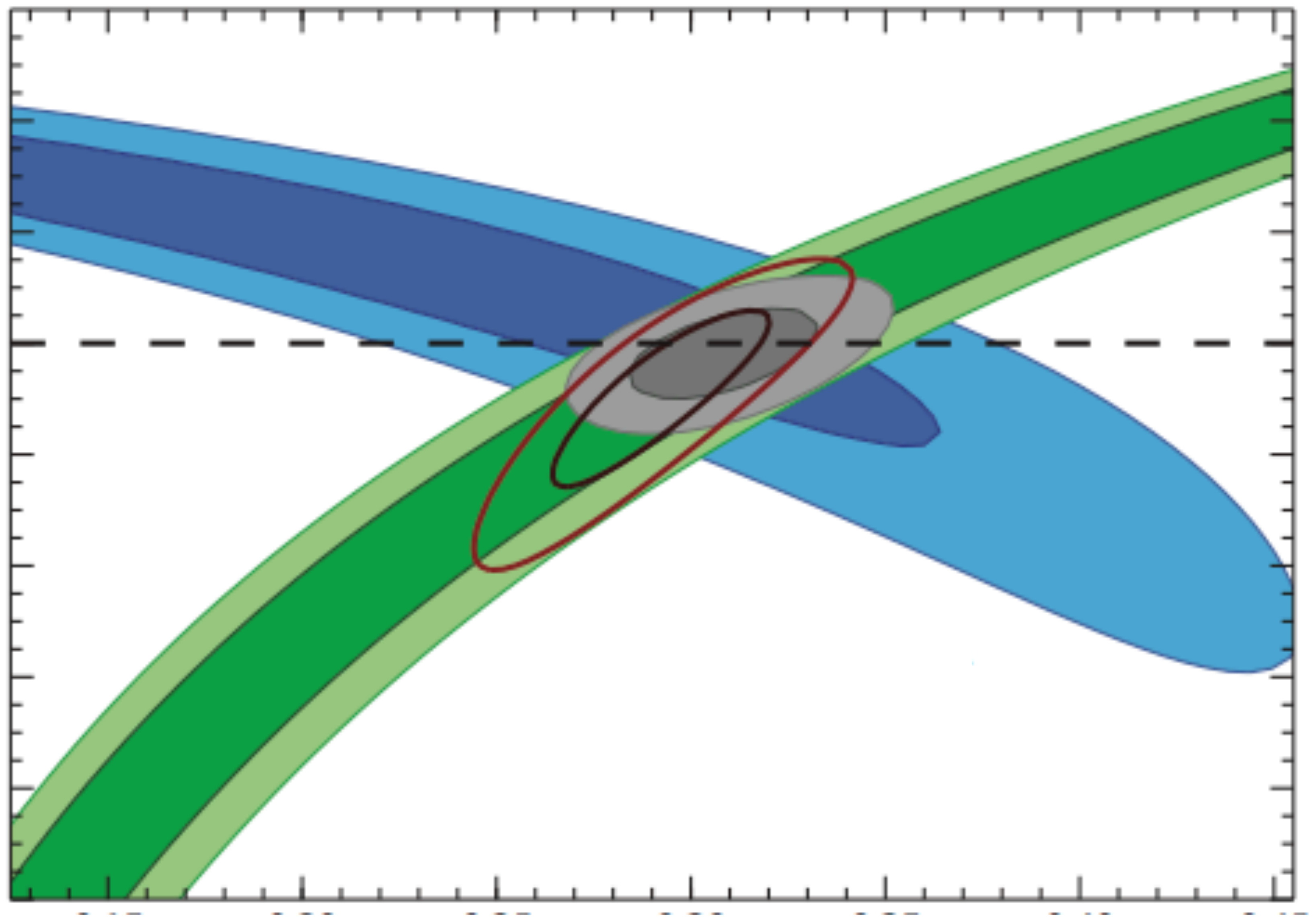

A roadmap:

- Identify and fix the problematic lines.
- Establish a metric to quantify the consistency between data and model surface in higher dimensions.
- Parameterize the input assumptions: SED, N/O prescription, dust depletion pattern.
- Constrain the average values and identifies the source of scatters.

Precision gas astrophysics in the same style as precision cosmology

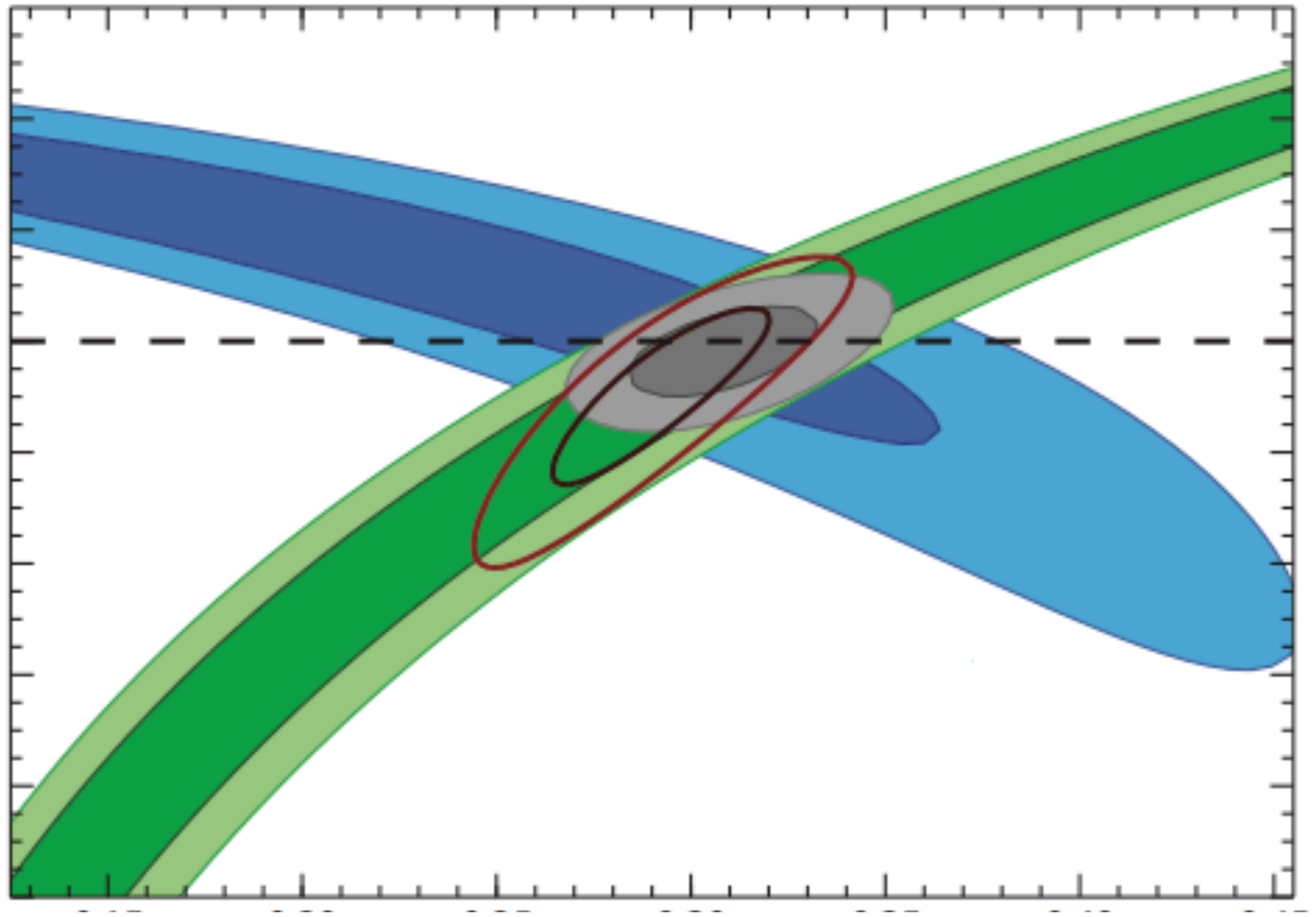

A roadmap:

- Identify and fix the problematic lines.
- Establish a metric to quantify the consistency between data and model surface in higher dimensions.
- Parameterize the input assumptions: SED, N/O prescription, dust depletion pattern.
- Constrain the average values and identifies the source of scatters.
- Unify the metallicity, ionization parameter measurements

Precision gas astrophysics in the same style as precision cosmology

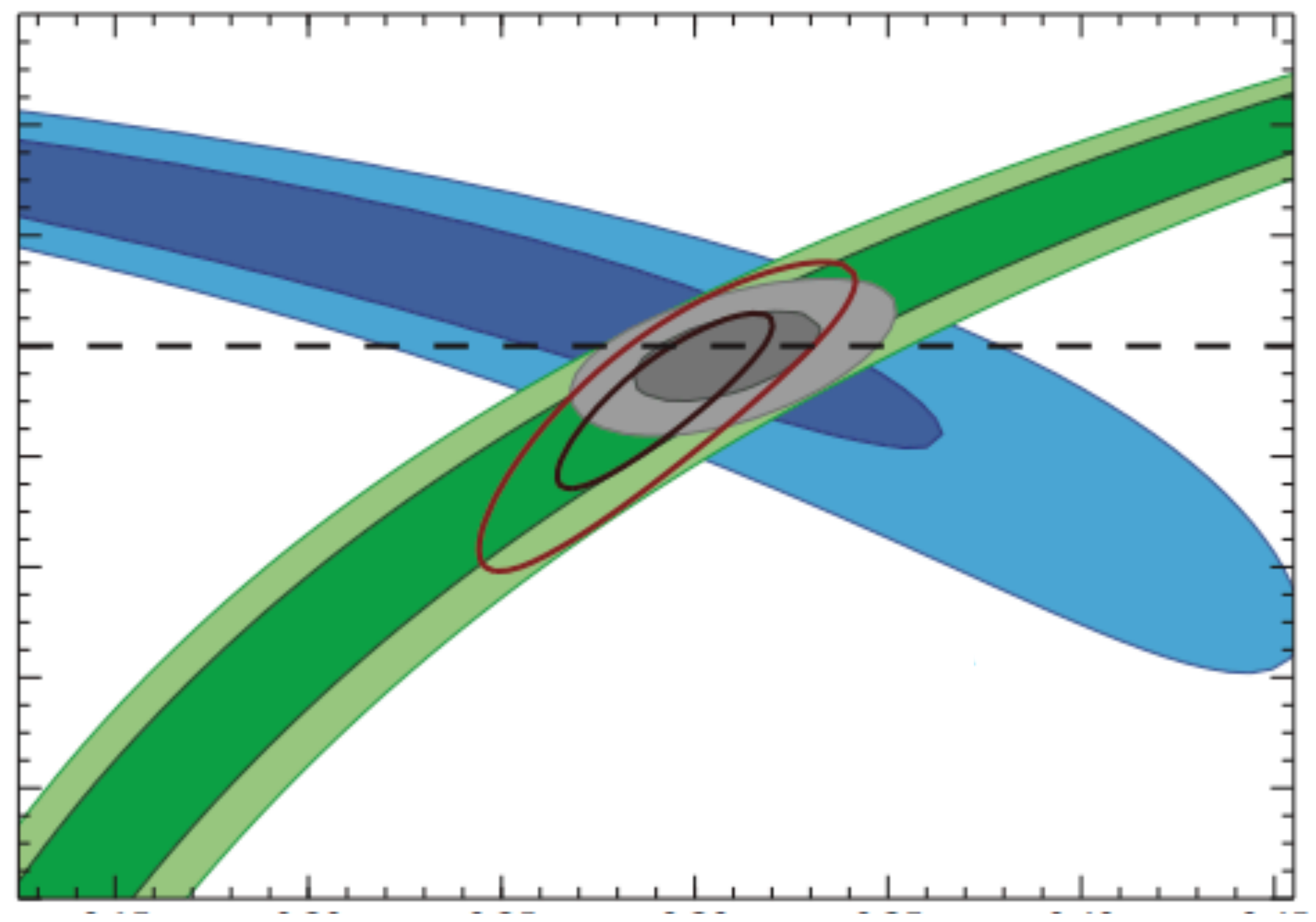

A roadmap:

- Identify and fix the problematic lines.
- Establish a metric to quantify the consistency between data and model surface in higher dimensions.
- Parameterize the input assumptions: SED, N/O prescription, dust depletion pattern.
- Constrain the average values and identifies the source of scatters.
- Unify the metallicity, ionization parameter measurements
- More accurate SF history and baryon-cycling history; better understanding of the feedback of SF and AGN.

Understand the microphysics of feedback

- Microphysics of feedback
  - Direct temperature and density measurements in multiple zones.
  - Constrain the turbulent energy injection scale through velocity power spectrum and emissivity power spectrum (Medina et al. 2014)
  - Measure outflow velocity to discern the dominant energy and momentum source (Kim et al. 2018, Raskutti et al. 2017)
  - Map the magnetic field lines using intensity gradient and velocity gradient techniques (Lazarian et al. 2018, Hu et al. 2019)
- Connect small scale and large scale observations
  - Scale at which RMS turbulence velocity equals to sound speed : ~0.03 pc
  - Sizes of self-gravitating cores: ~0.1 pc
  - Molecular cloud and HII regions (tens of pc)
  - MaNGA resolution ~ 1-2 kpc

Need to bridge the small and large scales!

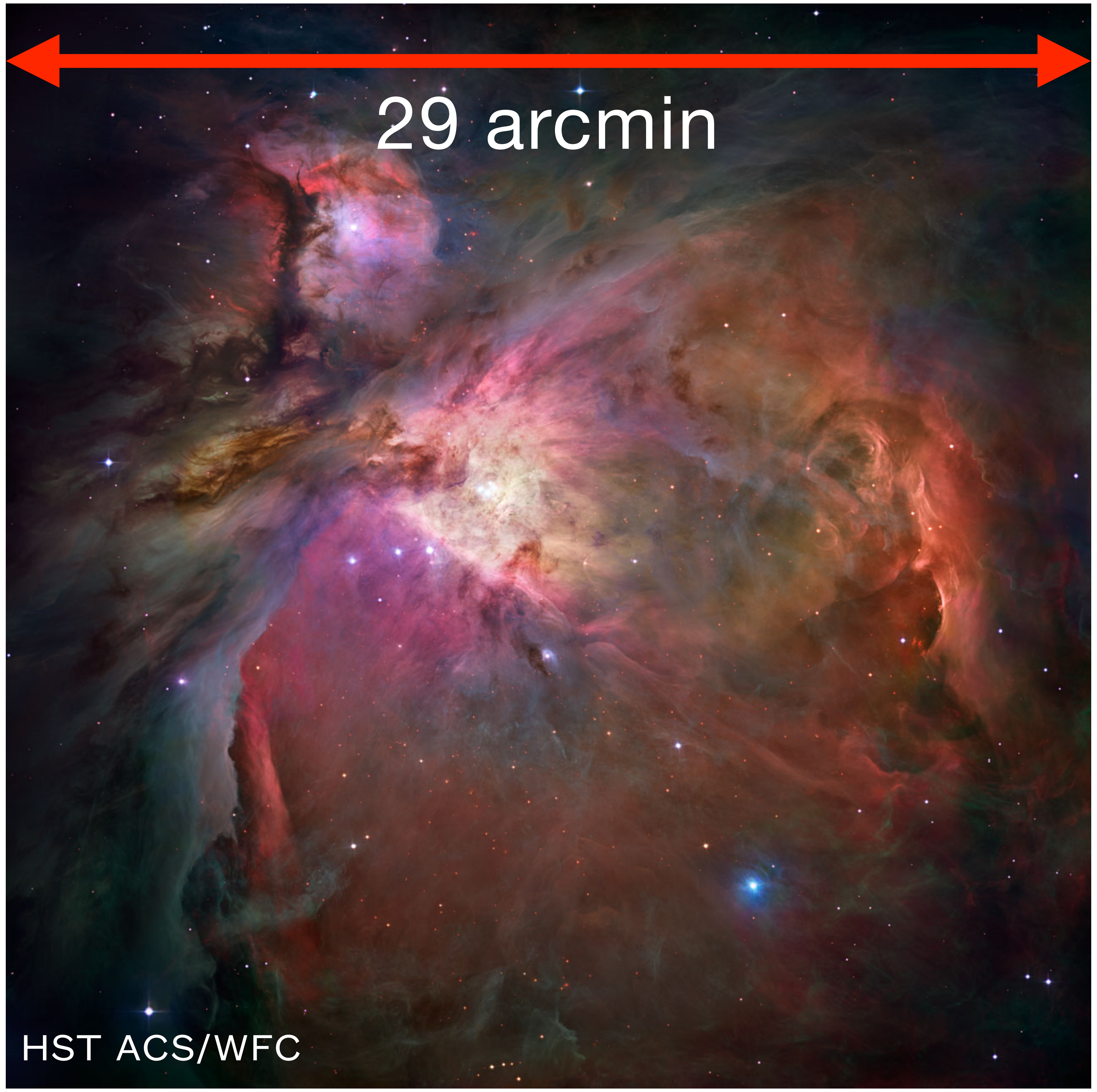

1 arcsec = 0.002 pc

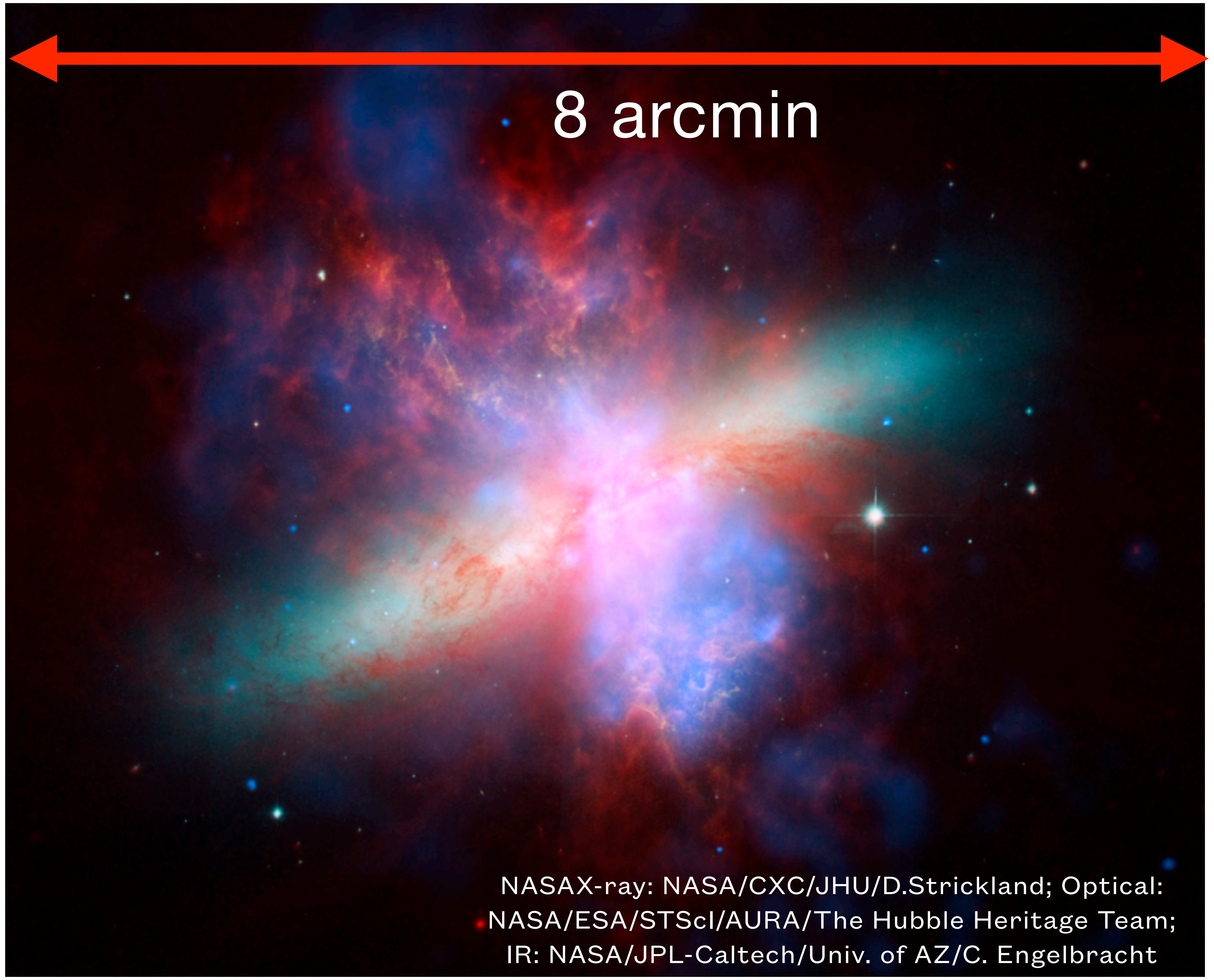

1 arcsec = 170 pc

How to cover the intermediate scale: 0.1-100pc

To resolve 0.1pc

- Resolving 0.1pc on the ground without AO (seeing 1”)
  ➡ Distance < 20kpc
  ➡ Sources in the MW
- Distances of MW HII regions: 0.4 -3 kpc
  ➡ requires a spatial resolution of 10-20”.
- We do not need large telescopes — they have too fine a plate scale, which is an overkill in spatial resolution.
  A small telescope of 15-30 cm and fast focal ratio would suffice!

How to cover the intermediate scale: 0.1-100pc

To cover 100pc

- Dynamic range = spatial coverage / spatial resolution
- Dynamic range of an instrument is set by the total number of independent spectral traces:

  Biggest MaNGA bundle: ~12

  All MaNGA bundles combined: ~40

  VLT/MUSE: ~120 (24 spectrographs)
- Cover a dynamic range of 1000 (0.1-100 pc) needs a dedicated survey instrument with lots of spectrographs!
- The same system would be able to cover LMC/SMC at 10pc resolution and cover M31/M33 at 100pc resolution.

Need a moderately high spectral resolution

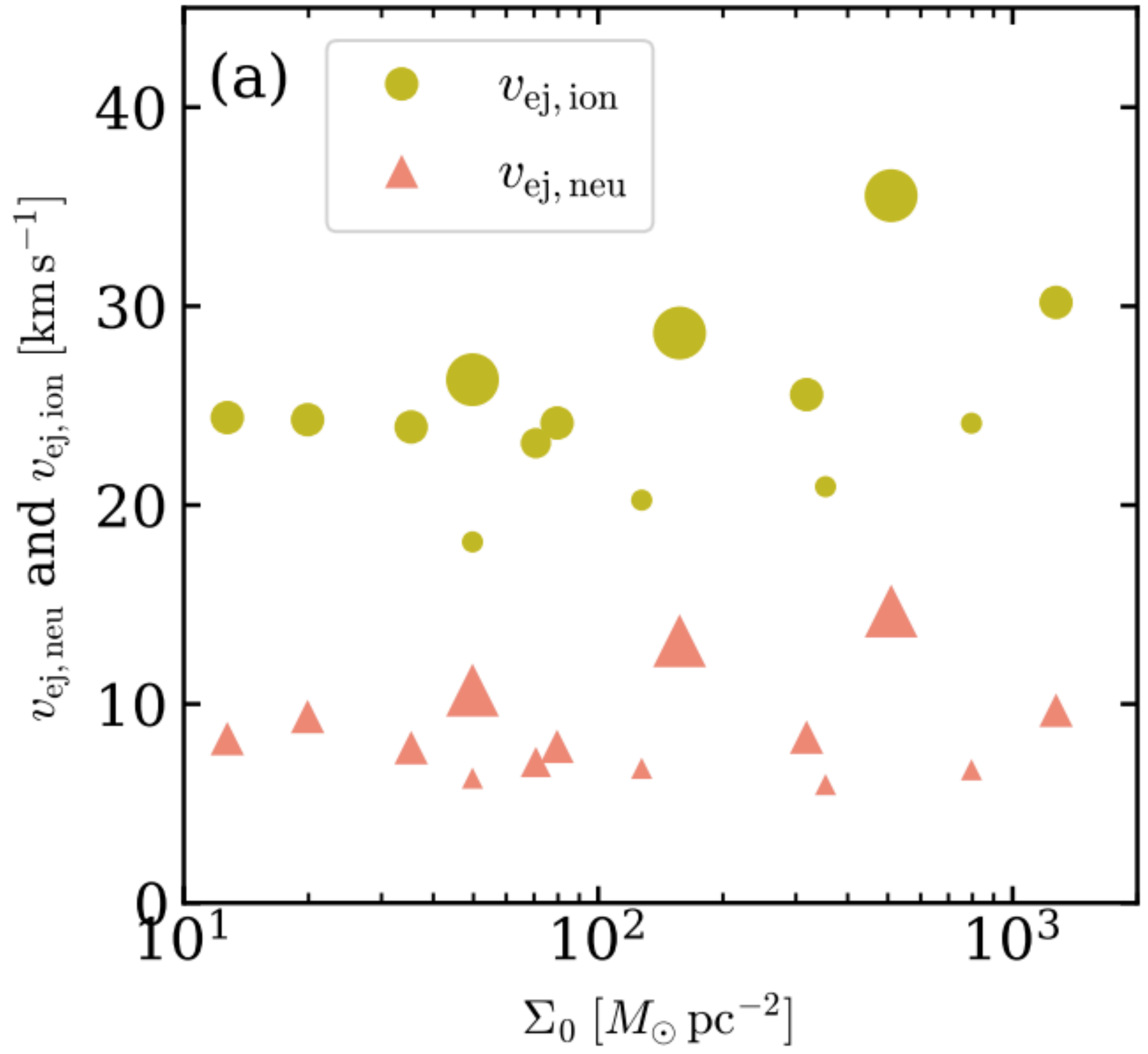

Ionized outflows are on the order of 20km/s.

Require R~15,000

Kim, Kim, Ostriker (2018b)

Need a moderately high spectral resolution

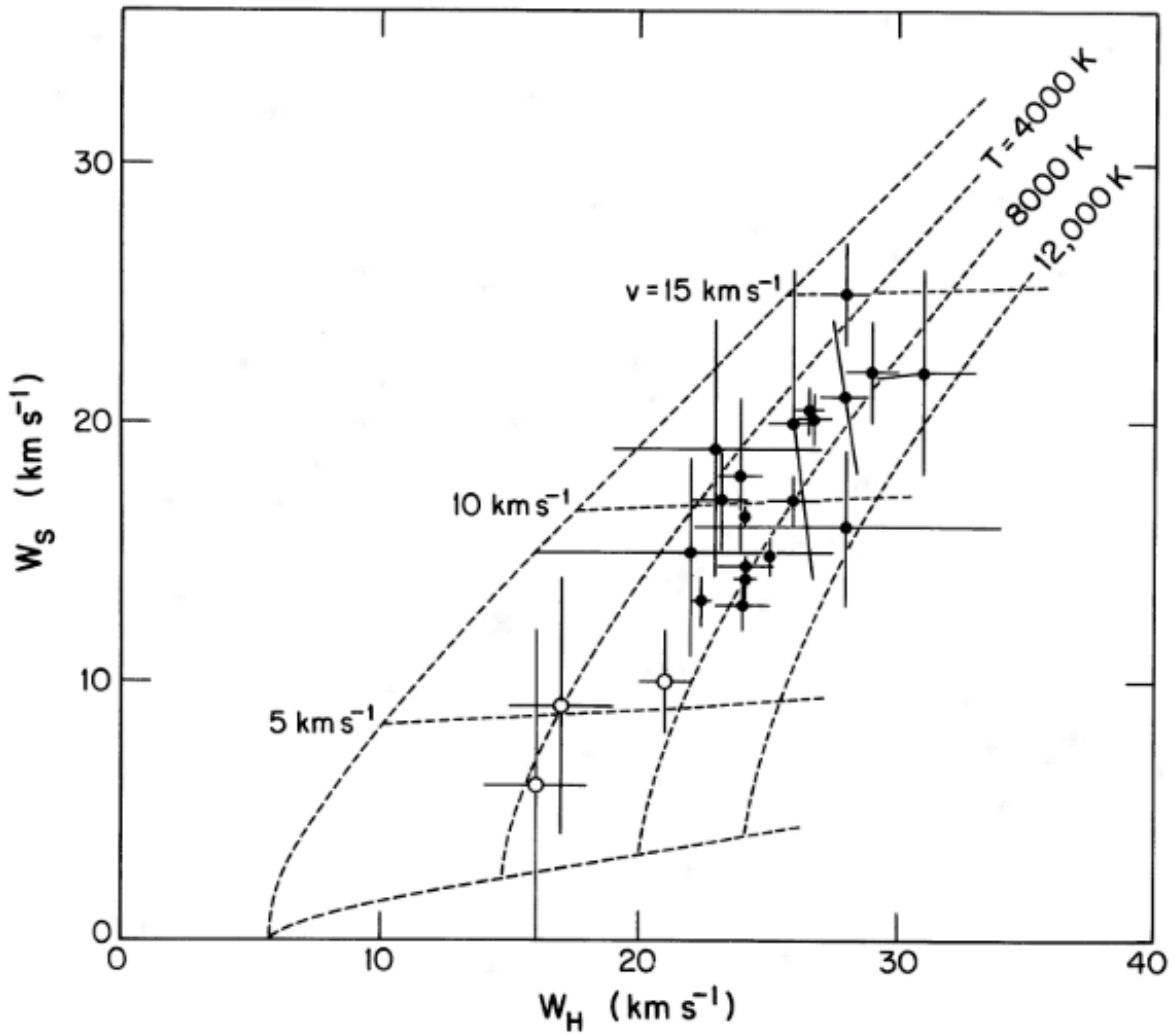

Reynolds (1988)

High resolution can help separate thermal from non-thermal broadening

- Light atoms (H) has both thermal and non-thermal broadening
- Heavy atoms (like O, N, S) is dominated by non-thermal broadening

Science Requirements

Science Requirements

- Spectroscopically map the scale of
  0.1 pc - 100 pc in the Milky Way
  10 pc - 5 kpc in the LMC and SMC
  100pc - 50 kpc in the M31 and M33

Science Requirements

- Spectroscopically map the scale of
  0.1 pc - 100 pc in the Milky Way
  10 pc - 5 kpc in the LMC and SMC
  100pc - 50 kpc in the M31 and M33

- Resolve 20km/s FWHM in velocity; R>=15,000

Science Requirements

- Spectroscopically map the scale of
  0.1 pc - 100 pc in the Milky Way
  10 pc - 5 kpc in the LMC and SMC
  100pc - 50 kpc in the M31 and M33

- Resolve 20km/s FWHM in velocity; R>=15,000

- Need an array of high spectral resolution integral field spectrograph paired with small telescopes

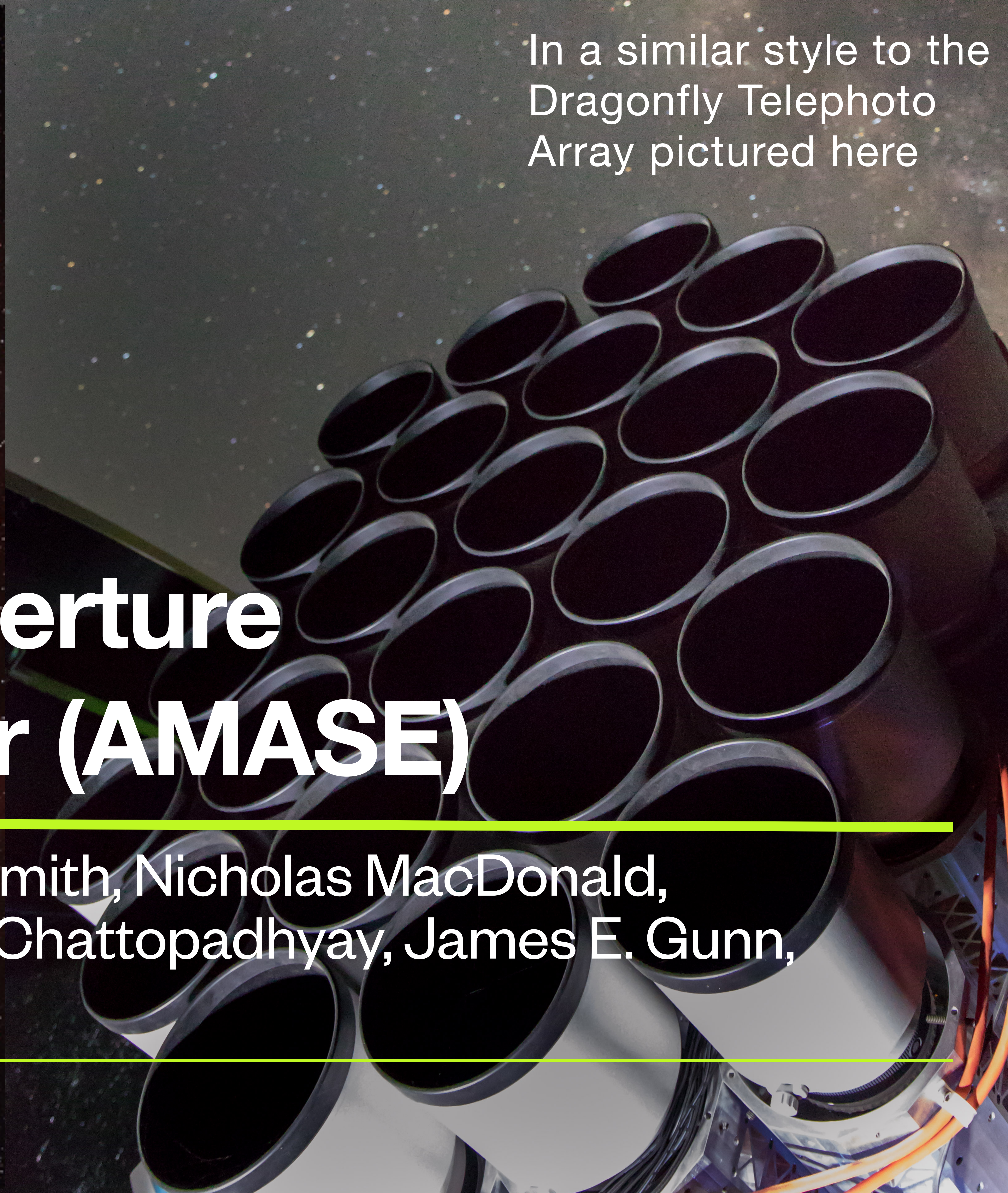

In a similar style to the Dragonfly Telephoto Array pictured here

Affordable Multiple Aperture Spectroscopy Explorer (AMASE)

Renbin Yan, Matthew Bershady, Michael Smith, Nicholas MacDonald, Dmitry Bizyaev, Kevin Bundy, Sabaysachi Chattopadhyay, James E. Gunn, Kyle Westfall, Marsha Wolf

Image credit: John Corban

Strategy to improve cost-effectiveness

- Generally, reduce beam width to enable the use of commercial off-the-shelf components, and take advantage of technology advances in CMOS sensors and lens coatings
- Thinner fibers

  ➡ shorter collimator focal length (for fixed spectral resolution)

  $$R = \frac{f_{\mathrm{coll}}}{d_{\mathrm{fiber}}} \frac{\lambda A}{r}$$

  ➡ smaller beam width

  ➡ smaller optics

- Thinner fibers

  ➡ less demagnification in order to use small-pixel CMOS sensors

Technology advance in CMOS

- Compared to top-end CCDs
  - Comparable quantum efficiency
  - Lower read noise
  - Higher electron capacity per unit area
  - Fast readout
  - Much lower cost

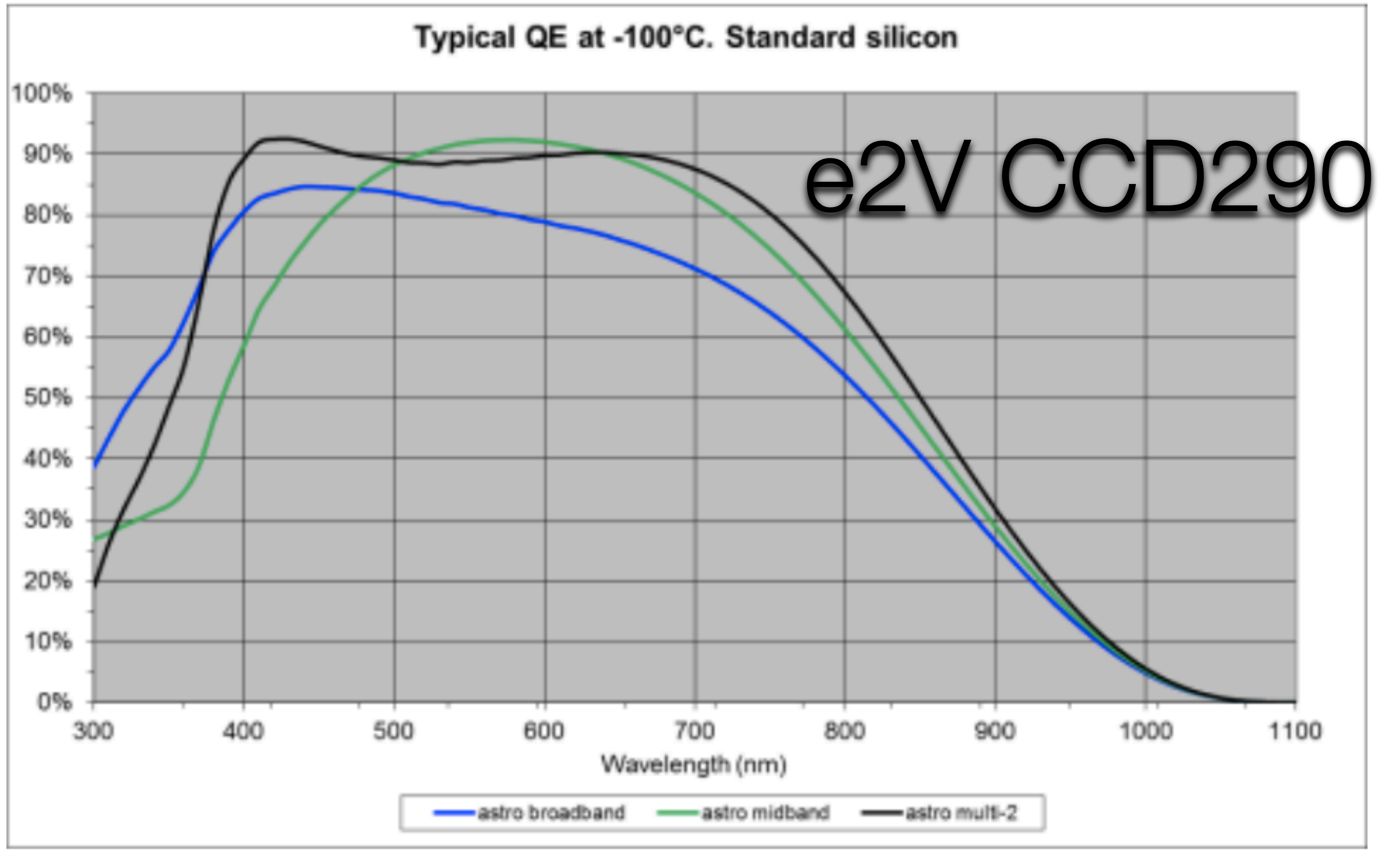

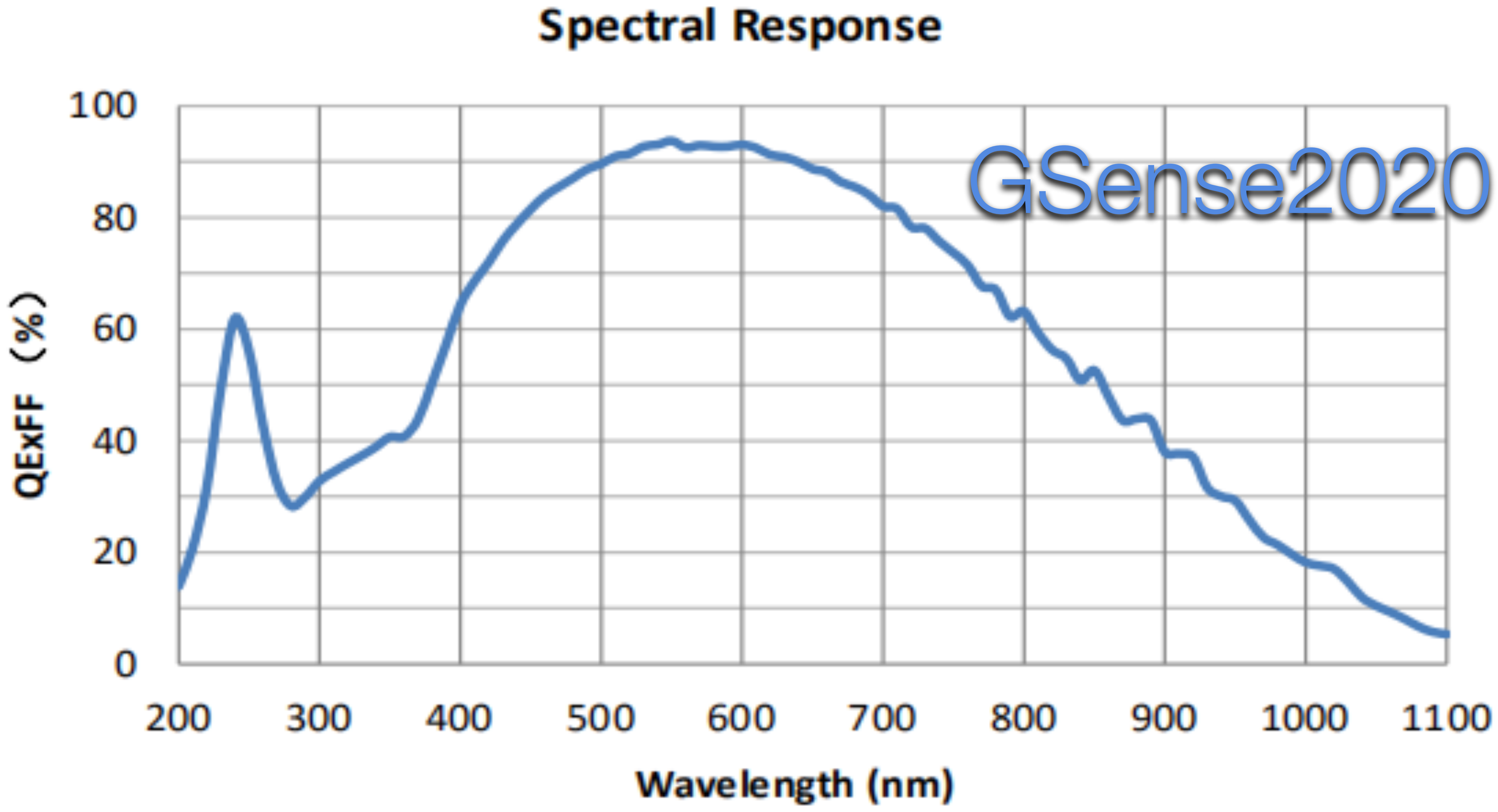

Technology advance in CMOS

- Compared to top-end (
  - Comparable quantum
  - Lower read noise
  - Higher electron capa
  - Fast readout
  - Much lower cost

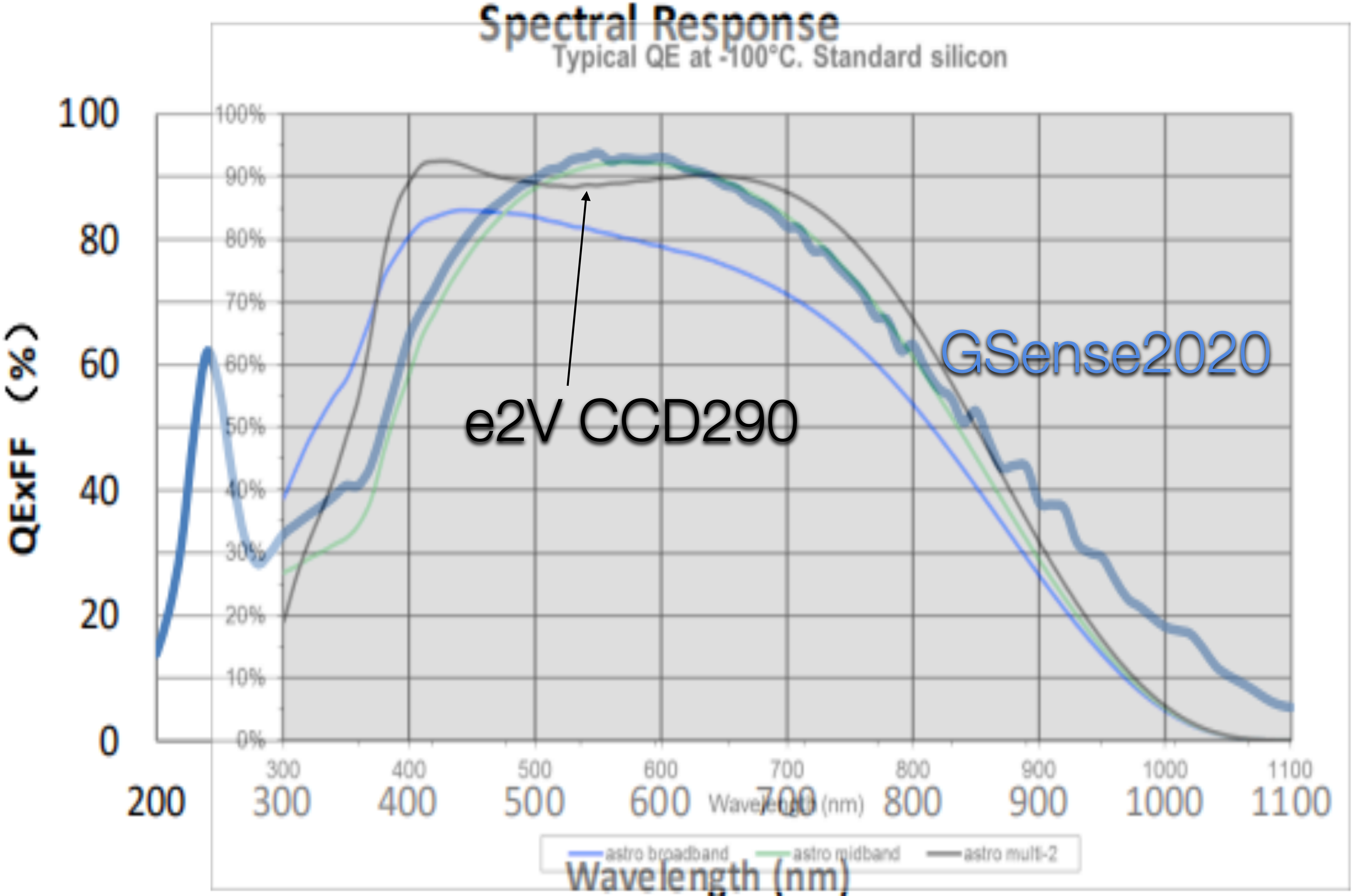

The sensor we chose

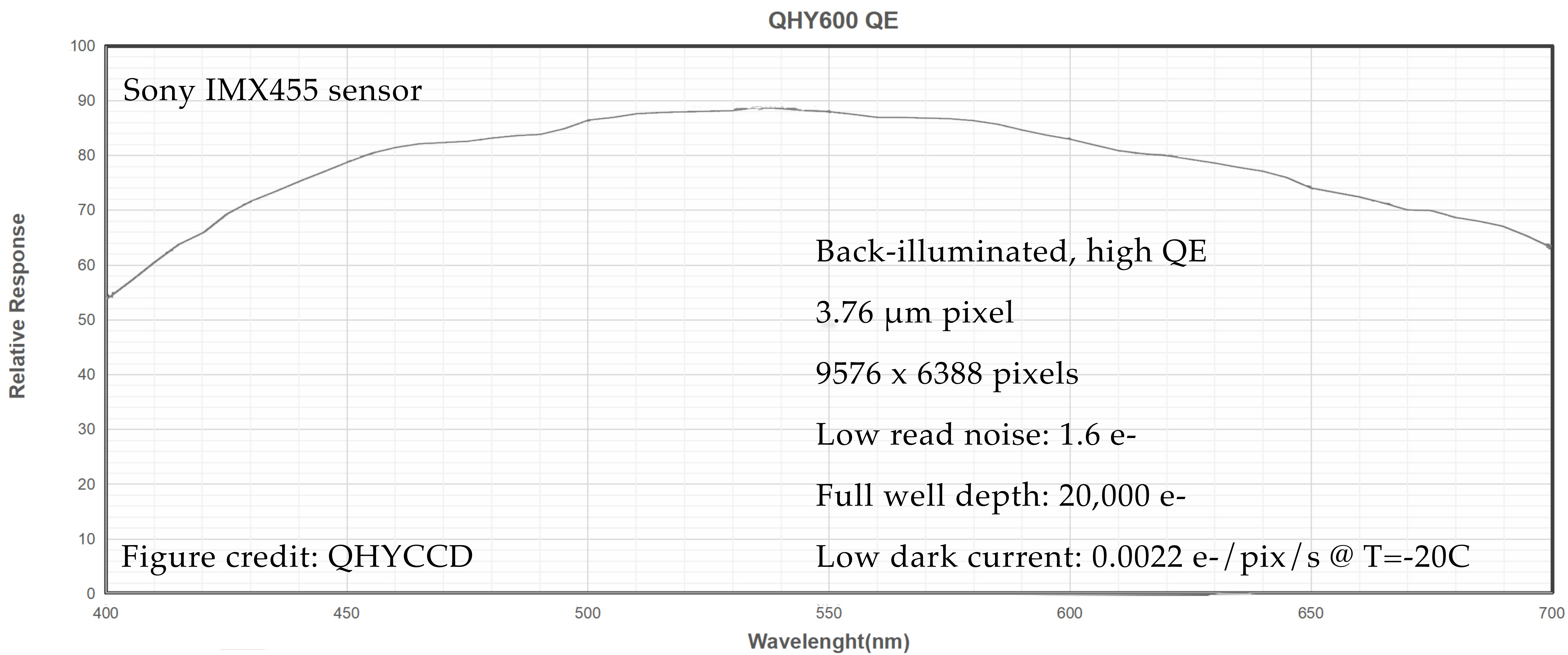

Commercial Photographic lenses with advanced coating technology

Canon

Nano-crystal coating used to improve throughput and reduce scattered light.

Nikon

Newly released super fast (f/0.95) Nikon lens designed for point sources in dark background!

Ray tracing: 1-2 um RMS spot

Spectrograph design for AMASE-P

- 50μm-core fiber =>   26” on the sky
- 547 fibers per spectrograph
- Blue channel: 4640-5092A (HeII, Hβ, [OIII])
  Red channel: 6250-6850A ([OI], Hα, [NII], [SII])
- Spectral Resolution: R~15,000
- Custom dichroic and VPH grisms.
- Nikon 58mm f/0.95 lens as camera
- Water-cooling yields ΔT= -45C

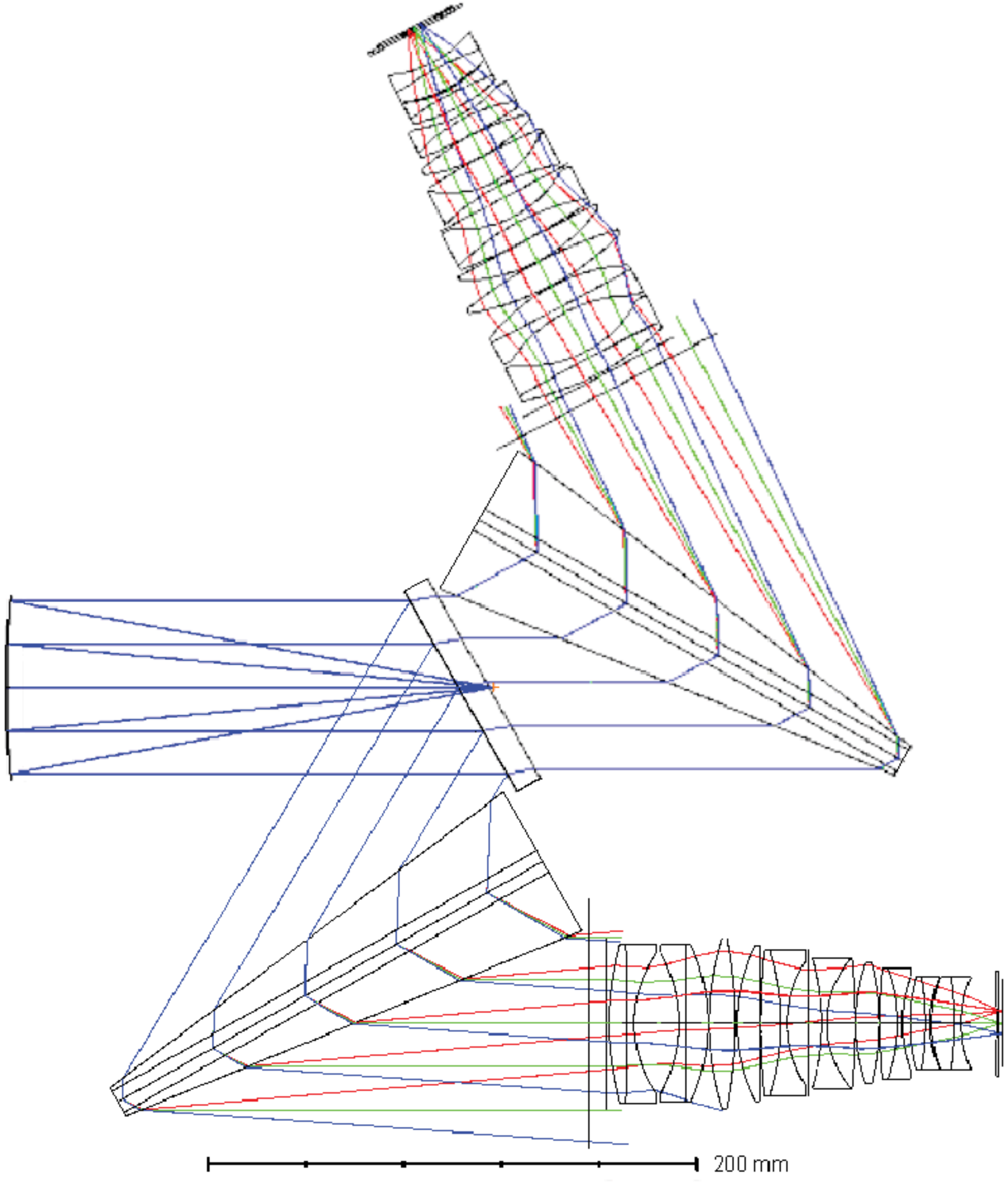

Optomechanics

- Mounted on a bench of 60x60 cm
- Collimator mount and detector cooler are available off the shelf.
- All hardware cost total:
  USD $184K, and much cheaper if massively replicated.

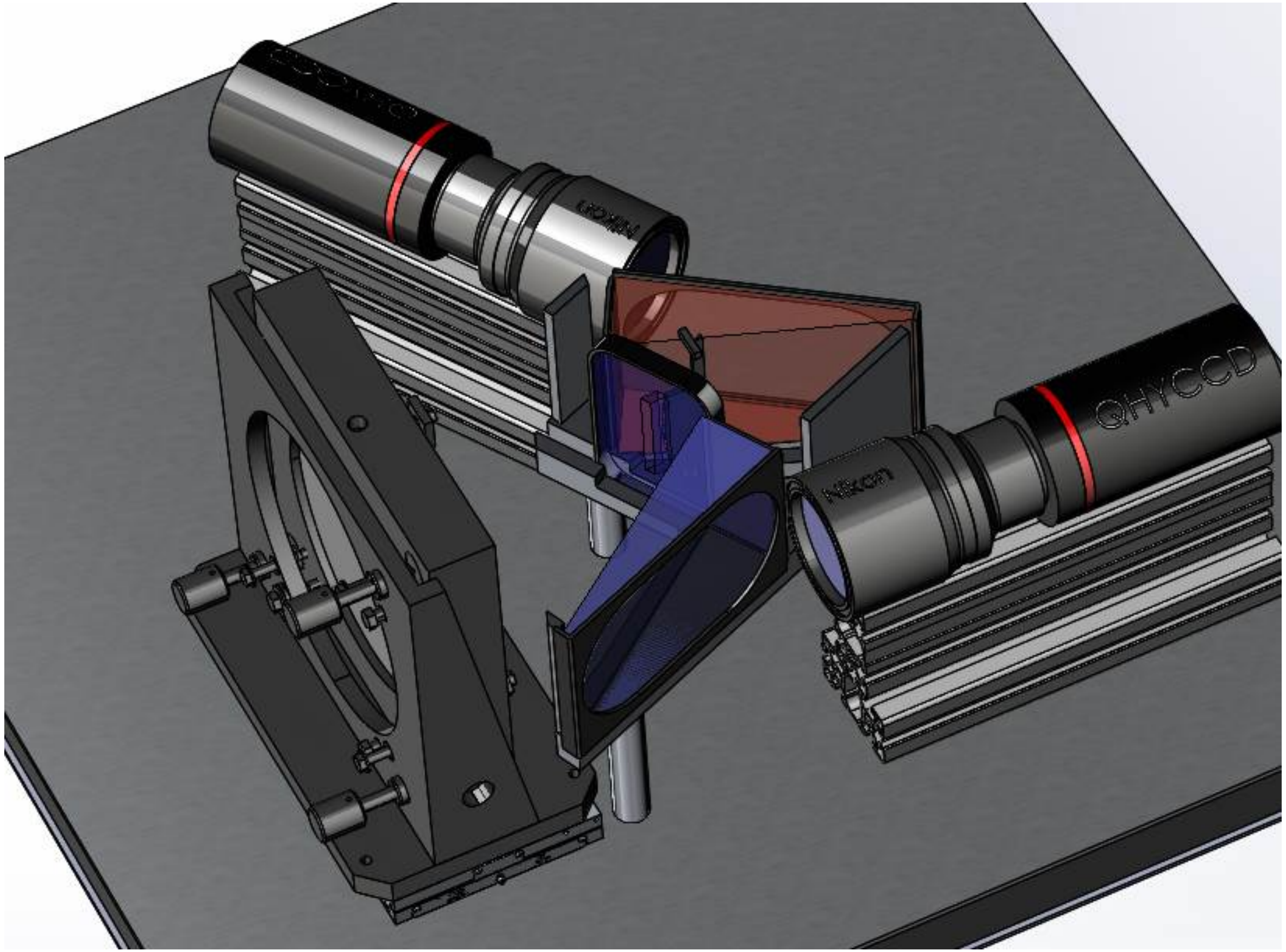

Telescope and Calibration System

- Telescope: Canon 400mm f/2.8 lens
- 20 arcmin across, hexagonal fiber-bundle in MaNGA style, fill factor 31%, covering 79 sq. arcmin at a time.
- Acquisition/Guiding/Focus-monitoring using on-axis NIR light (λ>750nm)
- Pre-set focus offset for bundle to smooth the near-field illumination within fibers (26”)
- Calibration cone in front for on-the-field calibration.

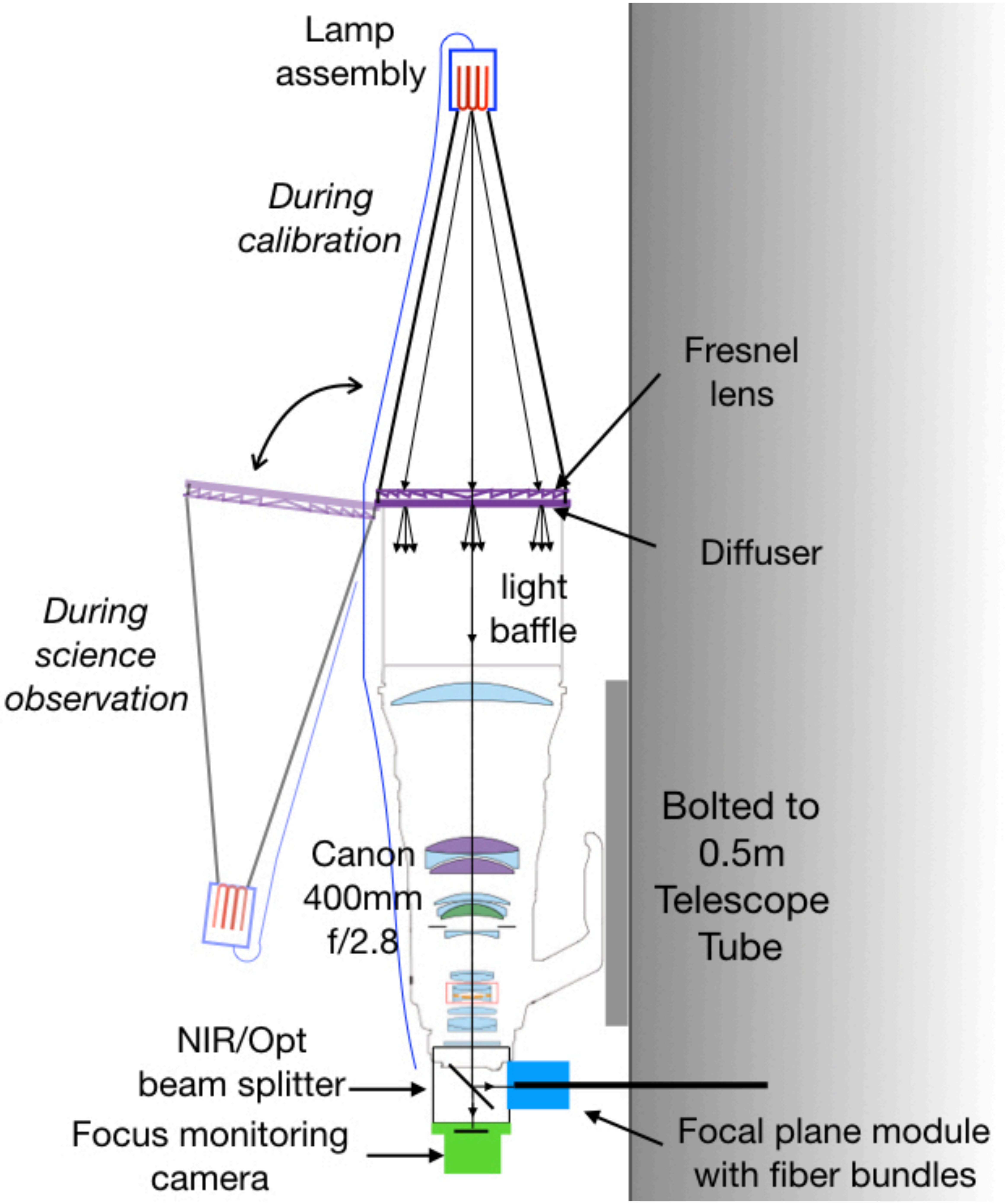

Preliminary Lab Testing — Throughput

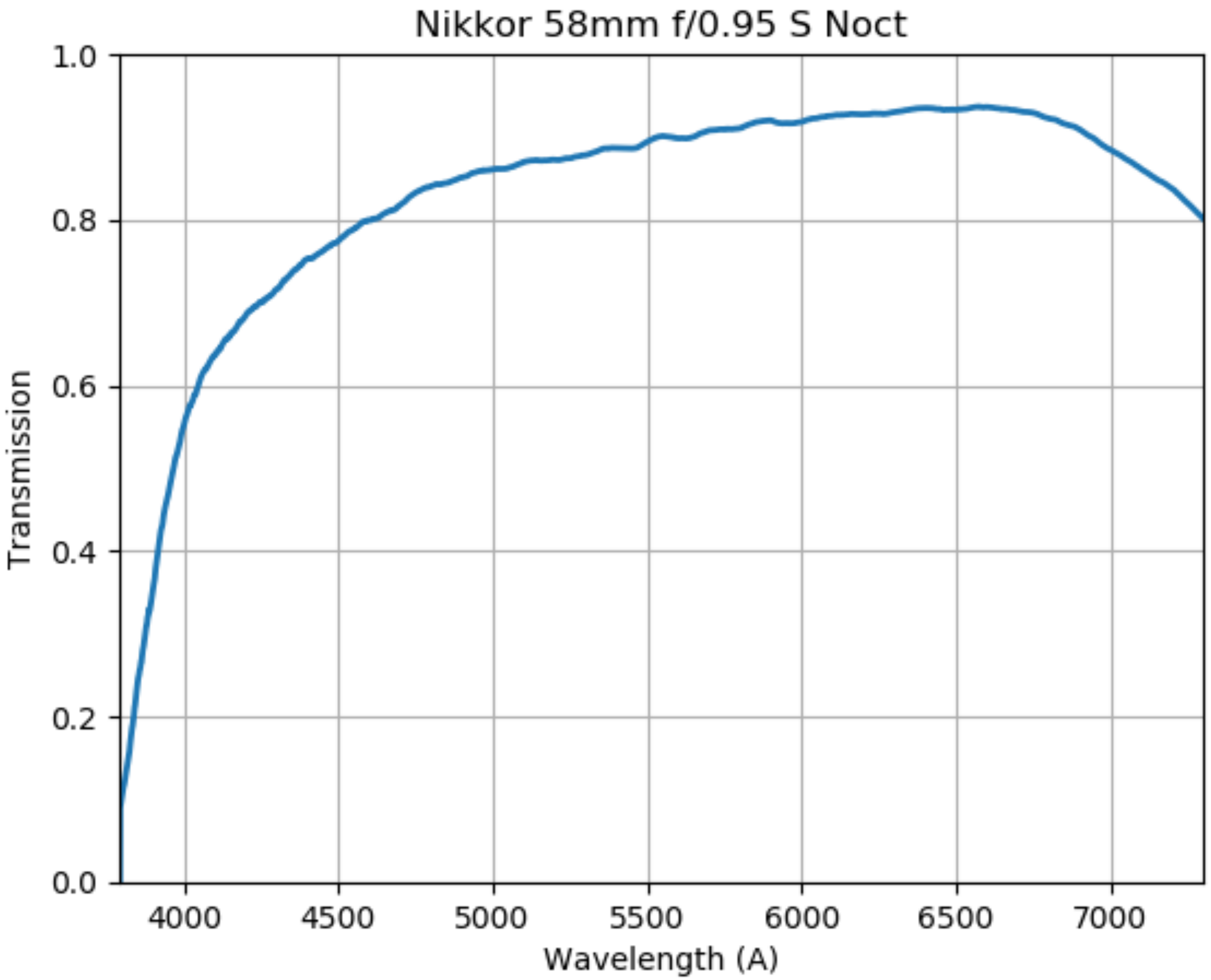

- The chosen Nikon lens has excellent throughput.

Lab Testing — Positioning of thin fibers

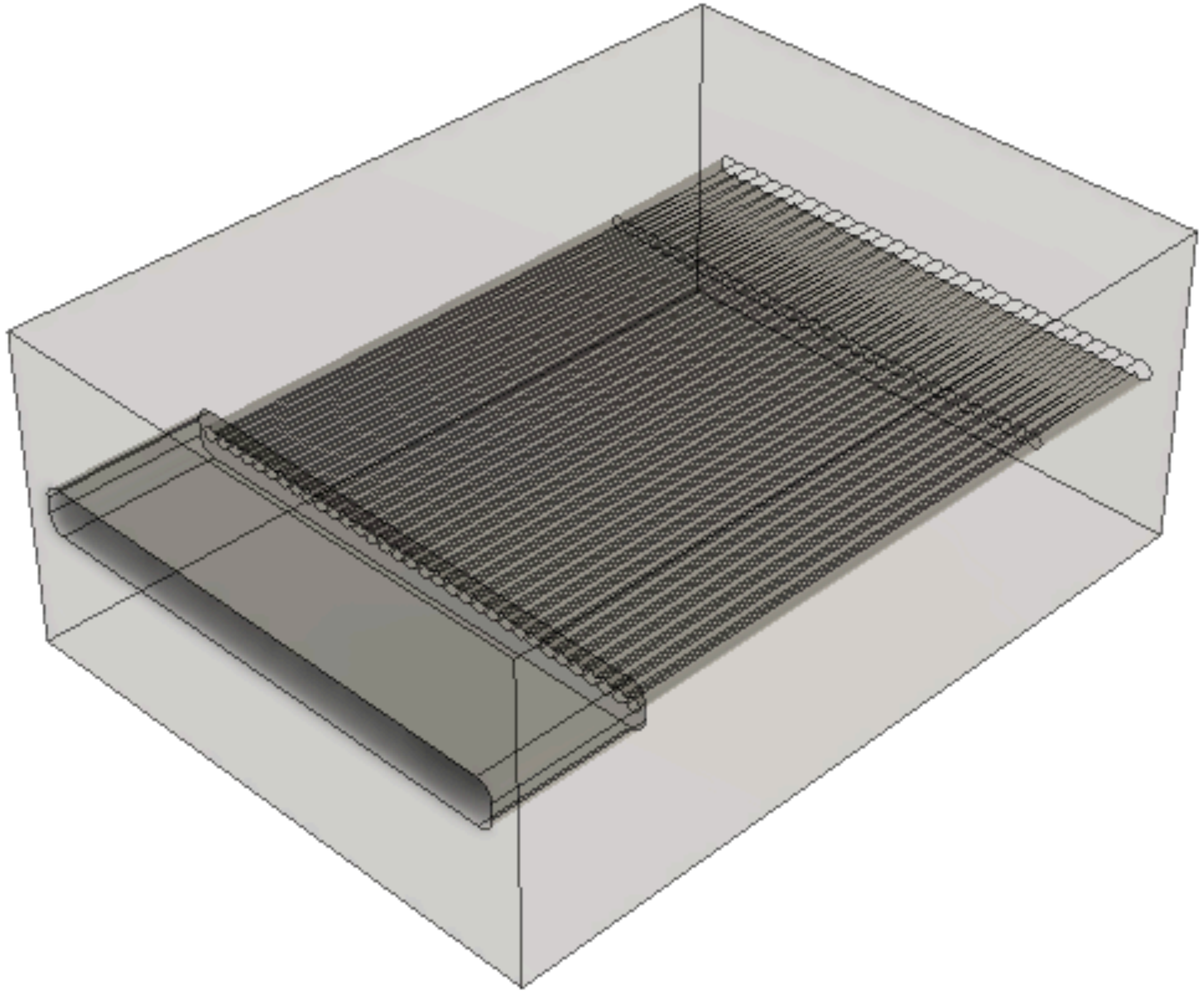

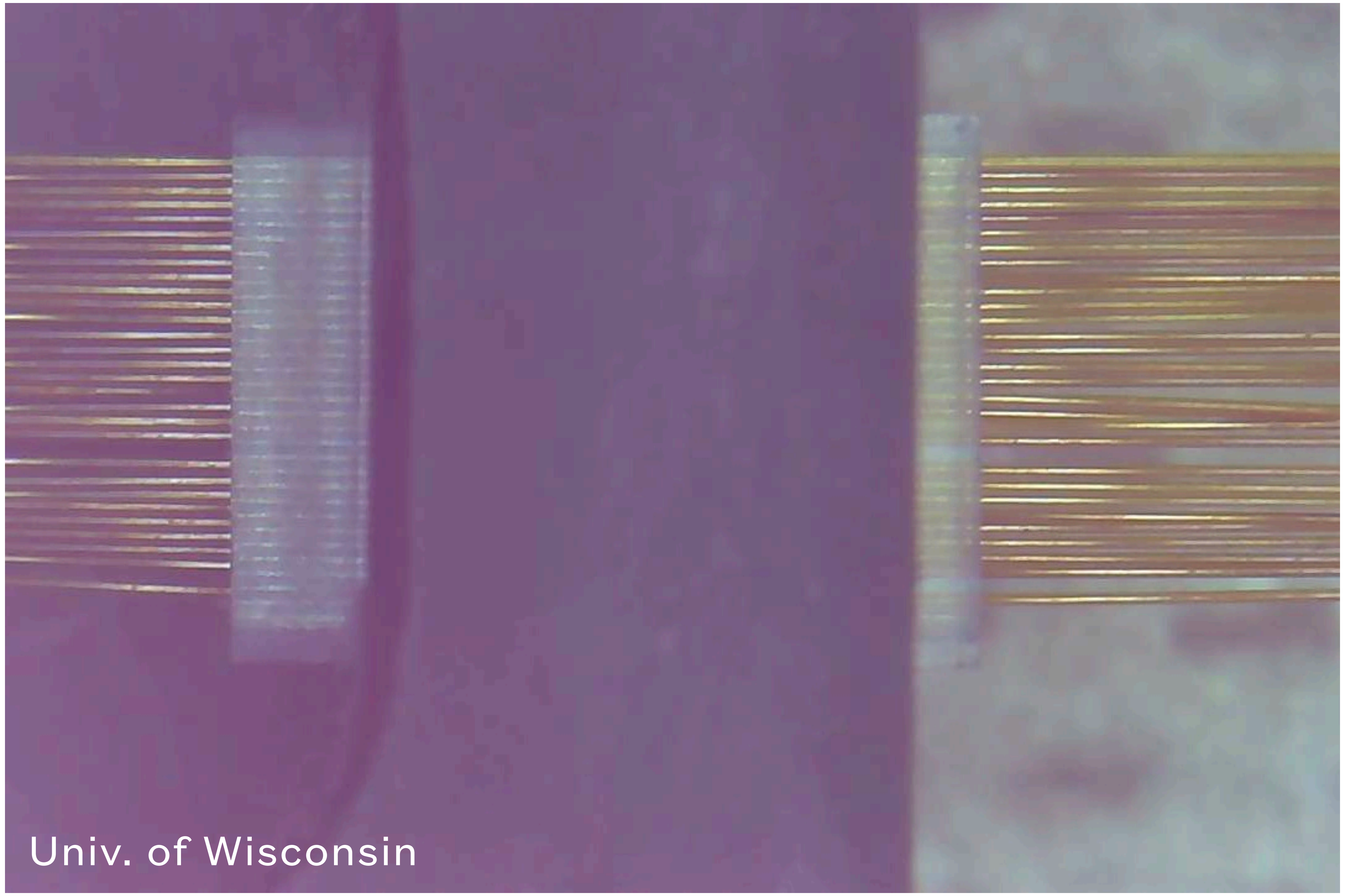

Lab Testing — Image Quality

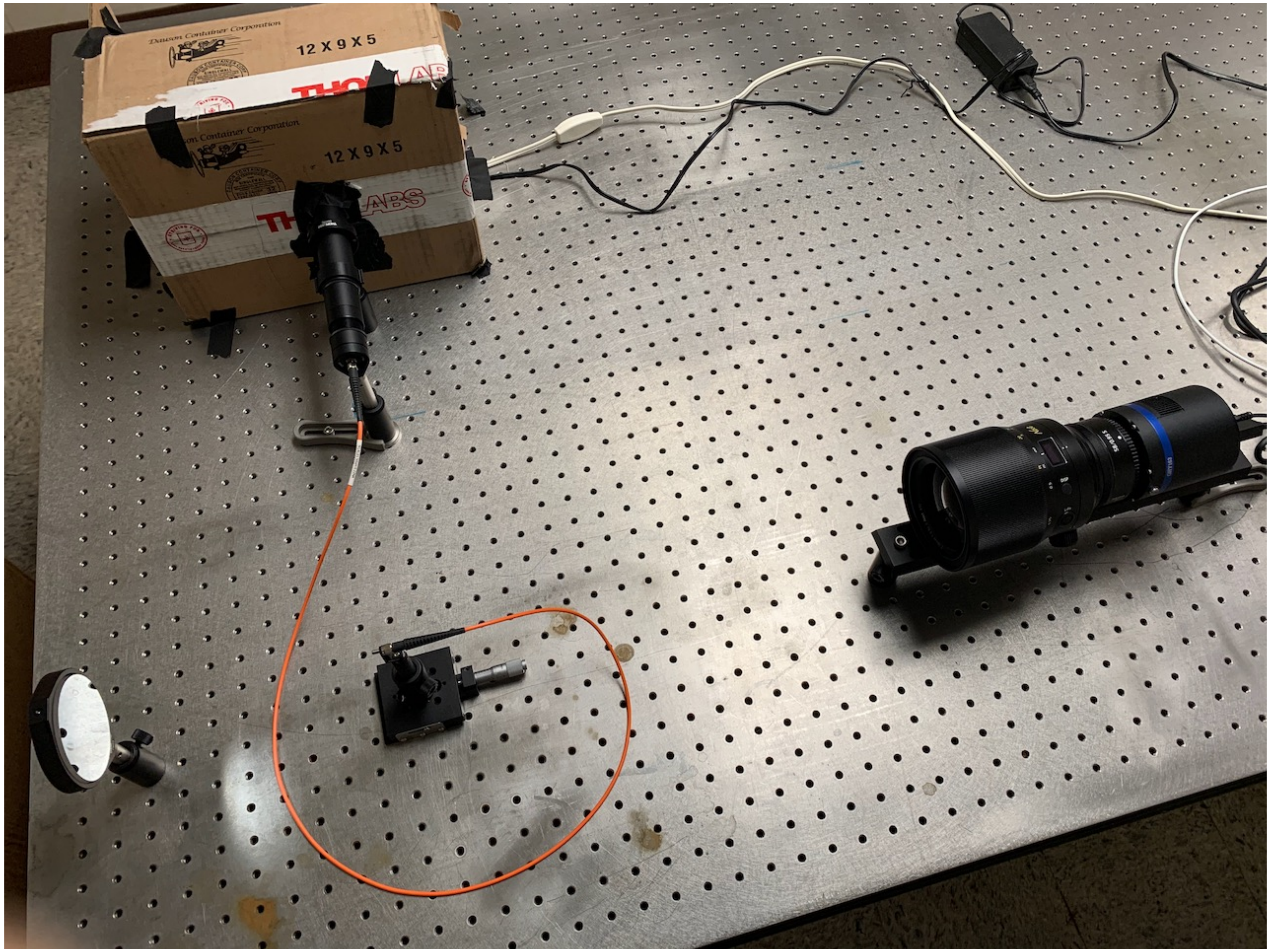

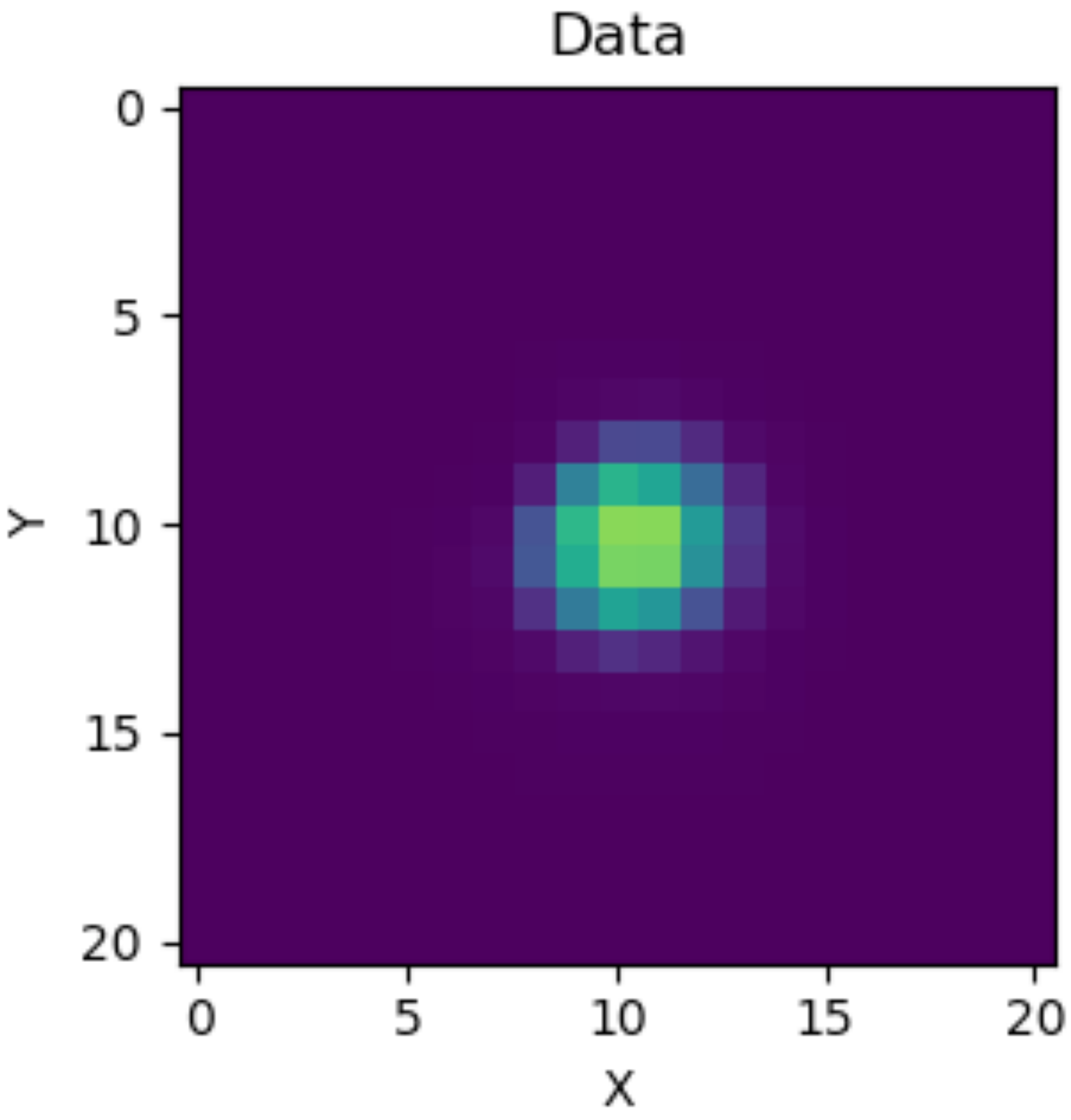

Cost-effectiveness and Expected Sensitivity

- Etendue = (input beam solid angle) x (fiber area) x (efficiency)
- Using DESI as a reference

  Per-fiber etendue: AMASE-P = 18% DESI
  Per-fiber cost: AMASE-P = 11% DESI
- AMASE-P is 60% more cost-effective than DESI, with 4-5 times higher spectral resolution, covering 18% of the bandpass as DESI.
- With an array of 100 spectrographs (US$18M), we can map 1/4 of the sky in 4 years, probing down to 1 Rayleigh.

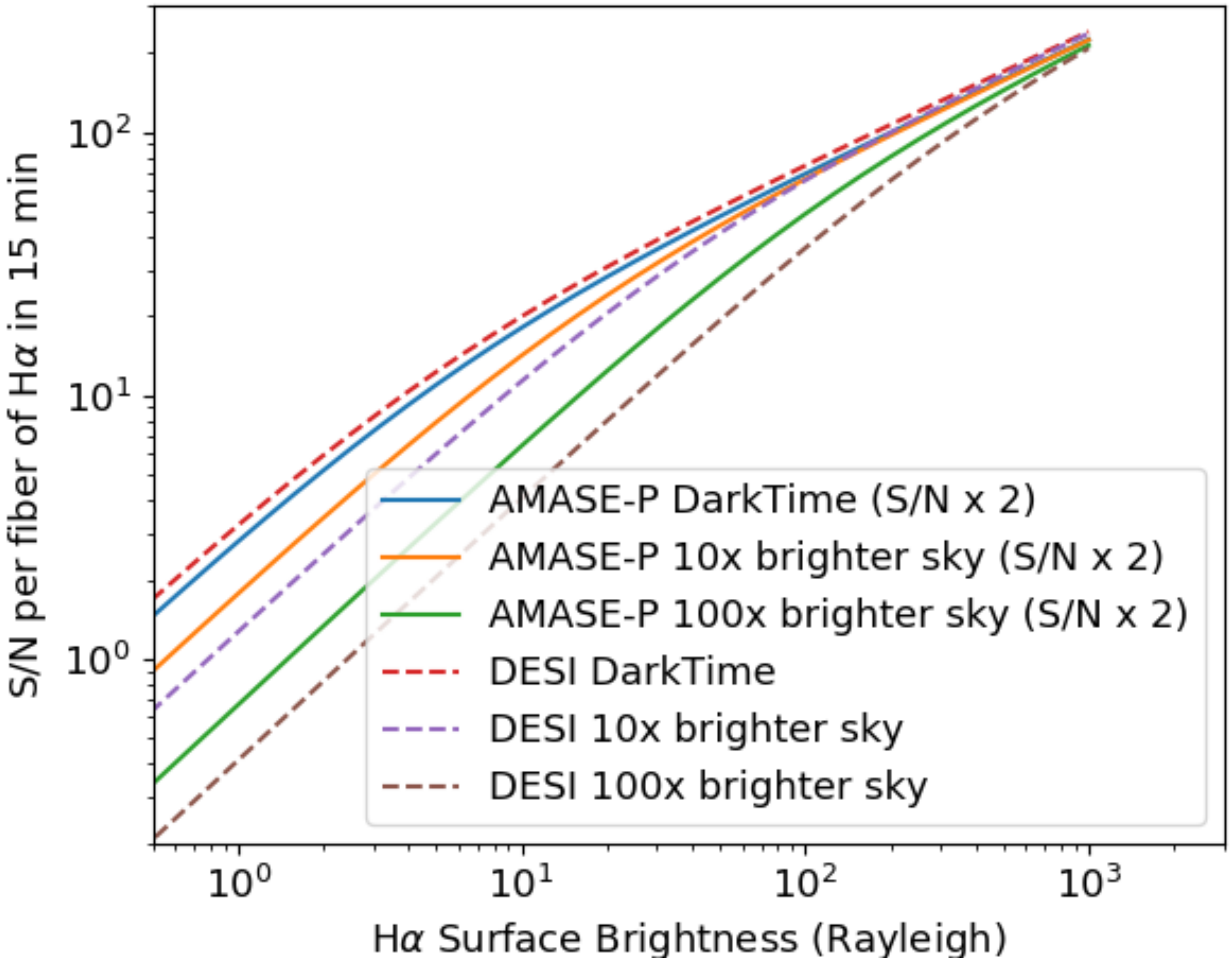

Other potential applications

- Intensity mapping at R~3500 will measure the redshift space distortion, and complement SPHEREx
  - Reduce resolution to R~3500, more efficient design, cheaper gratings and dichroics.
  - Connect to arrays of 50cm f/3.6 telescopes to get a spatial resolution of 6”.
- Multi-object or large monolithic IFS for 6.5m SSST or other large telescopes
  - 50um fiber would be 0.44” on the 6.5m, matching the best seeing condition.
  - A fiber-based MUSE-like instrument.

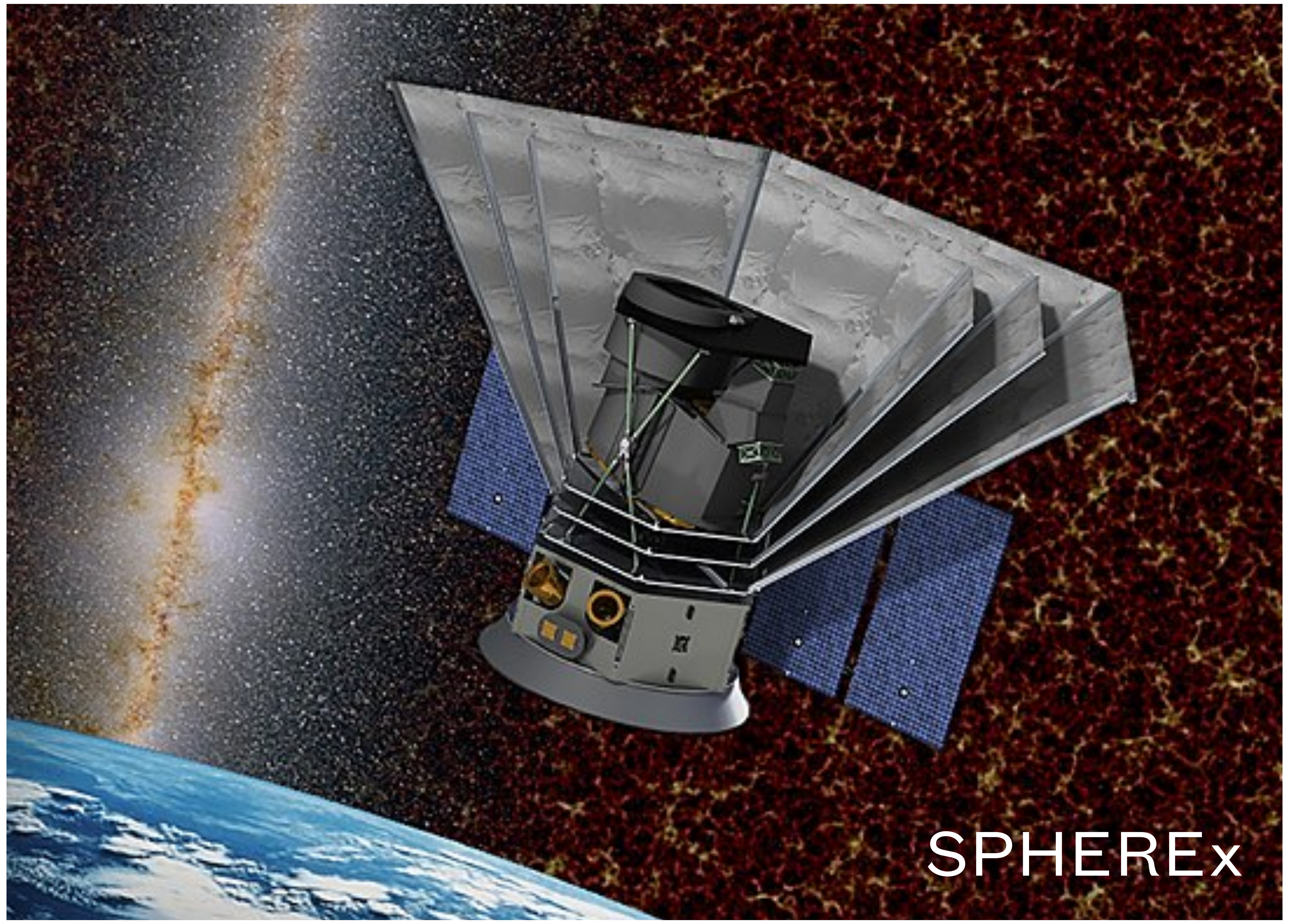

Summary

- Warm ionized gas is a critical component for understanding star formation and feedback
- New methodology is putting strong constraints on photoionization model assumptions that are previously under-constrained. It also helps us identify lines that are discrepant with the models.
- Developing this method to higher dimensions would help constrain all the model assumptions, and help metallicity calibrators to converge, leading us to an era of precision astrophysics of warm ionized gas
- Further constraining the star-forming region models and understanding feedback require new observations probing the intermediate scales and with high spectral resolution.
- The AMASE-P and AMASE instrument will help achieve this goal.

N/O prescription inconsistency

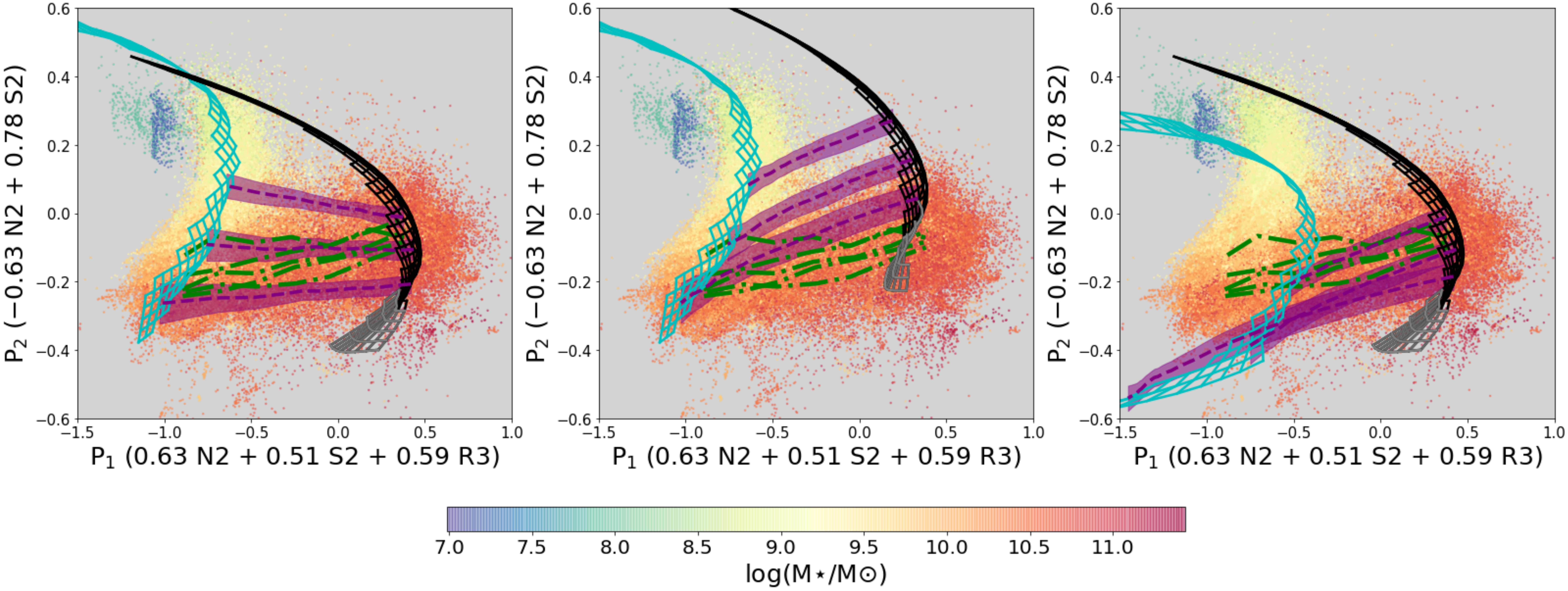

More meaningful demarcations

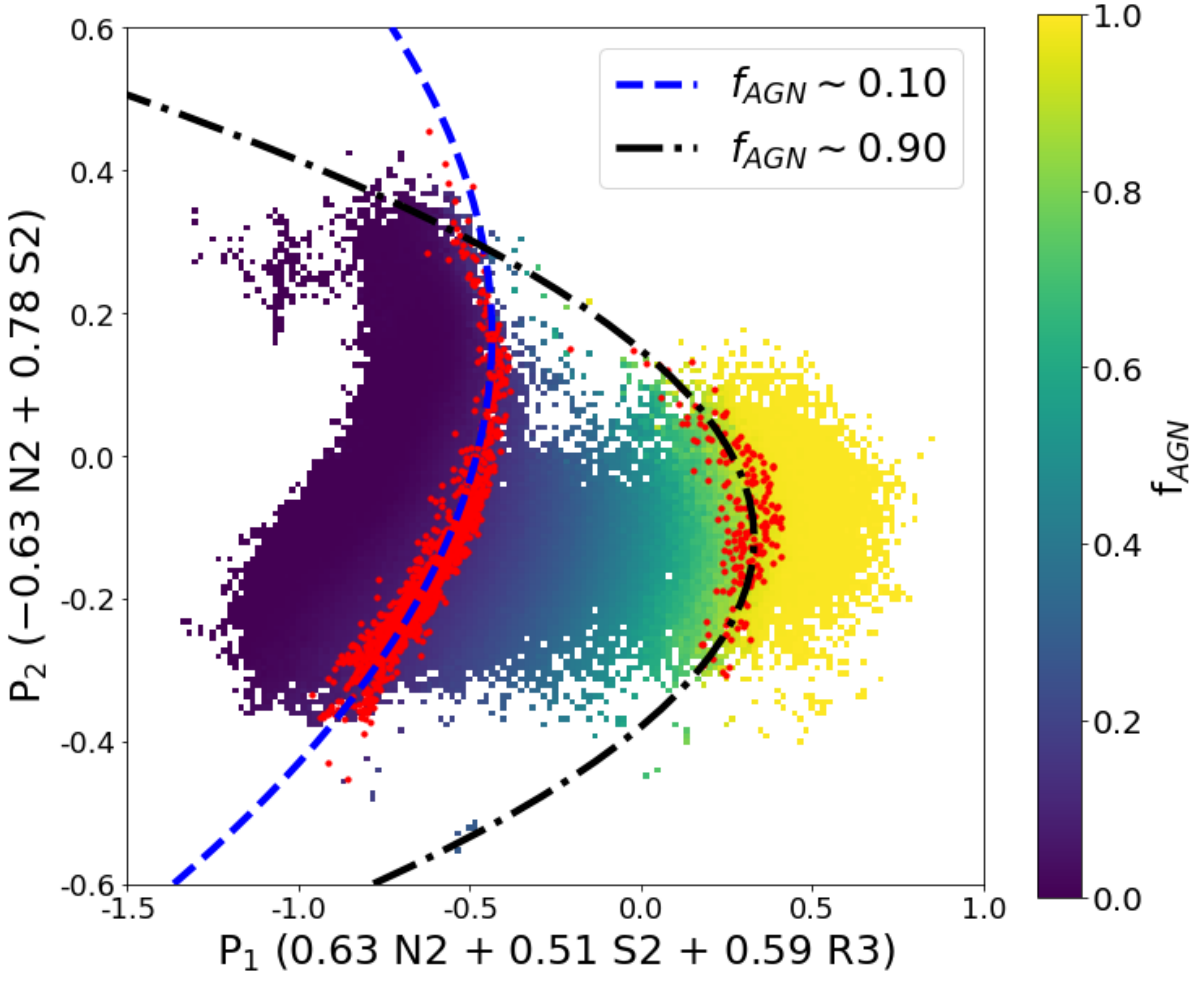

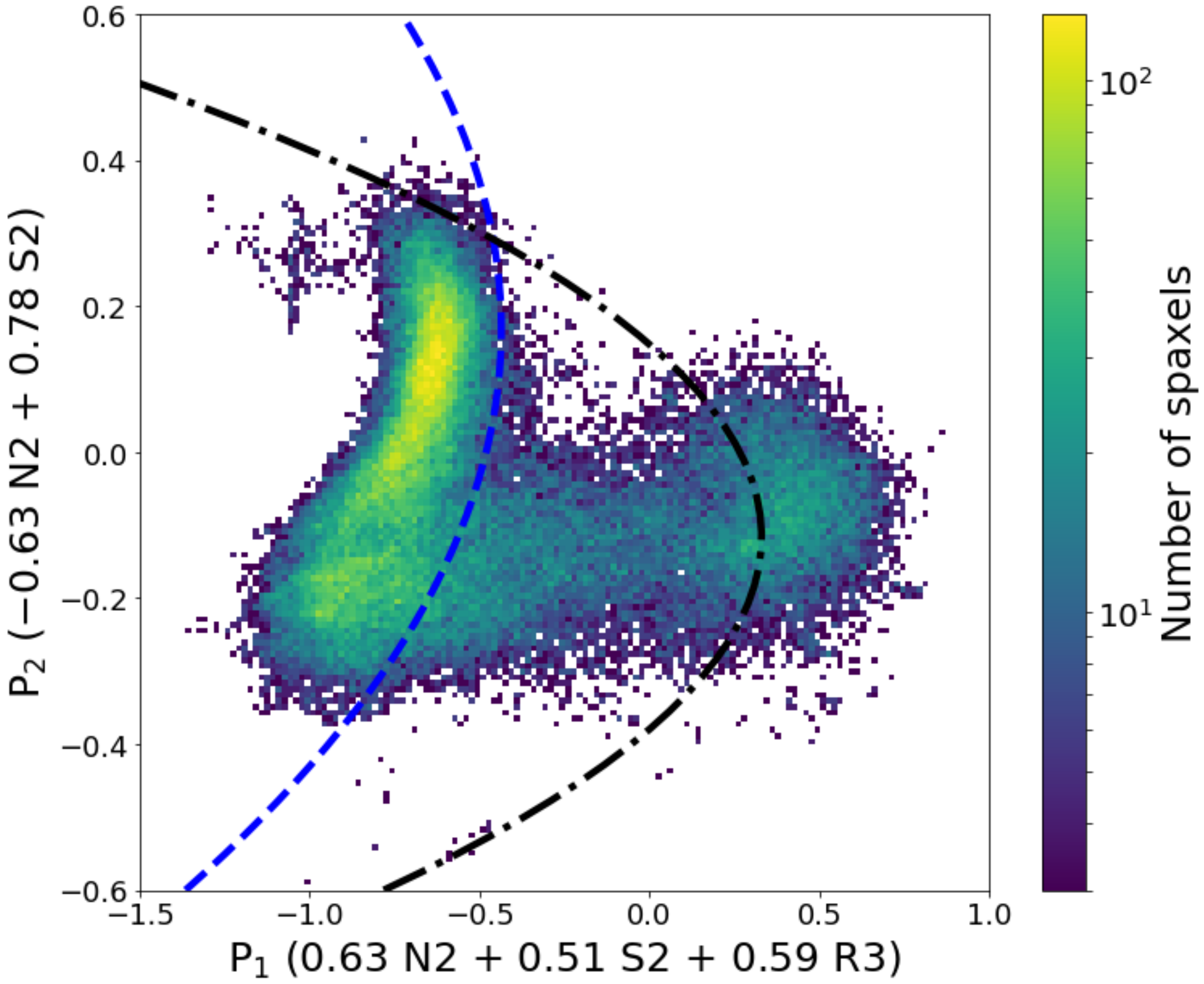

Seyfert/LI(N)ER separation in the P3 direction

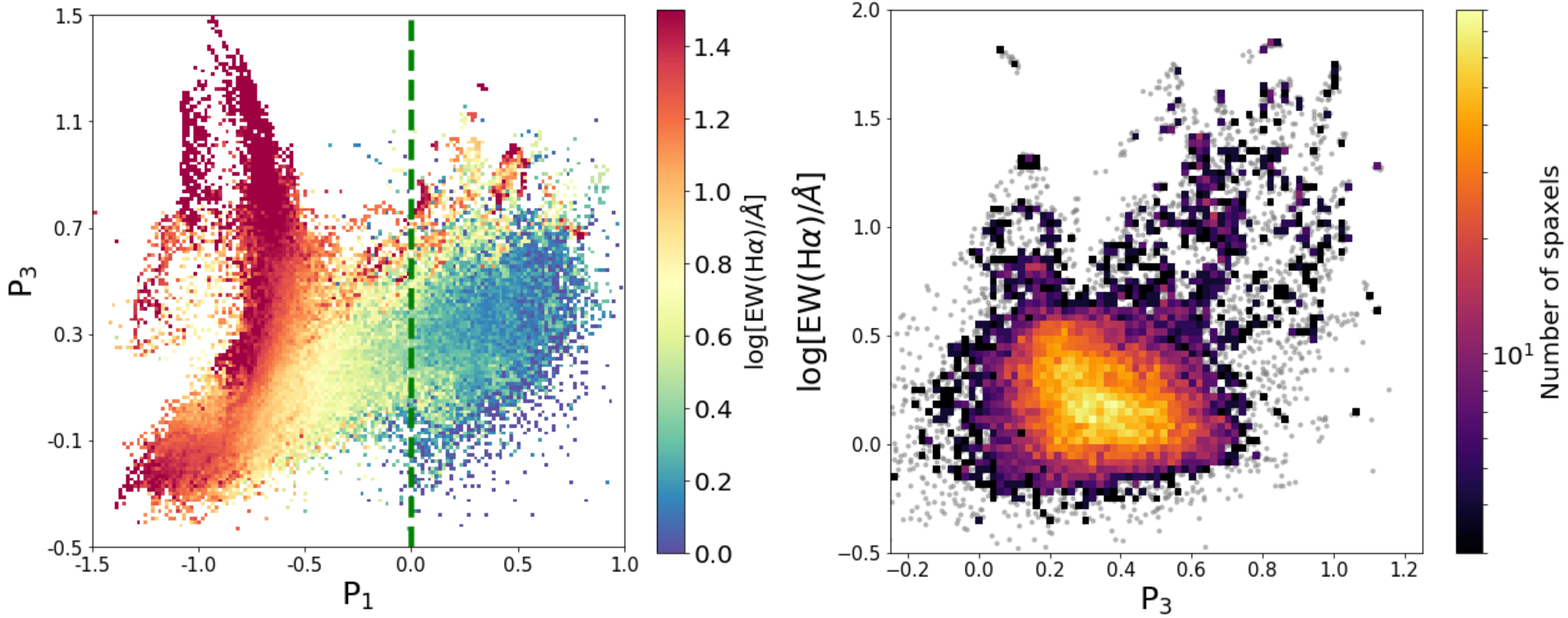

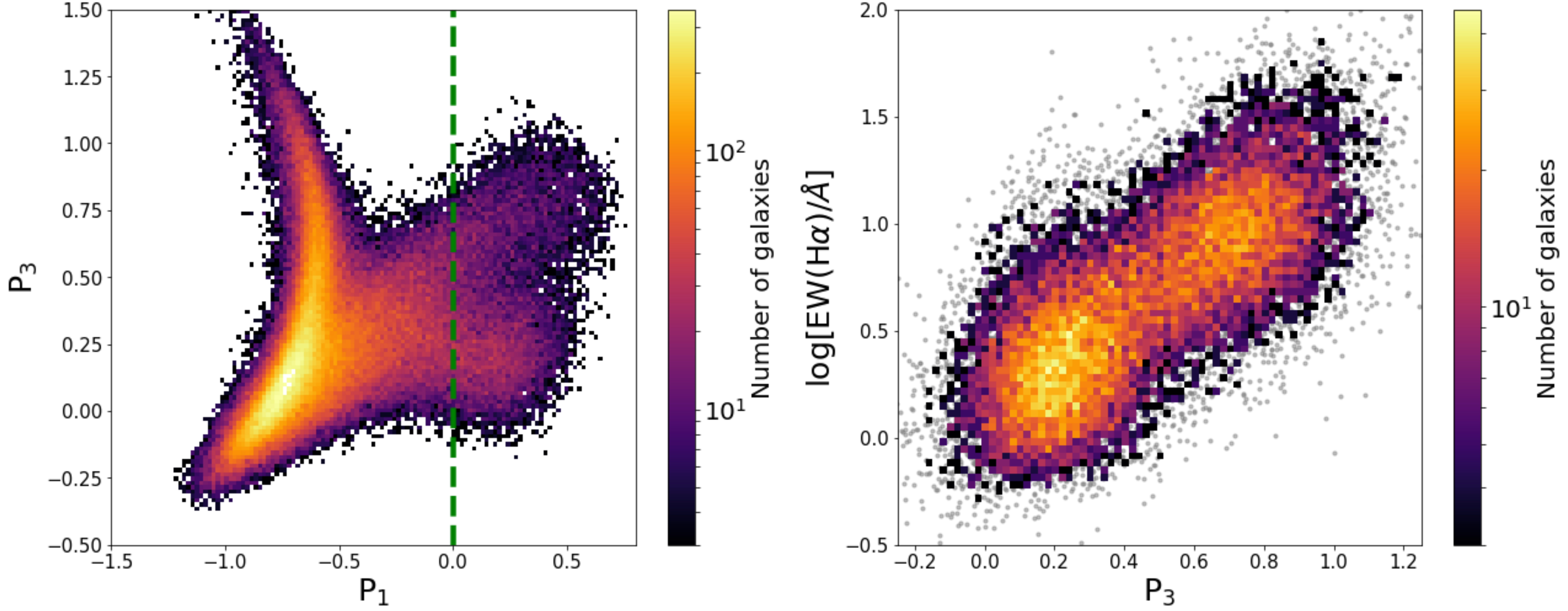

1.50
1.25
1.00
0.75
0.50
0.25
0.00
−0.25
−0.50
P3
−1.5
−1.0
−0.5
0.0
0.5
P1
10^2
10^1
Number of galaxies
2.0
1.5
1.0
0.5
0.0
−0.5
log[EW(Hα)/Å]
−0.2
0.0
0.2
0.4
0.6
0.8
1.0
1.2
P3
10^1
Number of galaxies